

PACIFIC EARTHQUAKE ENGINEERING RESEARCH CENTER

Flow-Failure Case History of the Las Palmas, Chile, Tailings Dam

R. E. S. Moss

Department of Civil and Environmental Engineering
California Polytechnic State University

T. R. Gebhart

California Department of Transportation

J. D. Frost

Department of Civil and Environmental Engineering
Georgia Tech

C. Ledezma

School of Engineering
Pontificia Universidad Catolica de Chile

PEER Report No. 2019/01

Pacific Earthquake Engineering Research Center
Headquarters at the University of California, Berkeley

January 2019

Disclaimer

The opinions, findings, and conclusions or recommendations expressed in this publication are those of the author(s) and do not necessarily reflect the views of the study sponsor(s), the Pacific Earthquake Engineering Research Center, or the Regents of the University of California.

Flow-Failure Case History of the Las Palmas, Chile, Tailings Dam

R. E. S. Moss

Department of Civil and Environmental Engineering
California Polytechnic State University

T. R. Gebhart

California Department of Transportation

J. D. Frost

Department of Civil and Environmental Engineering
Georgia Tech

C. Ledezma

School of Engineering
Pontificia Universidad Catolica de Chile

PEER Report No. 2019/01
Pacific Earthquake Engineering Research Center
Headquarters at the University of California, Berkeley

January 2019

ABSTRACT

This report documents the flow failure of the Las Palmas tailings dam that was induced by the 27 February 2010 Maule Chile M8.8 earthquake. The Las Palmas site is located in Central Chile in Region VII near the town of Talca. Construction of the tailings dam occurred between 1998 as part of a gold mining operation and was no longer in active use.

The ground shaking from the earthquake induced liquefaction of the saturated tailings material and resulted in a flow failure that ran out upwards of 350 m, flowing downslope in two directions. This report is broken into three sections:

1. A summary of the construction and flow failure of the Las Palmas tailings dam;
2. Details on the field investigations at the site, including the 2010 GEER reconnaissance, 2011 litigation support [DICTUC 2012], and the recent PEER–NGL-funded 2017 investigation; and
3. Back-analysis of the flow failure by Gebhart [2016] to estimate the residual strength.

The goal of this work is to provide a “high-quality” flow-failure case history to augment the existing database. The existing database is composed of roughly thirty case histories of varying quality (e.g., Weber et al. [2015] and Kramer and Wang [2015]). Herein, the term “high-quality” means that the *in situ* measurements were made in a controlled and repeatable manner, and that the back-analysis of the residual strength was performed considering static and dynamic effects of the slide mass. The results from this research indicate that the median back-analyzed residual strength of the liquefied material is ~ 8.3 kPa (~ 173 psf) at a pre-earthquake vertical effective stress of 2 atm (~ 200 kPa or 4000 psf), which is correlated to a median SPT blow count of $N_{1,60} \sim 2.5$, a median CPT tip resistance of $q_{c1} \sim 1.3$ MPa, and a median shear-wave velocity of $V_{S1} \sim 172$ m/sec. The back analyzed residual strength has a nominal coefficient of variation of 5.5% determined using a sensitivity analysis.

ACKNOWLEDGMENTS

This research is a compilation of prior work and more recent field investigations. The initial reconnaissance was performed by GEER members and was funded by the U.S. National Science Foundation (NSF) through the Geotechnical Engineering Program under Grant No. CMMI-1266418. The work by Professor Ledezma and colleagues at Pontificia Universidad Católica de Chile was funded through litigation support. The work by Tristan Gebhart was performed as part of his Master's Degree at Cal Poly, San Luis Obispo. The most recent field investigations were funded through the PEER–NGL program, with support by the California Department of Transportation and the U.S. Nuclear Regulatory Commission.

Thanks go to NSF, the NGL program, Professor Ricardo Moffat and the employees of LMMG, and Professor Joe Weber, with special thanks to Professor Jon Stewart who provided a careful and detailed review of a draft report that helped vastly improve the presentation and communication of this study.

Any opinions, findings, and conclusions or recommendations expressed in this material are those of the authors and do not necessarily reflect those of the sponsoring organizations, PEER, or the Regents of the University of California.

CONTENTS

ABSTRACT	iii
ACKNOWLEDGMENTS	v
CONTENTS	vii
LIST OF TABLES	ix
LIST OF FIGURES	xi
1 INTRODUCTION	1
2 LAS PALMAS TAILINGS DAM CONSTRUCTION AND FAILURE	3
3 GEER INVESTIGATIONS	7
4 LITIGATION-SUPPORTED FIELD INVESTIGATIONS	13
5 PEER NGL-FUNDED INVESTIGATIONS	21
6 BACK-ANALYSIS OF RESIDUAL STRENGTH	35
7 COMPREHENSIVE RESULTS	41
7.1 Resistance Measurements	41
7.2 Residual Strength	47
7.3 Effective Stress	47
7.4 Comparison with Existing Database	48
8 SUMMARY AND CONCLUSIONS	53
REFERENCES	55
APPENDIX GEOPHYSICAL DATA PROCESSING	57

LIST OF TABLES

Table 2.1	Ground shaking recorded in Talca (after Boroschek et al. [2012]).	4
Table 4.1	Summary of field and lab data performed by DICTUC [2012]; from Gebhart [2016].	14
Table 5.1	Showing co-location of different field tests.	23
Table 6.1	Summary of materials and properties used in modeling the tailings failure.	39
Table 7.1	Shear-wave velocity of "weak" layers for each profile.	43
Table 8.1	Summary mean and coefficient of variation.	53

LIST OF FIGURES

Figure 2.1	Location of Las Palmas tailings dam; regional inset and local with coordinates.	5
Figure 2.2	Construction Stages 1-4 of tailings embankments (from DICTUC, [2012]).....	6
Figure 3.1	Upper scarp of failed tailings impoundment looking southwest (from GEER [2010]).	7
Figure 3.2	Upper scarp of failed tailings impoundment looking northeast (from GEER [2010]).	8
Figure 3.3	Aerial photograph showing scarp, longitudinal cracks, and the location of the tailings dams (after DICTUC [2012] and Gebhart [2016]).....	8
Figure 3.4	Sand-boil tailings along flow path (S35.18872, W71.75777) looking up towards the scarp is shown in Figures 3.2 and 3.3 (from GEER [2010]).	9
Figure 3.5	Gravelly cover layer over oxidized and unsaturated tailings, S35.184679 S, W71.759410 (from GEER [2010]).	10
Figure 3.6	Terrestrial laser scanning with a Riegl z420 LIDAR unit at the Las Palmas Mine tailings dam failure. The system uses a PC for data acquisition and a car battery to power the laser (from GEER [2010]).	11
Figure 3.7	Detailed LIDAR of head scarp of Las Palmas tailings dam failure (from GEER [2010]).	12
Figure 4.1	Location of SPT borings performed by DICTUC [2012], with the depth of each boring shown in parenthesis. The intact and failed material zones are delineated.	14
Figure 4.2	Histogram of corrected SPT blow counts, $(N_1)_{60}$, from the field investigations (from Gebhart [2016]).	15
Figure 4.3	Boring B1 performed by DICTUC [2012]; from Gebhart [2016].	16
Figure 4.4	Boring B2 performed by DICTUC [2012]; from Gebhart [2016].	17
Figure 4.5	Boring B3 performed by DICTUC [2012]; from Gebhart [2016].	18
Figure 4.6	Boring B4 performed by DICTUC [2012]; from Gebhart [2016]).	19
Figure 4.7	Boring B5 performed by DICTUC [2012]; from Gebhart [2016].	20

Figure 5.1	Portable “ramset” mobilized for Las Palmas field investigations because of the difficult access conditions. The reaction weight was provided by water tanks and truck. The ramset is the white hydraulic jack in the middle. The black box with orange cord to the right is the hydraulic pump.	21
Figure 5.2	Location of CPT soundings with respect to prior SPT borings.	22
Figure 5.3	Shown is a 10-m circular array at location G5. Passive measurements were made of ambient noise from a generator, foot falls, and other.	23
Figure 5.4	Locations of passive circular array measurements with respect to CPT soundings and SPT borings.....	24
Figure 5.5	CPT1 cone tip, sleeve, and pore pressure measurements. Location S35.184242 W71.759540; elevation ~155 m.	25
Figure 5.6	CPT2 cone tip, sleeve, and pore pressure measurements. Location S35.184297 W71.760284; elevation ~155 m.	26
Figure 5.7	CPT3 cone tip, sleeve, and pore pressure measurements. Location S35.184350 W71.761197; elevation ~153 m.	27
Figure 5.8	Location G1 <i>VS</i> measurements. Location S35.184242 W71.759540; elevation ~155 m.....	28
Figure 5.9	Location G2 <i>VS</i> measurements. Location S35.184297 W71.760284; elevation ~155 m.....	29
Figure 5.10	Location G3 <i>VS</i> measurements. Location S35.184350 W71.761197; elevation ~153 m.....	30
Figure 5.11	Location G5 <i>VS</i> measurements of flow slide material. Location S35.185729 W71.758658; elevation ~140 m.	31
Figure 5.12	Location G6 <i>VS</i> measurements of translated block material. Location S35.186669 W71.758161; elevation ~134 m.	32
Figure 5.13	Comparison of G5 and G6 <i>VS</i> measurements.....	33
Figure 6.1	Marked image showing flow failure runout following two directions, east and south (from Gebhart [2016]).	36
Figure 6.2	Evidence of sand boils in the flow failure debris (from GEER [2010]).	37
Figure 6.3	Modeled slope failure progression sequence in AutoCAD (from Gebhart [2016]).	37
Figure 6.4	Modeled slope failure progression sequence in Slope/W (from Gebhart [2016]).	38
Figure 6.5	Example trial of incremental momentum method (IMM) after Weber [2015].	40

Figure 7.1	Histogram of blow counts in saturated tailings material, with fines correction (borings B-2,3,4).....	42
Figure 7.2	CPT1 overburden corrected tip resistance with histogram of boxed region thought to best represent the tailings material susceptible to liquefaction and flow failure. The mean and median are approximately 1.83 MPa with a CoV of 0.40.....	44
Figure 7.3	CPT2 overburden corrected tip resistance. This sounding is thought to represent material not highly susceptible to liquefaction because of wall material and interlayering. The boxed region mean is 2.94 MPa, median 1.86 MPa, with a CoV of 0.52.	45
Figure 7.4	CPT3 overburden corrected tip resistance. This sounding is in the center of a region that experienced liquefaction but did not exhibit failure in a flow failure. The boxed regions have a mean of 1.3 MPa, median 1.4 MPa, with a CoV of 0.06.....	46
Figure 7.5	Tornado plot sensitivity analysis of post-liquefaction residual strength (from Gebhart [2016]).....	47
Figure 7.6	Geometry used to estimate the effective stress on the failure plane at the time of failure (from Gebhart [2016]).....	48
Figure 7.7	Las Palmas data ellipse with respect to Seed and Harder [1990].	48
Figure 7.8	Las Palmas data point (SPT) with respect to Olson and Stark [2002].....	49
Figure 7.9	Las Palmas data point (CPT) with respect to Olson and Stark [2002].	50
Figure 7.10	Las Palmas data point with respect to Kramer and Wang [2015].....	51
Figure 7.11	Las Palmas data point with respect to Weber et al. [2015].....	52

1 Introduction

The 27 February 2010 Maule, Chile, earthquake is the seismic event that resulted in the failure for this case history. The sixth largest recorded earthquake since 1900, this event occurred at 3:34 am local time with a moment magnitude of 8.8 and was centered off the coast of Bio Bio, Chile. The hypocenter was located at an approximate depth of 35 km (21.7 miles), 95 km (60 miles) off the coast, and 335 km (210 miles) southwest of the capital of Santiago.

Maximum recorded acceleration was 0.94 g at a station located in the city of Angol, Chile (www.terremotosuchile.cl/red_archivos/RENAMAULE2010R2.pdf). Strong earthquake shaking exceeded a minute in some locations for a total duration up to nearly two minutes. The rupture occurred on the shallow-inclined fault conveying the Nazca plate eastward and downward beneath the South American plate. Thrust faulting occurred on the interface between both plates due to a plate convergence of approximately 7 m (23 ft) per century. The fault rupture at depthplane exceeded 100 km (60 miles) in width and nearly 500 km (300 miles) parallel to the coast [Hayes 2010]. Rupture initiated beneath the coast and propagated westward, northward, and southward, causing tectonic deformation that triggered a tsunami.

The ground shaking resulted in pervasive damage of lifelines, e.g., roadways, bridges, railroads, and road embankments. In total, approximately 523 people were killed, 12,000 injured, and 800,000 displaced, and 370,000 houses, 4000 schools, and 79 hospitals were damaged or destroyed [USGS 2010]. The tailings dam of the Las Palmas gold mine experienced liquefaction-induced flow failure due to strong ground shaking, which produced a run out of a third of a kilometer [GEER 2010]. The flow failure resulted in fatalities and caused environmental degradation of the surrounding area.

This report summarizes the following:

- Construction and subsequent failure of the Las Palmas tailings dam
- Reconnaissance investigations performed by the GEER team [GEER 2010]
- Field investigations performed by Professor C. Ledezma and colleagues [DICTUC 2012] where standard penetration test (SPT) measurements were made
- PEER (Pacific Earthquake Engineering Research Center)-NGL (next generation liquefaction)-funded field investigations where cone penetration tests (CPT) and shear-wave velocity (V_S) measurements were made

- Back-analysis of the failure by Gebhart [2016] that estimated the liquefied residual strength, and effective stress at the time of failure.

The objective of this report is to provide a “high-quality” flow-failure case history to add to the existing liquefied residual strength database.

2 Las Palmas Tailings Dam Construction and Failure

The construction of the Las Palmas gold mine tailings dam (Figure 2.1) began in 1981 [DICTUC 2012]. The dam was built upon existing ground that was downward sloping toward the south and east, with approximate maximum upper slope of 4:1 (horizontal to vertical) above the dam and maximum lower slope of 15:1 (horizontal to vertical) below. The dam was constructed in four phases (Figure 2.2), which occurred between 1981–1998. Each stage included initial construction of containment embankments and hydraulic fill placement of tailings materials. Construction of containment walls or embankments typically utilize the sandy, more granular fraction of the tailings material to provide increased strength

Construction documents indicate use of both upstream and centerline construction methods to build containment embankments. Stage 1 construction spanned from the end of 1981–1986, covering the upper half of the slope. Stage 2 construction spanned from 1986–1992, initiating the covering of the lower half of the slope. Stage 3 construction continued from 1992–1997, containing the largest volume of material and spanning the entire length of the slope, covering both Stages 1 and 2. The final construction of Stage 4 spanned from 1997–1998, covering approximately the same area as Stage 1 [DICTUC 2012]. After closure of the facility, the tailings area was partially covered with a thin 6-in. layer of gravelly material.

Limited available information indicates that during Stage 4, the down-slope embankment was built nearly atop the down-slope embankment built during Stage 1 [DICTUC 2012]. Stage 3 covered the entire area, which resulted in a continuous potentially weak horizontal plane between the lower and upper material. During the earthquake Stage 4 acted as a driving mass at the head of the slope. The boundary between Stage 3 and the material below it became the zone in which liquefaction occurred.

The strong ground shaking resulted in liquefaction of susceptible tailings material. The flow failure took two paths: an easterly and southerly direction. The leading edge of the easterly flow traveled approximately 165 m (540 ft), whereas the southerly flow traveled roughly 350 m (1150 ft) based on air photos rendered into CAD [Gebhart 2016]. Approximately 231,660 m³ (303,000 yds³) of material displaced in roughly two equal halves; see the slope stability analyses presented herein.

Strong ground shaking as measured in the town of Talca is shown in Table 2.1 below (after Boroschek et al. [2012]). The Las Palmas site is located roughly 20 km NNW from Talca in a direction closer to the 2010 rupture plane, so ground shaking at the site [ignoring two-dimensional (2D) site response effects] can reasonably be assumed to be in line with that recorded in Talca.

Table 2.1 Ground shaking recorded in Talca (after Boroschek et al. [2012]).

Code Station (Rrup)	Channel	PGA (g)	PGV (cm/s)	PGD (cm)	5% damped PSa (g)					Arias Intensity (m/s)	Significant Duration (sec)	Central Freq. (Hz)
					0.1sec	0.2sec	1sec	2sec	3sec			
TAL (66 km)	L	0.48	28	4	0.77	1.22	0.31	0.13	0.05	11.61	69.9	5.14
	T	0.42	34	7	1.01	1.79	0.38	0.19	0.08	11.06	71.9	5.14



Figure 2.1 Location of Las Palmas tailings dam; regional inset and local with coordinates.

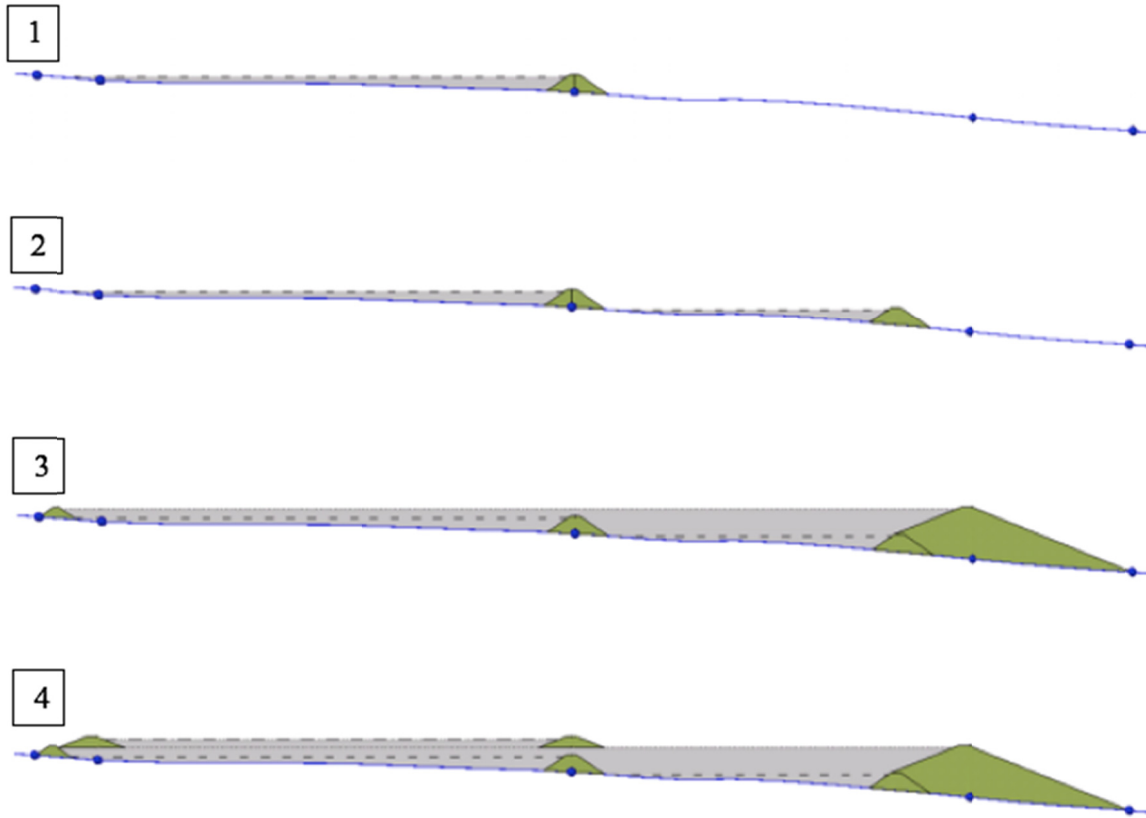


Figure 2.2 Construction Stages 1-4 of tailings embankments (from DICTUC [2012]).

3 GEER Investigations

The Las Palmas site was investigated by GEER personnel on 11 March 2010, with a follow-up visit on 28 March 2010 to collect LIDAR and *V**S* measurements. The reconnaissance team found the flow failure marked by a large scarp (Figures 3.1–3.3) and sand boils throughout the failed material (Figure 3.4) and other locations. Figure 3.5 shows the ground cracking and layered nature of the underlying tailings materials. The only eyewitnesses of the flow failure were killed; therefore, it is not known if the event was primarily co-seismic or post-seismic in nature. Because of the observed sand boils and the large distance of runout, the subsequent analysis assumed that this failure could be characterized as liquefaction initiation, followed by post-liquefaction flow-failure deformations that were not seismic-loading dependent.



Figure 3.1 Upper scarp of failed tailings impoundment looking southwest (from GEER [2010]).



Figure 3.2 Upper scarp of failed tailings impoundment looking northeast (from GEER [2010]).



Figure 3.3 Aerial photograph showing scarp, longitudinal cracks, and the location of the tailings dams (after DICTUC [2012] and Gebhart [2016]).



Figure 3.4 Sand-boil tailings along flow path (S35.18872, W71.75777) looking up towards the scarp is shown in Figures 3.2 and 3.3 (from GEER [2010]).



Figure 3.5 Gravelly cover layer over oxidized and unsaturated tailings, S35.184679 S, W71.759410 (from GEER [2010]).

LIDAR measurements of the failed slope were performed. The terrestrial LIDAR technique [three-dimensional (3D) laser scanning] consists of sending and receiving laser pulses to build a point file of 3D coordinates of the scanned surface. The time of travel for a single pulse reflection is measured along a known trajectory that computes the distance from the laser and the position of a point of interest. Using this methodology, data collection occurs at rates of thousands of points per second, generating a “point cloud” of 3D coordinates. LIDAR measurements were conducted by Dr. Rob Kayen as part of the reconnaissance efforts, and the point-cloud data was processed by the third author, Professor David Frost.

A laser scanner was used to conduct a tripod-mounted survey (Figure 3.6). Multiple scans were collected during each site survey to fill in “shadow zones” of locations not directly in the line-of-sight of the laser and to expand the range and density of the point data. Data were collected at a rate of 8000 points per second, scanning a range of 360° in the horizontal direction and 80° in the vertical direction. For all sites, a project coordinate system was used to register and reference multiple scan locations into one large project file. No global geo-referencing using differential GPS was performed. Scanning and registration were performed using Riscan-Pro. Point-cloud processing and surface modeling of the data was performed using I-SiTE software specifically designed to handle laser-scan data.

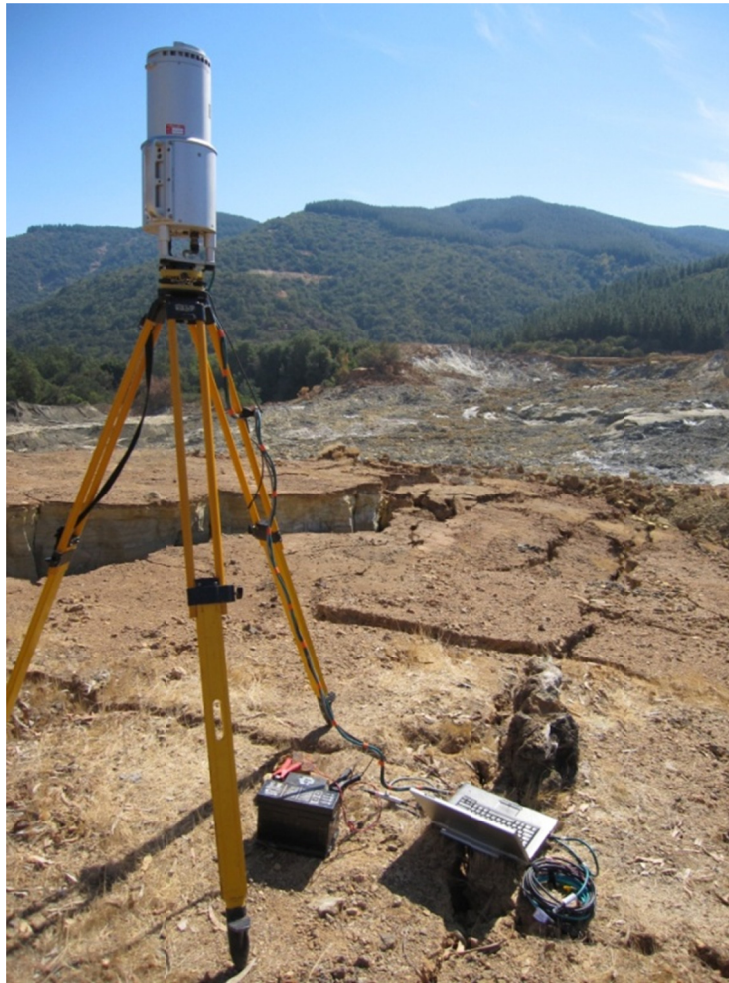


Figure 3.6 Terrestrial laser scanning with a Riegl z420 LIDAR unit at the Las Palmas Mine tailings dam failure. The system uses a PC for data acquisition and a car battery to power the laser (from GEER [2010]).

The registration of LIDAR data involves merging two, or more, individual scans data to form a single model of the reconnaissance site area, termed the “registration process.” A best fit translation and rotation registration process—using millions of points—aligns the overlapping data within a pair of point-cloud datascans.

Point data from each set of scans were subjected to a series of filters to remove non-ground surface and extraneous laser returns from the point clouds. Points reflected from vegetation and other non-ground conveyance features were manually cropped from each of the point clouds. Next, an isolated point filter was used to remove single-point instances occurring above the land surface. These isolated points are usually a result of reflections from moisture in the atmosphere. Topographic filters that select the lowest point in the point clouds were used to remove vegetation from point clouds. Here, the entire dataset was divided into 5 to 10 cm square bins, and only the lowest points within the bins were selected.

The final product of LIDAR data processing is 3D surface models. A linear interpolation method is used to process the surface models to generate surface edges of the triangular irregular network (TIN) facets between points. Triangular irregular network models represent a topographic surface of each area. After filtering, a TIN surface was generated from each scan file using either a spherical surface algorithm (curved facets) or a linear topographic algorithm (flat facets); see Figure 3.7.



Figure 3.7 Detailed LIDAR of head scarp of Las Palmas tailings dam failure (from GEER [2010]).

4 Litigation-Supported Field Investigations

In support of ongoing litigation concerning this flow failure, the fourth author (Professor Christian Ledezma) and colleagues performed field investigations to gather subsurface information on the failure material [DICTUC 2012]. Between June 2–26, 2011, they conducted geotechnical exploration including borings with SPT measurements. Five 4-in. diameter exploratory borings were advanced to depths ranging from 8.5–21.0 m (28–70 ft) below ground surface, typically terminating in the competent native material below the tailings. As indicated in Figure 4.1, these locations are within the non-displaced portion of the dam. Borings B-1 and B-5 were located within the containment embankments, and borings B-2, B-3, and B-4 were located within the tailings material. The drill rig was equipped with an automatic safety hammer to obtain blow counts, with an estimated efficiency of approximately 60%. Corrected ($N_{1,60}$) SPT blow counts for fine and coarse-grained materials were between single digits to the lower teens range: see Figure 4.2. The field crew encountered groundwater in four of five SPT borings at depths ranging from 5–13 m (17–43 ft) below the ground surface, which is thought to be not grossly dissimilar to the ground water present at the time of the earthquake. Vane shear testing was also performed in conjunction with some of the borings to measure the peak strength of the intact material (see Table 4.1). Subsequent laboratory testing was performed on samples acquired from the drilling operation. The following bore logs (Figures 4.3–4.7) and laboratory data (see Table 4.1) were compiled by Gebhart [2016] and used to guide subsequent investigations.

Table 4.1 Summary of field and lab data performed by DICTUC [2012]; from Gebhart [2016].

Location	Field Test	Location	Depth		Soil Type	Strength		Unit Wt. (pcf)		Fail Strain (%)	Lab Strength Testing			
			(m)	(ft)		Cohesion (psf)	Φ (°)	Total	Dry		CU	Cyclic Triaxial	UC	Sample Method
B-1	SPT	"Wall"	6-6.5	20	SM	800	26	100	95	5.5	X	-	-	Shelby
			16.0-16.5	54	ML	-	-	-	-	-	-	X	-	-
		Bedrock	18.5-19.25	62	SC-SM	7000	-	138	127	0.8	-	-	X	HQ3 cutting tip
			20.0-21.0	67	SC	19500	-	131	116	1	-	-	X	HQ3 cutting tip
	Vane Shear	"Wall"	5	17	SM	520	-	-	-	-	-	-	-	-
			7	23	SM	1486	-	-	-	-	-	-	-	-
9			30	SM	1486	-	-	-	-	-	-	-	-	
12			40	ML	520	-	-	-	-	-	-	-	-	
14			46	ML	632	-	-	-	-	-	-	-	-	
B-2	Vane Shear	"Bowl"	7	23	ML	780	-	-	-	-	-	-	-	
			13	43	ML	818	-	-	-	-	-	-	-	
B-3	Vane Shear	"Bowl"	5	17	ML	780	-	-	-	-	-	-	-	
			8	26	ML	502	-	-	-	-	-	-	-	
B-4	SPT	"Bowl"	-	-	-	-	-	-	-	-	-	-	-	
B-5	SPT	"Wall"	5.0-5.5	17	ML	5600	-	110	96	8.3	X	X	-	Undisturbed
			10.0-10.5	34	ML	-	-	-	-	-	-	X	-	-

CU: Consolidated Undrained
 UC: Unconfined Compressive

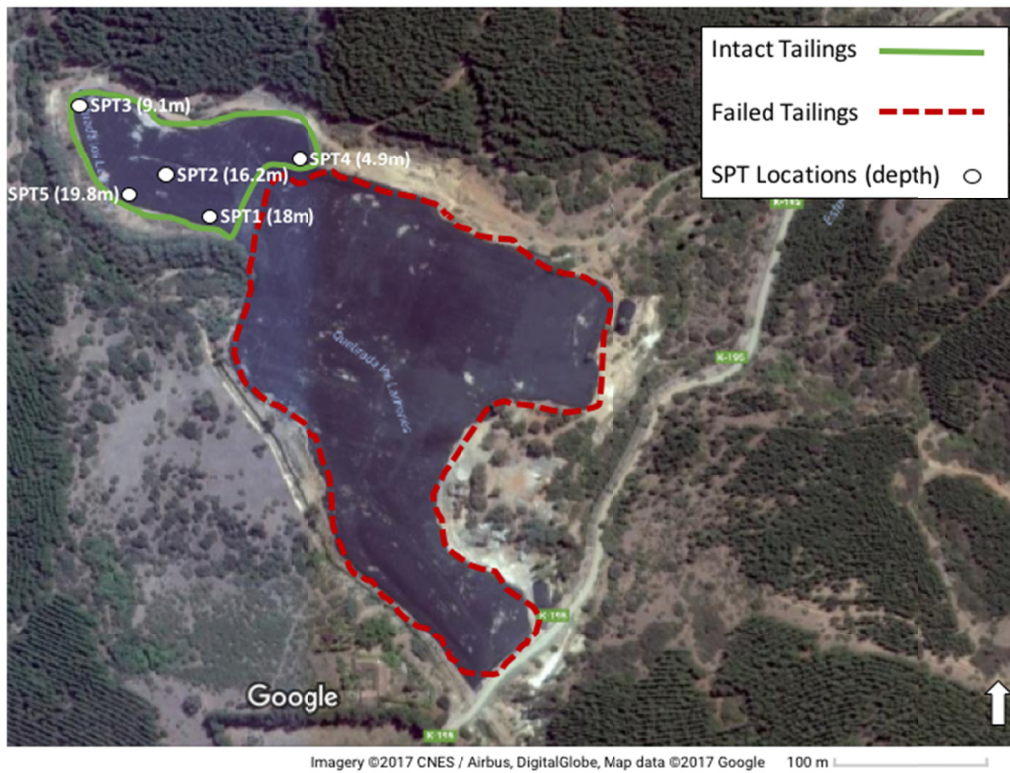


Figure 4.1 Location of SPT borings performed by DICTUC [2012], with the depth of each boring shown in parenthesis. The intact and failed material zones are delineated.

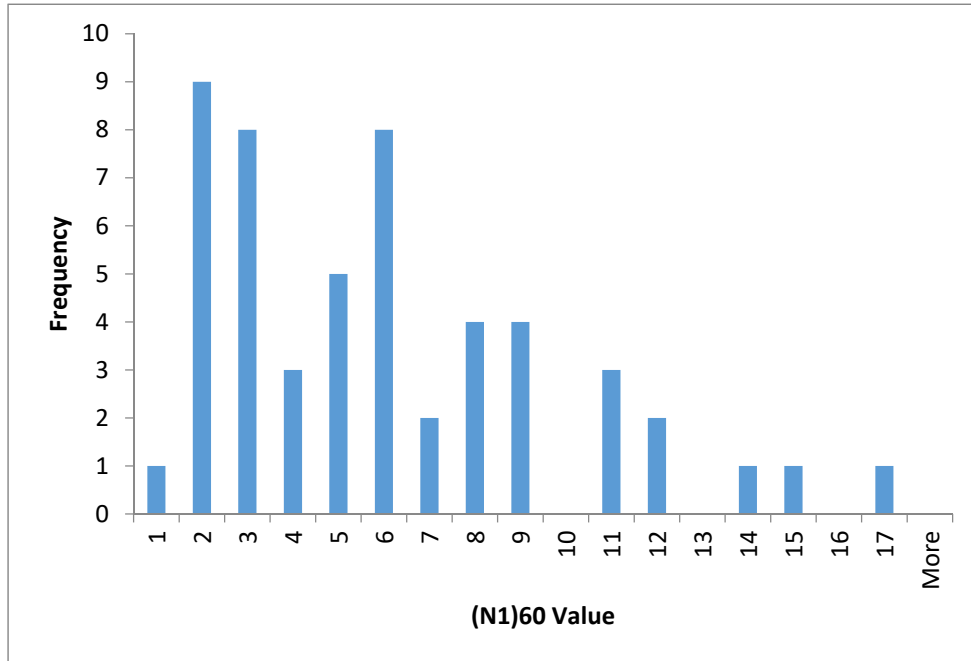


Figure 4.2 Histogram of corrected SPT blow counts, $(N_1)_{60}$, from the field investigations (from Gebhart [2016]).

PROJECT INFORMATION						DRILLING INFORMATION						
PROJECT: Las Palmas Tailings Dam						DRILL RIG:						
DRILLING LOCATION: Containment Wall						HOLE DIAMETER:						
DATE DRILLED:						SAMPLING METHOD:						
LOGGED BY:						HOLE ELEVATION:						
▼ Depth of Groundwater: 43 Feet						Boring Terminated At: 70 Feet						
DEPTH	SOIL DESCRIPTION	USCS	LITHOLOGY	SAMPLE	BLOWS/12 IN (N ₁) 60	FRICITION ANGLE, (degrees)	COHESION, C (psf)	WATER CONTENT (%)	MAXIMUM DRY DENSITY (pcf)	EXPANSION INDEX (EI)	FINES CONTENT (%)	PLASTICITY INDEX (PI)

0	SILTY SAND	SM			9	14		5-11%			35	NP
1					7	11			35			
2					11	16			33			
3					8	10			31			
4					4	4			31			
5					7	7			37			
6					9	8			43			
7					7	7			43			
8					6	6			43			
9					8	7			27			
10												
11												
12												
13												
14												
15												
16												
17												
18												
19												
20												
21												
22												
23												
24												
25												
26												
27												
28												
29												
30												
31	SANDY SILT:	ML			2	2		20-21%			77	2-4
32					6	4			77			
33					4	3			82.5			
34					4	3			82.5			
35					3	2			88			
36					5	3			77			
37					4	2			77			
38					3	2			65			
39					3	2			76			
40					2	1			76			
41												
42												
43												
44												
45												
46												
47												
48												
49												
50												
51												
52												
53												
54												
55												
56												
57												
58												
59												
60												
61	SILTY CLAYEY SAND: (BEDROCK)	SC-SM						8-13%				8-12
62					UC @							
63					62'							
64					UC @							
65					67'							
66												
67												
68												
69												
70												
71	BEDROCK	SC										
72												
73												
74												

Figure 4.3 Boring B1 performed by DICTUC [2012]; from Gebhart [2016].

PROJECT INFORMATION					DRILLING INFORMATION								
PROJECT: Las Palmas Tailings Dam					DRILL RIG:								
DRILLING LOCATION: Tailings					HOLE DIAMETER:								
DATE DRILLED:					SAMPLING METHOD:								
LOGGED BY:					HOLE ELEVATION:								
▼ Depth of Groundwater: 40 Feet					Boring Terminated At: 53 Feet								
DEPTH	SOIL DESCRIPTION	USCS	LITHOLOGY	SAMPLE	BLOWS/ 12 IN	(N ₁) 60	FRICITION ANGLE, (degrees)	COHESION, C (psf)	WATER CONTENT (%)	MAXIMUM DRY DENSITY (pcf)	EXPANSION INDEX (EI)	FINES CONTENT (%)	PLASTICITY INDEX (PI)

0	SANDY SILT	ML			8	12			12-32%			93	NP-4			
-1																
-2																
-3																
-4																
-5																
-6																
-7																
-8																
-9																
-10																
-11																
-12																
-13																
-14																
-15																
-16																
-17																
-18																
-19																
-20																
-21																
-22																
-23																
-24																
-25																
-26																
-27																
-28																
-29																
-30																
-31																
-32																
-33																
-34																
-35																
-36																
-37																
-38																
-39																
-40																
-41																
-42																
-43																
-44																
-45																
-46																
-47																
-48																
-49																
-50																
-51																
-52																
-53																
-54																
-55																

Figure 4.4 Boring B2 performed by DICTUC [2012]; from Gebhart [2016].

PROJECT INFORMATION					DRILLING INFORMATION								
PROJECT: Las Palmas Tailings Dam DRILLING LOCATION: Tailings DATE DRILLED: LOGGED BY:					DRILL RIG: HOLE DIAMETER: SAMPLING METHOD: HOLE ELEVATION:								
▼ Depth of Groundwater: 20 Feet					Boring Terminated At: 30 Feet								
DEPTH	SOIL DESCRIPTION	USCS	LITHOLOGY	SAMPLE	BLOWS/ 12 IN	(N ₁) 60	FRICITION ANGLE, (degrees)	COHESION, C (psf)	WATER CONTENT (%)	MAXIMUM DRY DENSITY (pcf)	EXPANSION INDEX (EI)	FINES CONTENT (%)	PLASTICITY INDEX (PI)

0	SANDY SILT	ML			10	15			5-19%				NP			
-1																
-2																
-3																
-4																
-5									7	11						83
-6																
-7																
-8																
-9									5	6						79
-10																
-11																
-12					6	6						76				
-13																
-14																
-15					5	5						90				
-16																
-17																
-18																
-19																
-20					2	2						81				
-21																
-22																
-23																
-24					10	9						75				
-25																
-26																
-27																
-28																
-29					7	6						73				
-30																

Figure 4.5 Boring B3 performed by DICTUC [2012]; from Gebhart [2016].

PROJECT INFORMATION						DRILLING INFORMATION							
PROJECT: Las Palmas Tailings Dam						DRILL RIG:							
DRILLING LOCATION: Tailings						HOLE DIAMETER:							
DATE DRILLED:						SAMPLING METHOD:							
LOGGED BY:						HOLE ELEVATION:							
▼ Depth of Groundwater: 17 Feet						Boring Terminated At: 28 Feet							
DEPTH	SOIL DESCRIPTION	USCS	LITHOLOGY	SAMPLE	BLOWS/12 IN	(N ₁) ₆₀	FRICION ANGLE, (degrees)	COHESION, C (psf)	WATER CONTENT (%)	MAXIMUM DRY DENSITY (pcf)	EXPANSION INDEX (EI)	FINES CONTENT (%)	PLASTICITY INDEX (PI)

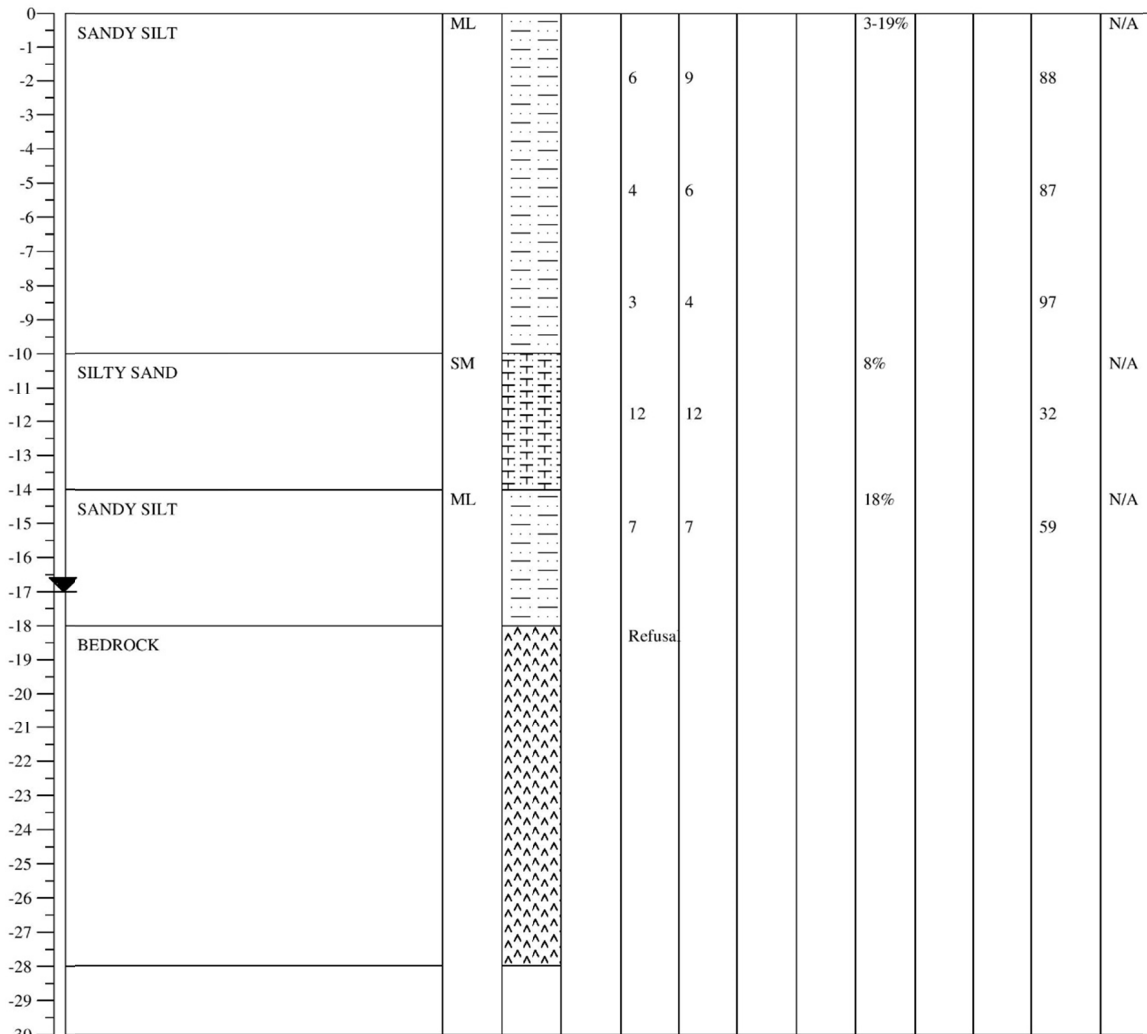


Figure 4.6 Boring B4 performed by DICTUC [2012]; from Gebhart [2016].

PROJECT INFORMATION					DRILLING INFORMATION								
PROJECT: Las Palmas Tailings Dam DRILLING LOCATION: Containment Wall DATE DRILLED: LOGGED BY:					DRILL RIG: HOLE DIAMETER: SAMPLING METHOD: HOLE ELEVATION:								
▼ Depth of Groundwater: Not Encountered					Boring Terminated At: 65 Feet								
DEPTH	SOIL DESCRIPTION	USCS	LITHOLOGY	SAMPLE	BLOWS/12 IN	(N) 60	FRICITION ANGLE, (degrees)	COHESION, C (psf)	WATER CONTENT (%)	MAXIMUM DRY DENSITY (pcf)	EXPANSION INDEX (EI)	FINES CONTENT (%)	PLASTICITY INDEX (PI)

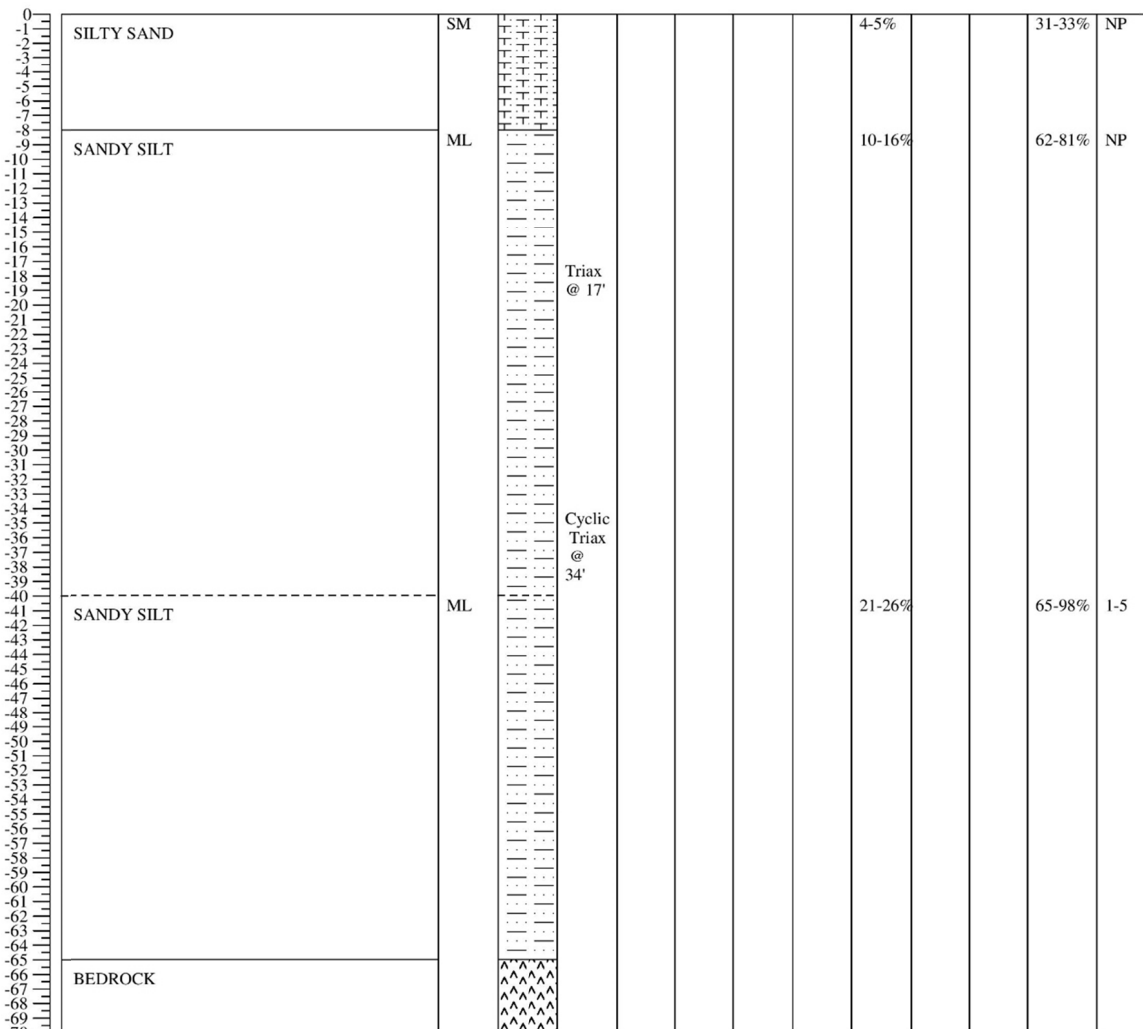


Figure 4.7 Boring B5 performed by DICTUC [2012]; from Gebhart [2016].

5 PEER NGL-Funded Investigations

The field investigations funded by PEER–NGL occurred over the time frame of 2017 June 20–23. The goal was to augment the existing SPT measurements with CPT and surface-wave measurements. Participants in the field investigations included the four authors of this report.

An initial site visit was conducted on June 20th. The CPT equipment was subsequently mobilized for three full days of field testing and included a portable CPT “ramset” (Figure 5.1), which is deployable in locations not accessible by typical CPT trucks, and a geophysical array of twelve geophones and accompanying seismograph for performing passive surface-wave measurements. Three CPT soundings were performed per ASTM 5778; the locations are shown in Figure 5.2, two of which were collocated with the SPT measurements.



Figure 5.1 Portable “ramset” mobilized for Las Palmas field investigations because of the difficult access conditions. The reaction weight was provided by water tanks and truck. The ramset is the white hydraulic jack in the middle. The black box with orange cord to the right is the hydraulic pump.

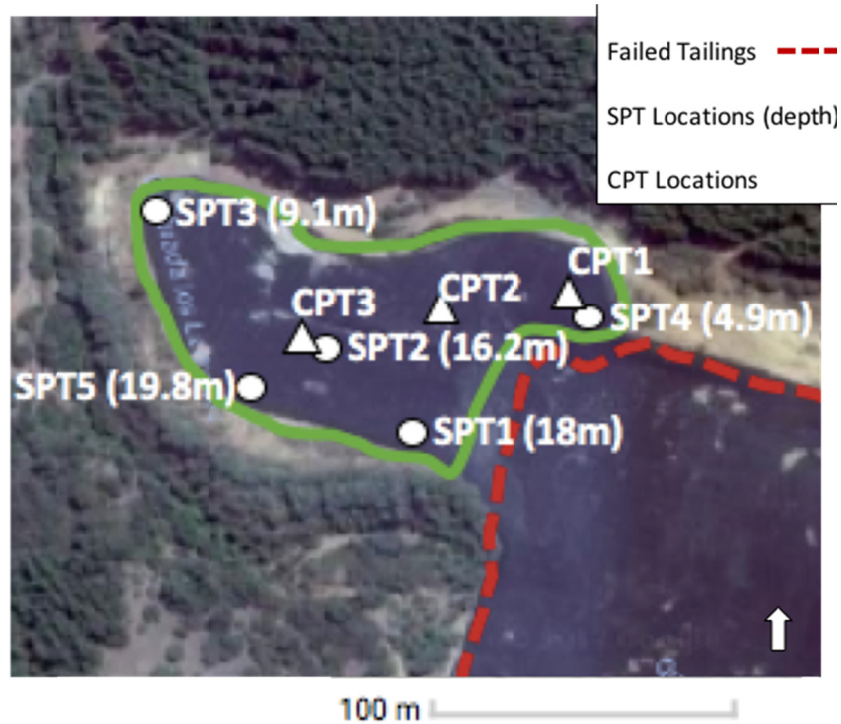


Figure 5.2 Location of CPT soundings with respect to prior SPT borings.

Passive surface-wave measurements were made using circular arrays of twelve 4.5 Hz vertical geophones (Figure 4.10). The locations of the passive measurements are shown in Figure 4.11. G1, G2, and G3 were collocated with the CPT measurements in the intact tailings. G5 and G6 were collocated in the failed portion of the tailings, where G5 was located in the flow failure and G6 in an intact block that was transported in the flow failure. The diameters of the arrays were 5 m, 10 m, and 20 m (16.40 ft, 32.81 ft, and 49.21 ft, respectively) fm, depending on the depth and resolution required. Recordings were made at a 2 m/sec sampling rate for 32 sec, with 10 of these recordings made for each array and concatenated for processing. Different array diameters were combined into single dispersion curves in those cases when it provided clearer resolution. Dispersion curves were arrived at using SPAC [Aki 1957] as coded in Geogiga Surface Plus [Geogiga 2017]. Dispersion curve picking and shear-wave velocity profile fittings were performed within Geogiga. To minimize interpretation uncertainty given the lack of prior knowledge of the stratigraphy, layering within a V/S profile was typically limited to three layers. The estimated shear-wave velocity profiles are shown in Figures 5.8–5.13, with a nominal coefficient of variation of 10% [Moss 2008]. The dispersion curve picks and profile fitting details are provided in the Appendix. Table 5.1 shows how the SPT, CPT, and V/S measurements are co-located with respect to each other.

Figures 5.5–5.7 show the results of the CPT, and Figures 5.8–5.13 shown the V/S data collected at the site. The CPT data was collected and processed by LMMG Geotecnia Limitada. The V/S data was collected and processed by the first author. Full reporting of the CPT and V/S measurements can be found in the Appendix.

Table 5.1 Showing co-location of different field tests.

CPT	VS	SPT	Coordinates
CPT1	G1	SPT4	S35.184242 W71.759540
CPT2	G2		S35.184297 W71.760284
CPT3	G3	SPT2	S35.184350 W71761197
		SPT1	
		SPT3	
		SPT5	
	G5		S35.185729 W71.758658
	G6		S35.186669 W71.758161



Figure 5.3 Shown is a 10-m circular array at location G5. Passive measurements were made of ambient noise from a generator, foot falls, etc.

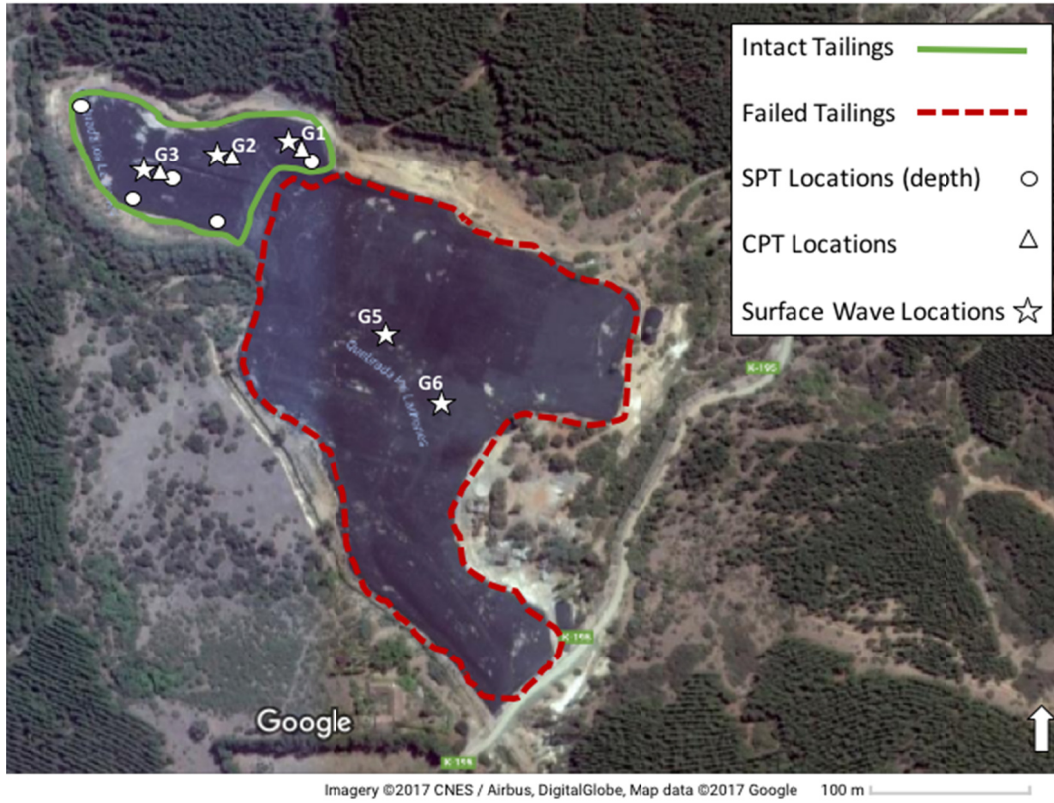


Figure 5.4 Locations of passive circular array measurements with respect to CPT soundings and SPT borings.

Project:

Location:

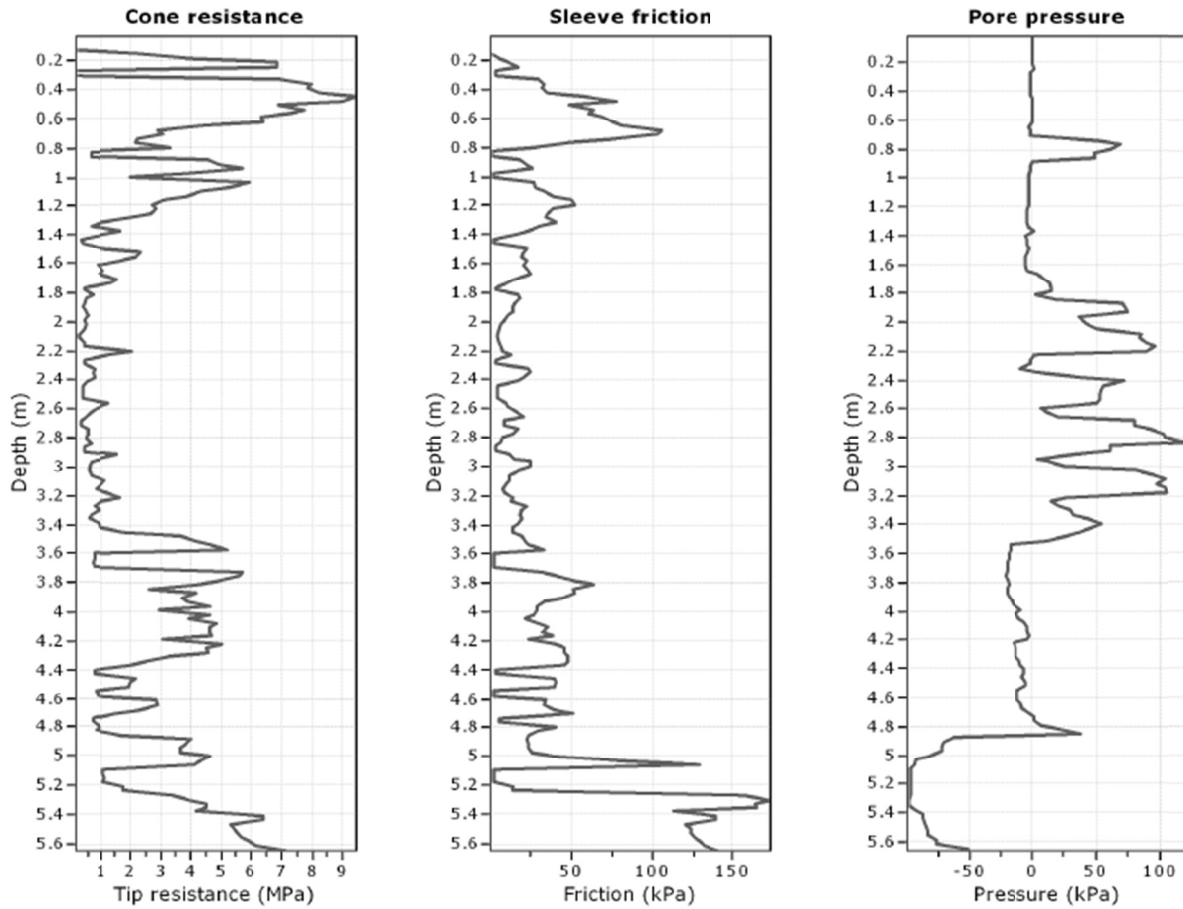


Figure 5.5 CPT1 cone tip, sleeve, and pore pressure measurements. Location S35.184242 W71.759540; elevation ~155 m.

Project:
Location:

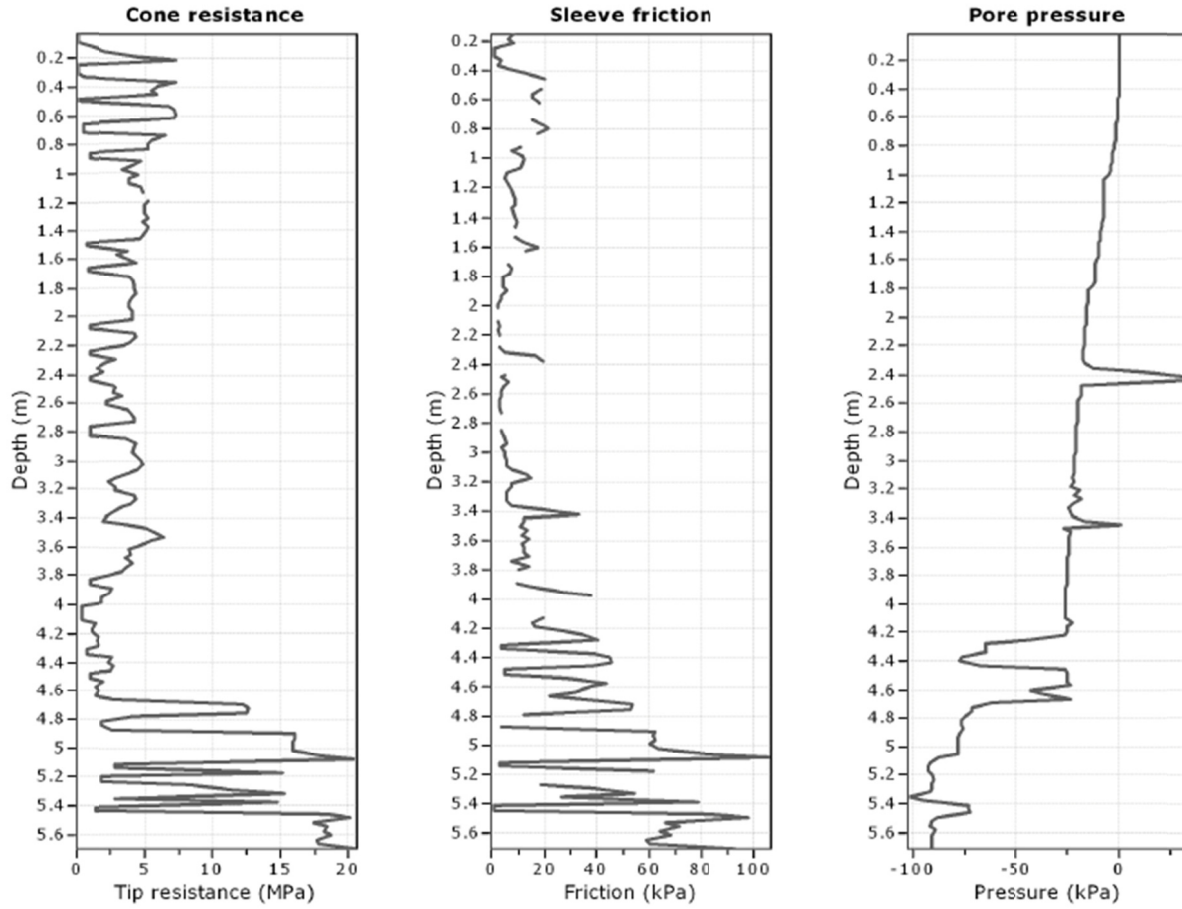


Figure 5.6 CPT2 cone tip, sleeve, and pore pressure measurements. Location S35.184297 W71.760284; elevation ~155 m.

Project:
Location:

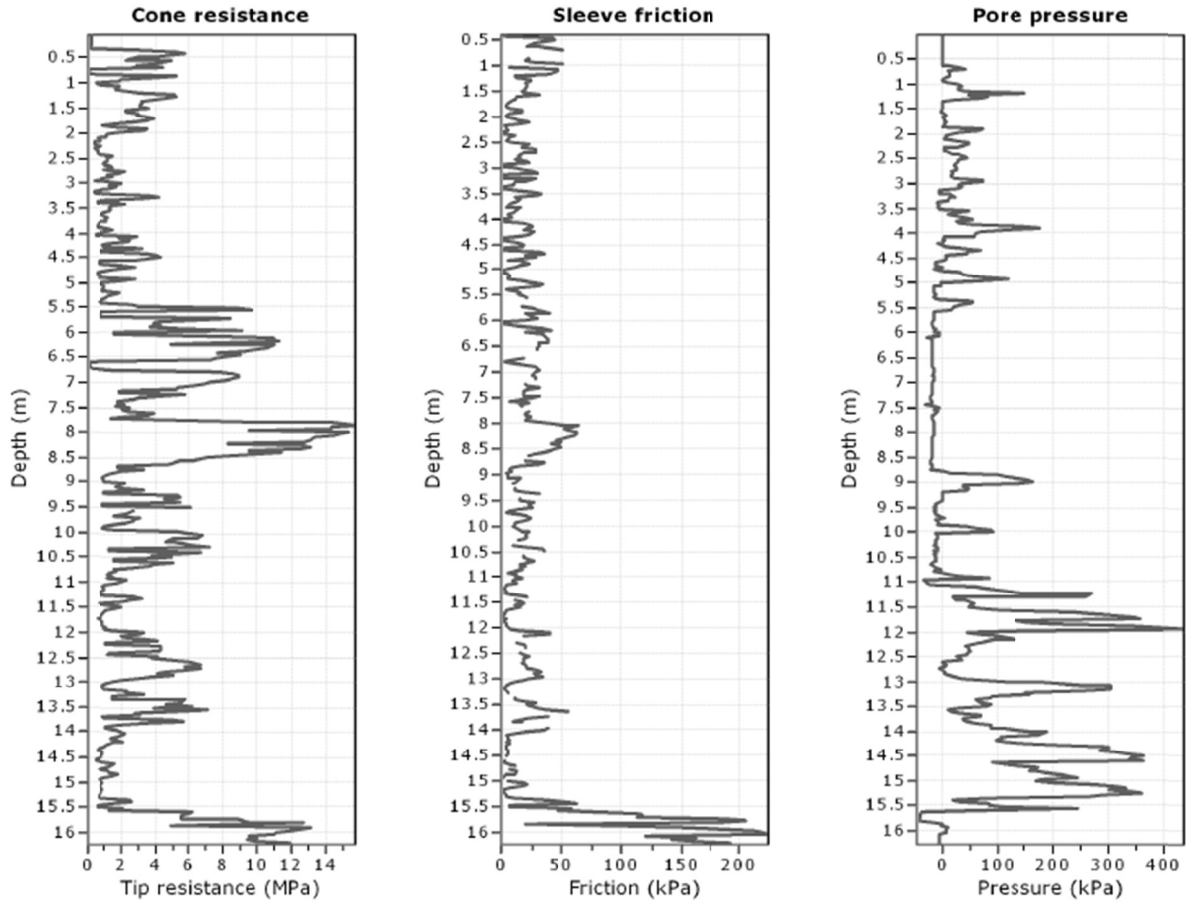


Figure 5.7 CPT3 cone tip, sleeve, and pore pressure measurements. Location S35.184350 W71.761197; elevation ~153 m.

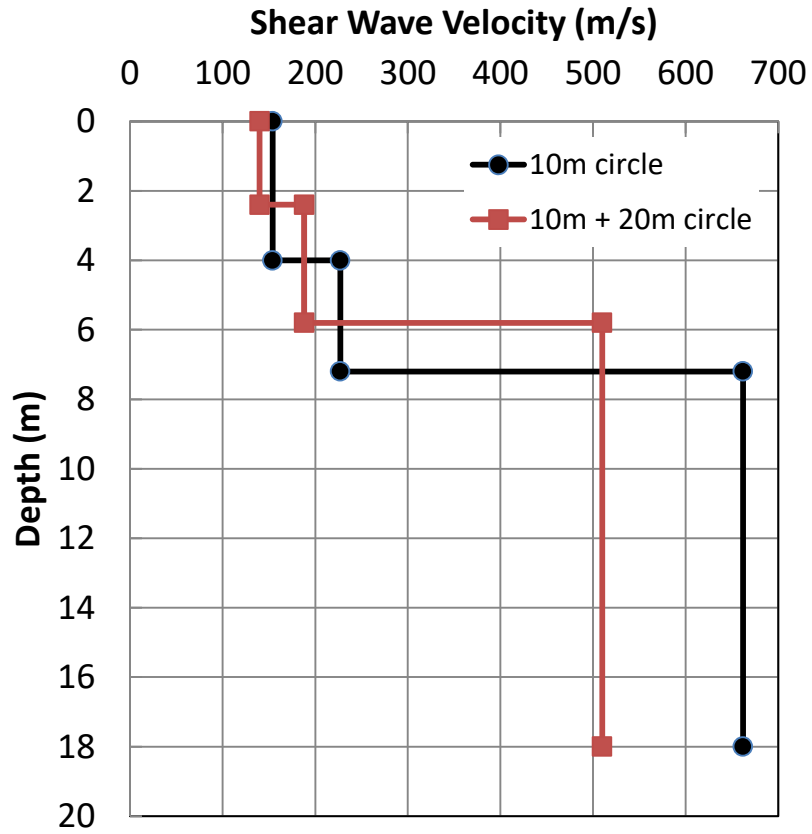


Figure 5.8 Location G1 VS measurements. Location S35.184242 W71.759540; elevation ~155 m.

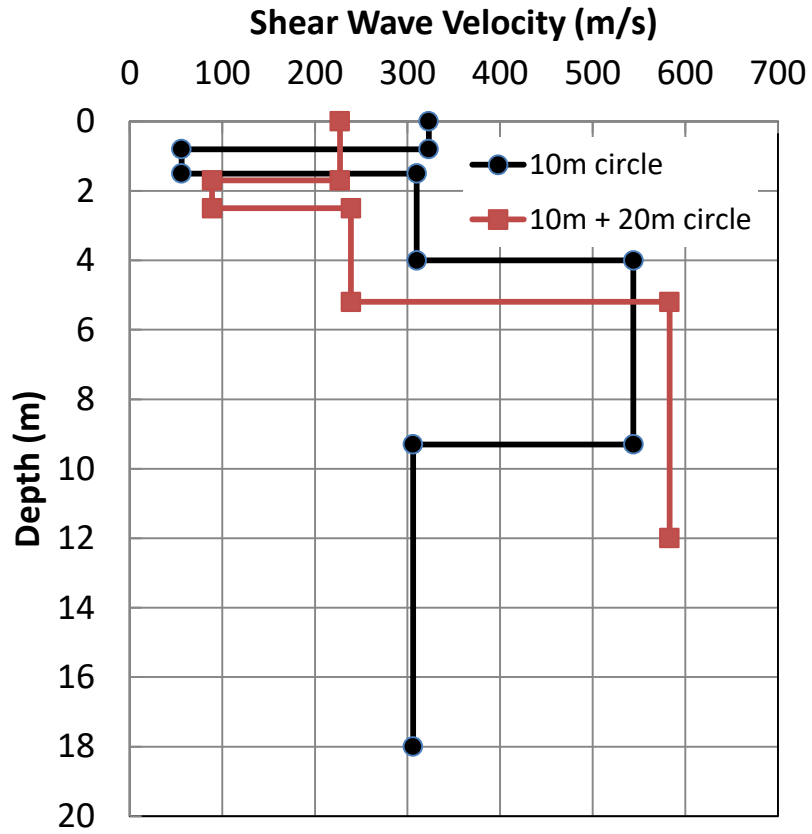


Figure 5.9 Location G2 VS measurements. Location S35.184297 W71.760284; elevation ~155 m.

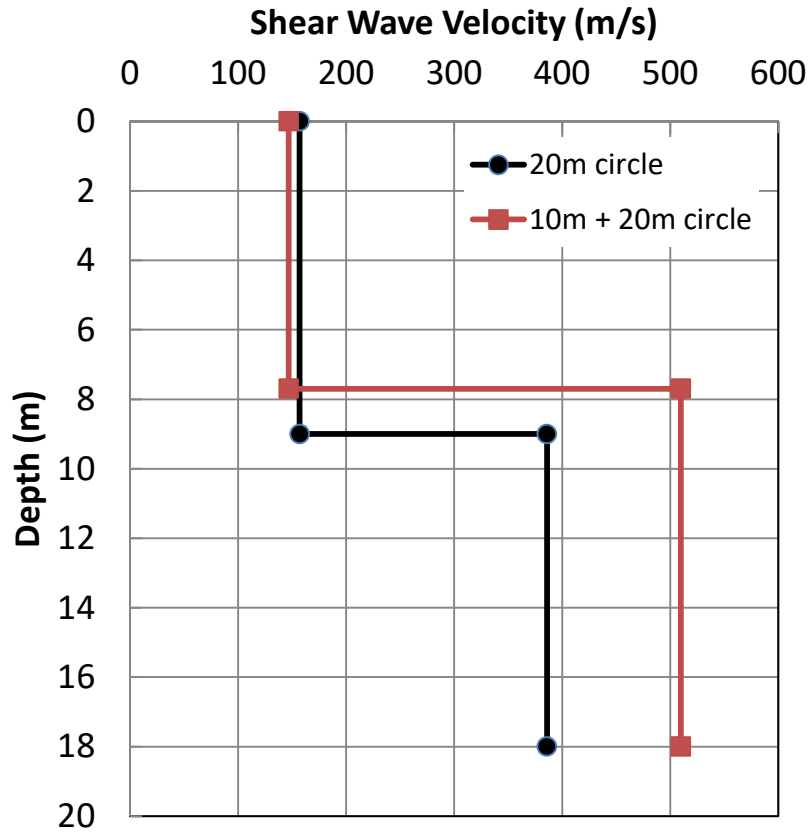


Figure 5.10 Location G3 VS measurements. Location S35.184350 W71.761197; elevation ~153 m.

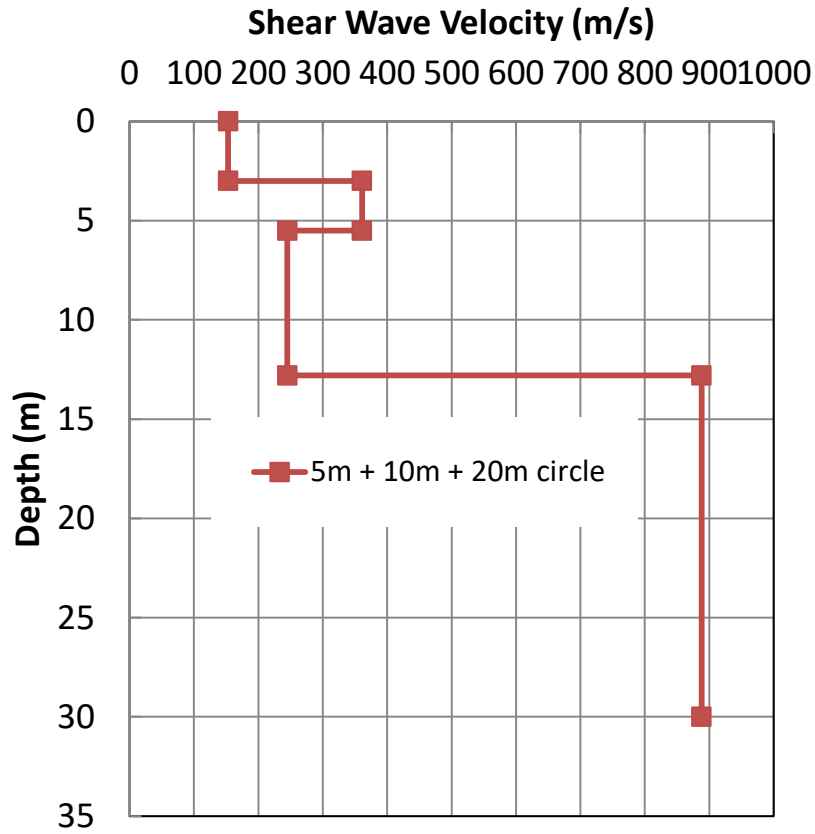


Figure 5.11 Location G5 VS measurements of flow slide material. Location S35.185729 W71.758658; elevation ~140 m.

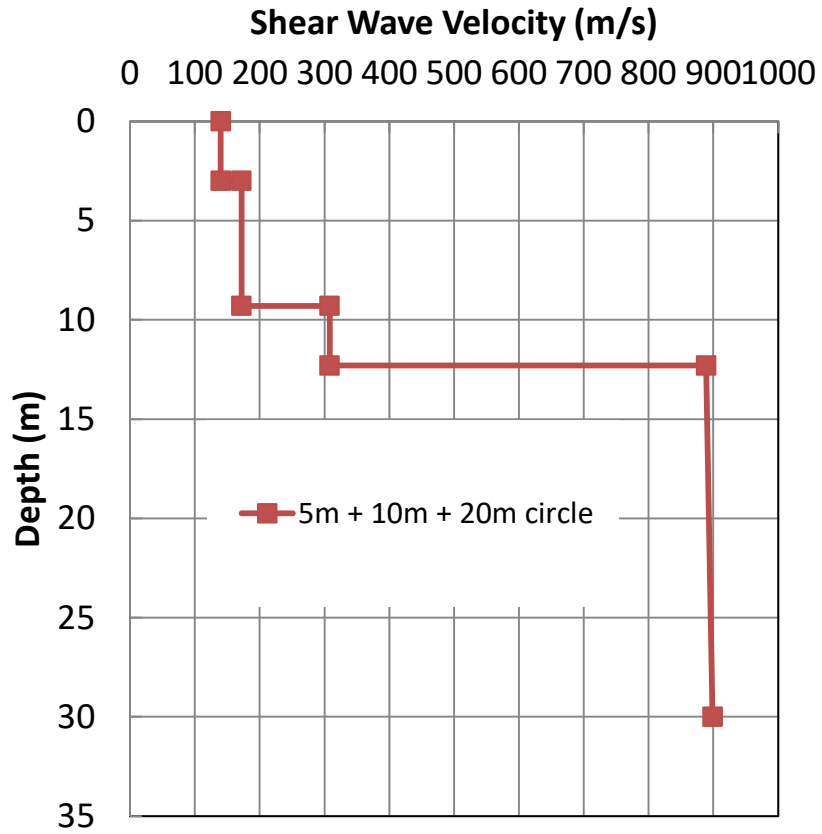


Figure 5.12 Location G6 VS measurements of translated block material. Location S35.186669 W71.758161; elevation ~134 m.

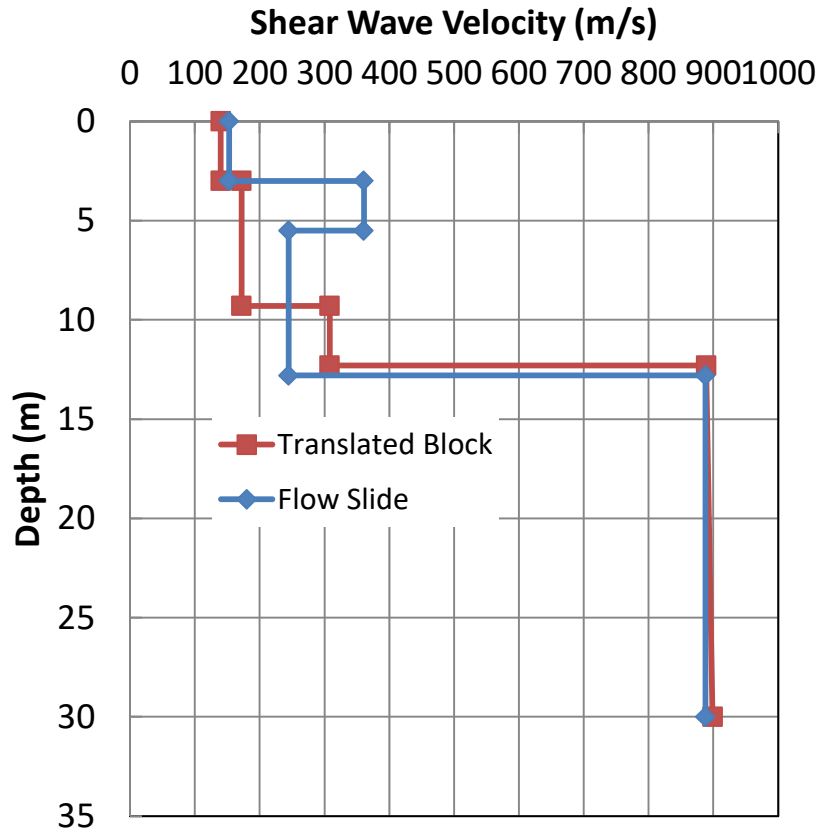


Figure 5.13 Comparison of G5 and G6 VS measurements.

6 Back-Analysis of Residual Strength

This section presents a back-analysis of the flow failure to estimate the residual strength of the liquefied material. A full description of this analysis and the details can be found in Gebhart [2016]. The strong ground shaking from the 2010 event resulted in liquefaction of some portion of the tailings material. The liquefied flow failure took two paths: an easterly and southerly direction. The leading edge of the easterly flow traveled approximately 165 m (540 ft), whereas the southerly flow traveled roughly 350 m (1150 ft). Based on the failed geometry plan view and the depth of the failed material, a total of approximately 231,660 m³ (303,000 yards³) of material displaced in roughly two equal halves; see Figure 6.1. The flow failure debris was approximately 1.5-4.0 m (5-13 ft) thick in some locations.

Boring logs indicate groundwater was located between depths of 5–13 m (17–43 ft) below the ground surface across the undisturbed portion of the tailings. This ground water table at the time of drilling is considered roughly representative of the ground water table at the time of the earthquake. This was corroborated by the location of seepage exiting the exposed failure slope in reconnaissance observations. Sand boils were also observed in numerous locations (Figure 6.2) throughout the failed mass, indicating saturated conditions of that material during failure.

Development of pre- and post-failure, 2D and 3D models of the Las Palmas tailings dam used AutoCAD Civil 3D (Auto Desk) and Slope/W (Geo-Slope International) was undertaken. These models considered:

- 2D and 3D detailed modeling of the wall geometry used for earthwork quantities
- Flow failure runout length estimation
- Creation of tailings dam cross sections
- Static and pseudo-static slope stability analysis

Pre-failure geometry was estimated using as-built information, aerial images, and existing intact embankments as a guide. Post-failure geometry is based on aerial images of the failed mass. The pre-and post-failure geometries were then used for “time” stepping from the beginning to the end of the failure event, mapping the change in geometry following the incremental momentum methodology (IMM) presented in Weber et al. [2015]. An initial intact slope cross-section area of approximately 33,000 ft² (3065 m²) is stepped through progressively more failed

slope geometries converging on the final failed slope cross-section area of approximately 12,000 ft² (1115 m²). This also applies to advancement of the toe of the slope, with displacement constrained to converge on a final observed displacement of approximately 165 m (540 ft). This yields an initial set of “time” steps that were treated as linear between each step because of the lack of prior knowledge.

The mass-property function of AutoCAD was used to calculate the centroid of mass for each step. This helped establish linear trends with respect to the following: (1) area loss and (2) centroid displacement of the failed mass. This process is iterative and requires repeated adjustment of cross-section geometry to converge upon a final solution. A typical step sequence for fully liquefied material can be seen in Figure 6.3. A similar analysis was performed for the situation where a weak layer liquefied, causing blocks of intact material to be carried downslope in the flow.

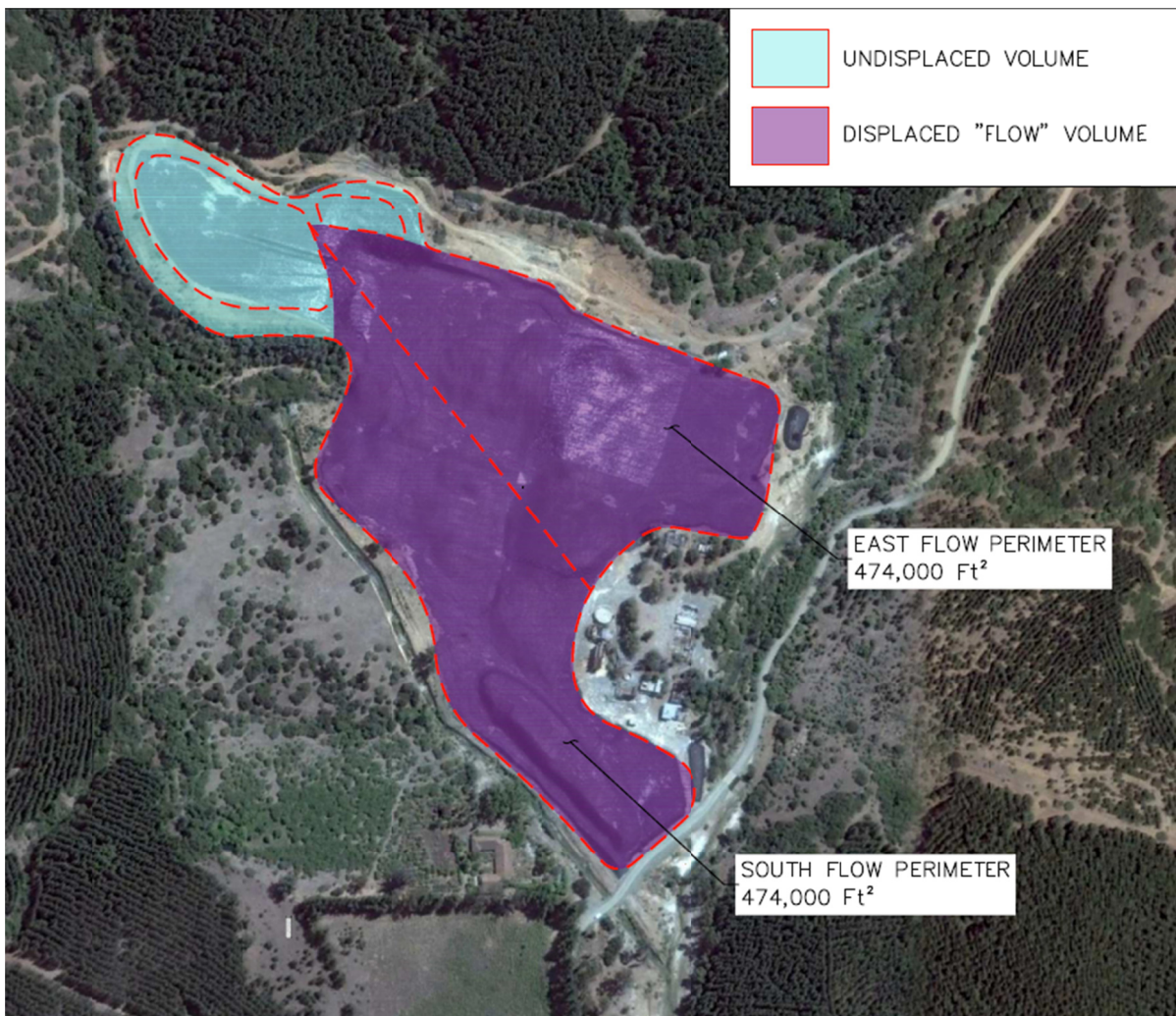


Figure 6.1 Marked image showing flow failure runout following two directions, east and south (from Gebhart [2016]).



Figure 6.2 Evidence of sand boils in the flow-failure debris (from GEER [2010]).

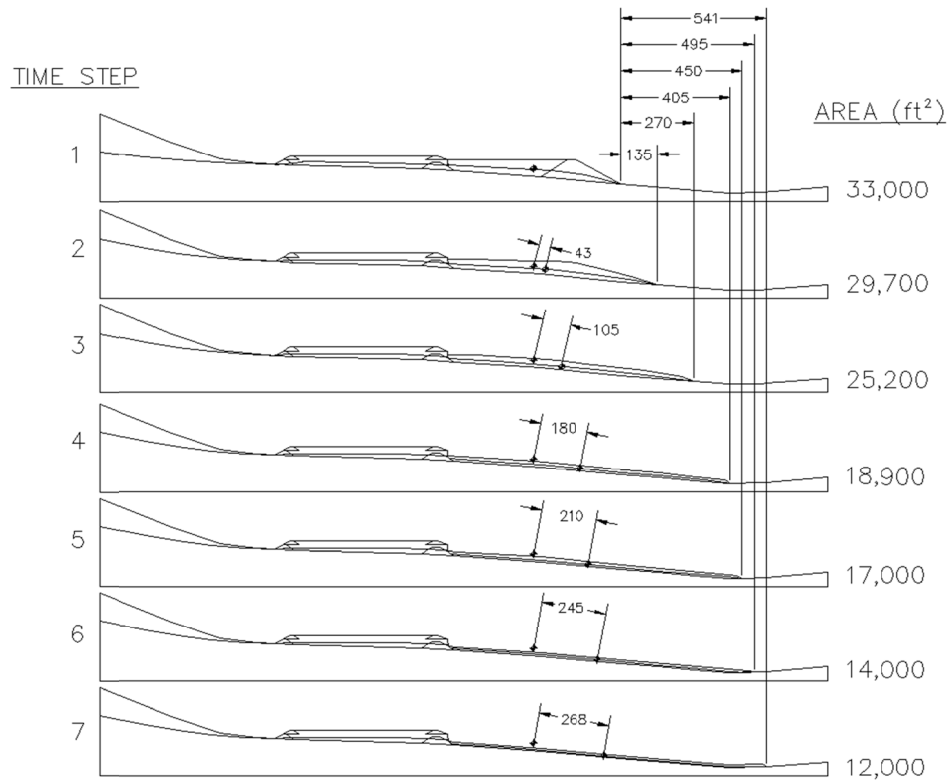


Figure 6.3 Modeled slope failure progression sequence in AutoCAD (from Gebhart [2016]).

The material properties used in the Slope/W model, which were based on the subsurface drilling investigations and IMM back-analysis, are shown in Table 6.1. The Morgenstern and Price method was used to solve the limit equilibrium problem with a pre-defined slip surface; see Figure 6.4.

The average of pre- and post-failure strengths are approximated for an initial run. This strength value is used for each step to execute a series of static LEM slope stability analyses without seismic effects. Slope/W produces the following output for further IMM analysis: driving force, resisting force, slide area, slide weight, and factor of safety.

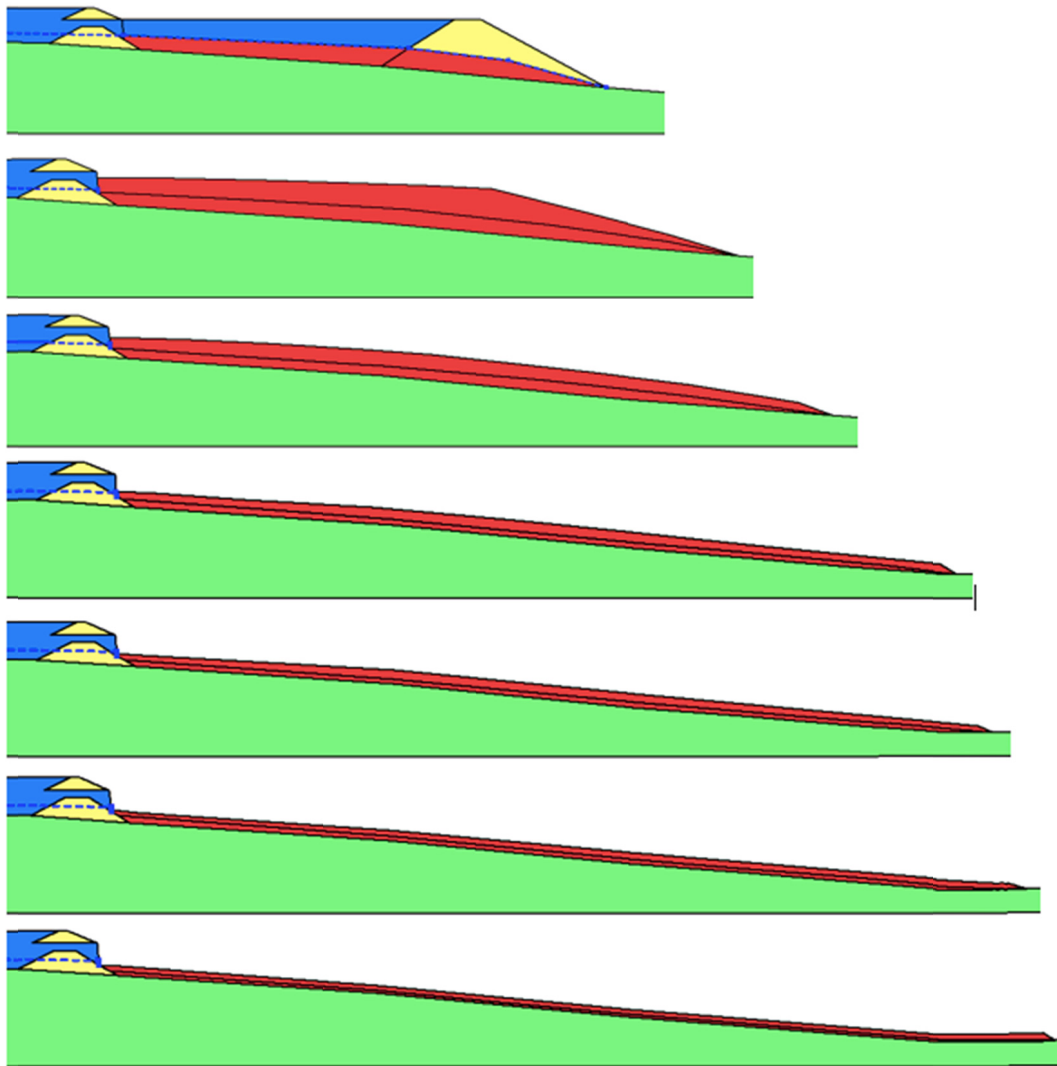


Figure 6.4 Modeled slope failure progression sequence in Slope/W (from Gebhart [2016]).

Table 6.1 Summary of materials and properties used in modeling the tailings failure.

Material type	Condition	Φ (°)	Cohesion (psf)	Unit Wt. (pcf)
Competent Native Material	-	(Unyielding)	(Unyielding)	(Unyielding)
Containment Walls	-	26	500	100
Non-Liquefied / Unsaturated Tailings	Undrained	0	500	95
	Drained	21	0	95
Liquefied / Saturated Tailings	-	0	(Varies)	100

A series of iterative calculations are performed, then the slide mass displacement for each step is calculated. This IMM process follows Newton’s second law of physics, rearranged to solve for acceleration as a function of the calculated force and calculated mass for each individual step:

$$a = F / m = F / (w / g) \tag{6.1}$$

where w is the weight of slide mass, g is gravity, and F is the net force, which equals the driving force–resisting force

Velocity is estimated through integration of the calculated acceleration; subsequently, displacement is determined through integration of the velocity function, both using the trapezoidal rule. These three parameters (acceleration, velocity, and displacement) are functions of time and are plotted on the y -axis; see Figure 6.5.

The parameter time (t) is estimated through the goal seek function in Excel and plotted on the x -axis. To accomplish this, a time value is selected to integrate each function (in order: acceleration, velocity, displacement) yielding a displacement of known value for each individual step. Each step is converged before proceeding to the next. This procedure is performed through all (7) steps, to converge on a final velocity of zero and the known final displacement.

The input residual strength is systematically changed, and the procedure repeated for each step in the analysis. Too large a residual strength value results in a premature reduction in velocity to zero and too small of a displacement; too small a residual strength value produces the opposite. The value best satisfying the final boundary conditions of zero velocity and known displacement represents the estimated post-liquefaction residual strength mobilized within the displaced mass. All of these analyses considered two possible failure modes: full-flow failure and layered liquefaction failure. As shown in Figures 6.3 and 6.4, full-flow failure is where the entire mass of the tailings liquefied. Layered liquefaction failure is where the weakest layer (as identified in the subsurface investigations)—which also “daylights” along the face of the slope—liquefied and carried block of intact material along with it downslope.

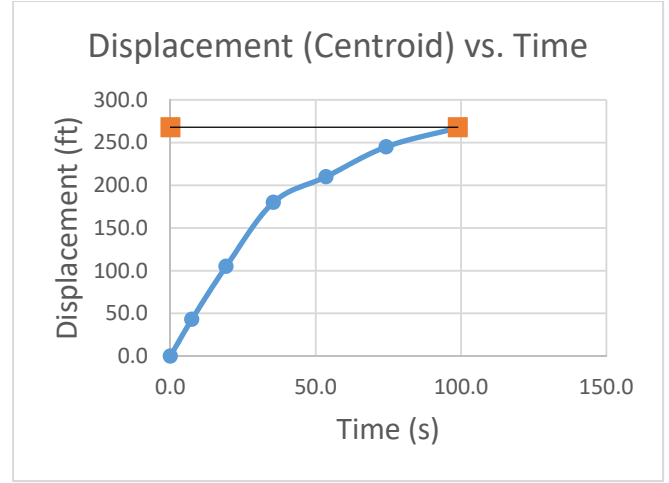
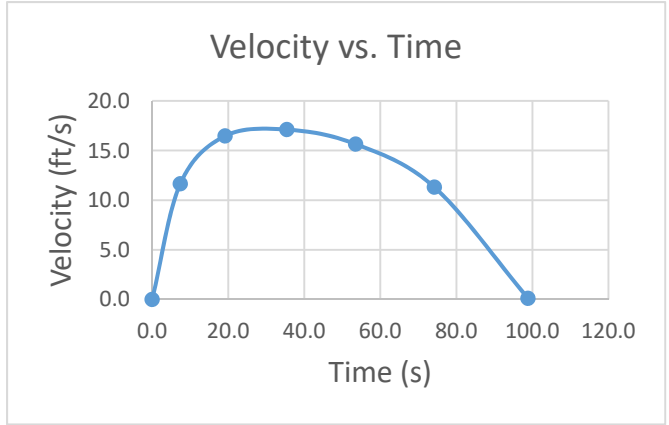
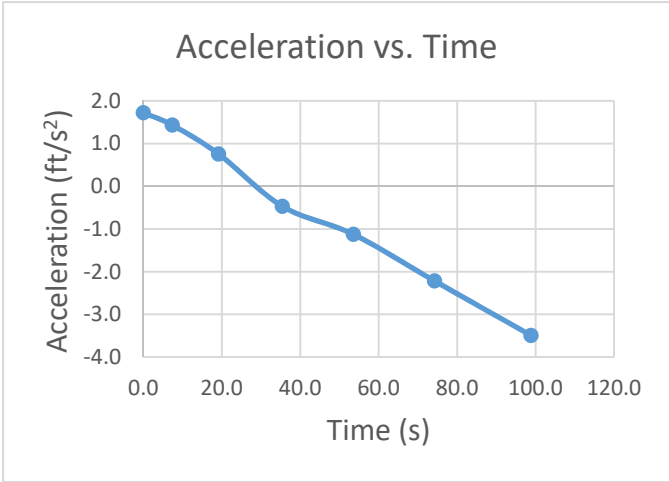


Figure 6.5 Example trial of incremental momentum method (IMM) after Weber [2015].

7 Comprehensive Results

The results in this report fall into three categories;

1. Resistance measurements representative of the pre-failure conditions of the material that liquefied and produced the flow failure;
2. Residual strength estimates of the liquefied material; and
3. Effective stress estimates of the pre-failure conditions at the depth of failure.

7.1 RESISTANCE MEASUREMENTS

Selection of a representative penetration resistance value of the Las Palmas dam for establishing post-liquefaction strength predictive correlations considered blow counts within what is interpreted as the saturated portion of the tailings material. Blow counts were corrected for factors related to overburden pressure and fines content; see Figure 7.1. Fines correction was per Equations (7.1) and (7.2) put forth by Cetin et al. [2004] to transform SPT $N_{1,60}$ values to $N_{1,60,CS}$ values. This fines correction accounted for two factors: (1) increased resistance to liquefaction as a function of fines content; and (2) adjustment of blow counts as a function of granular and fine grain material *in situ* resistance.

$$N_{1,60,CS} = N_{1,60} \times C_{fines} \quad (7.1)$$

$$C_{fines} = (1 + 0.004 \times FC) + 0.05 \times (FC / N_{1,60}) \quad (7.2)$$

In these equations, FC = percent fines content (by dry weight) expressed in percent (e.g., 20% fines is represented as $FC = 20.0$). Fines content less than 5% are represented as $FC = 0$, and fines content exceeding 35% are represented as $FC = 35.0$.

The averaged blow counts from the SPT measurements of intact material representative of liquefiable flow failure tailings were estimated at $N_{1,60} \approx 2.5$ and $N_{1,60,CS} \approx 5$ (Figure 6.6), with an estimated coefficient of variation of 25% [Kulhawy and Mayne 1990].

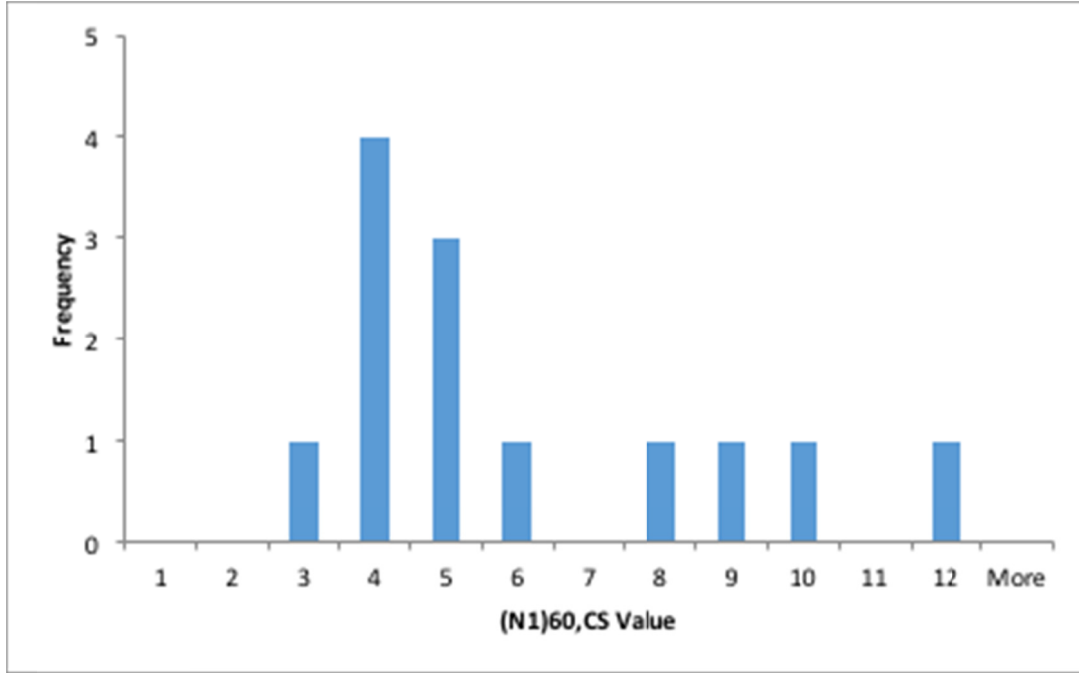


Figure 7.1 Histogram of blow counts in saturated tailings material, with fines correction (borings B-2, 3, and 4).

For the CPT, overburden corrections were performed using the equation below to arrive at q_{c1} and also corrected with the subsequent equation to arrive at the dimensionless Q_{tn} [Robertson and Cabal 2015].

$$q_{c1} = q_c \cdot (P_a / \sigma'_v)^n \quad q_{c1} = q_c \cdot (P_a / \sigma'_v)^n \quad (7.3)$$

where q_{c1} is the overburden stress normalized tip resistance (MPa); q_c is the raw tip resistance; P_a is one atmosphere of pressure ≈ 100 kPa – 0.1 MPa; σ'_v is the vertical effective stress (kPa); and n is the normalization exponent ≈ 0.5 .

Although the normalization exponent varies by soil type and stress conditions, a median value of 0.5 is typical for young normally consolidated sandy soils [Moss et al. 2006].

$$Q_{tn} \left[(q_t - \sigma_v) / P_a \right] \cdot (P_a / \sigma'_v)^n \quad (7.4)$$

where $q_t = q_c + u(1-a)$ is the pore pressure corrected tip resistance; u is the pore pressure measurement at the u_2 position; a is the cone factor ≈ 0.8 (typical for Gregg drilling cones; and σ_v is the vertical total stress (kPa).

The VS values have been overburden corrected (VS_1) for Holocene sands using the equation below, which uses a typical median normalization exponent of $n = 0.25$ [Andrus and Stokoe 2000].

$$VS_1 = VS \cdot (P_a / \sigma'_v)^n \quad (7.5)$$

The processed cone measurements are shown in Figures 7.2–7.4. Water table depths at the time of the measurements were estimated based on the pore pressure measurements and are shown in the figures with a triangle. The depth ranges thought to represent potentially liquefiable material with continuous stretches of low normalized penetration resistance are boxed. The histograms of the boxed regions are shown below each figure. CPT1 was located closest to the scarp where the material failed, CPT2 was positioned to intercept wall material, and CPT3 was located near the thickest portion of ponded tailings material.

Table 7.1 shows the stress normalized shear-wave velocity for the “weak” layers of the profiles measured. G2 was omitted because it appears to be non-liquefiable based on the CPT and VS profiles. Based on analysis of the normalized CPT and VS measurements, it appears the CPT3 and G3 are the most representative of intact material that resulted in flow failure in the unrestrained portion of the tailings. The interpreted measurements for this case history are then; $q_{c1} \sim 1.3$ MPa ($Q_m \sim 11.7$) and $VS_1 \sim 172$ m/sec, with an estimated coefficient of variation of 10% for the CPT [Kulhawy and Mayne 1990] and the same for VS [Moss 2008].

Table 7.1 Shear-wave velocity of "weak" layers for each profile.

Profile	Depth range (m)	Average VS_1 (m/sec)
G1	0 to 5	211
G2	na	na
G3	0 to 8	172
G5	0 to 3	222
G6	3 to 9	175

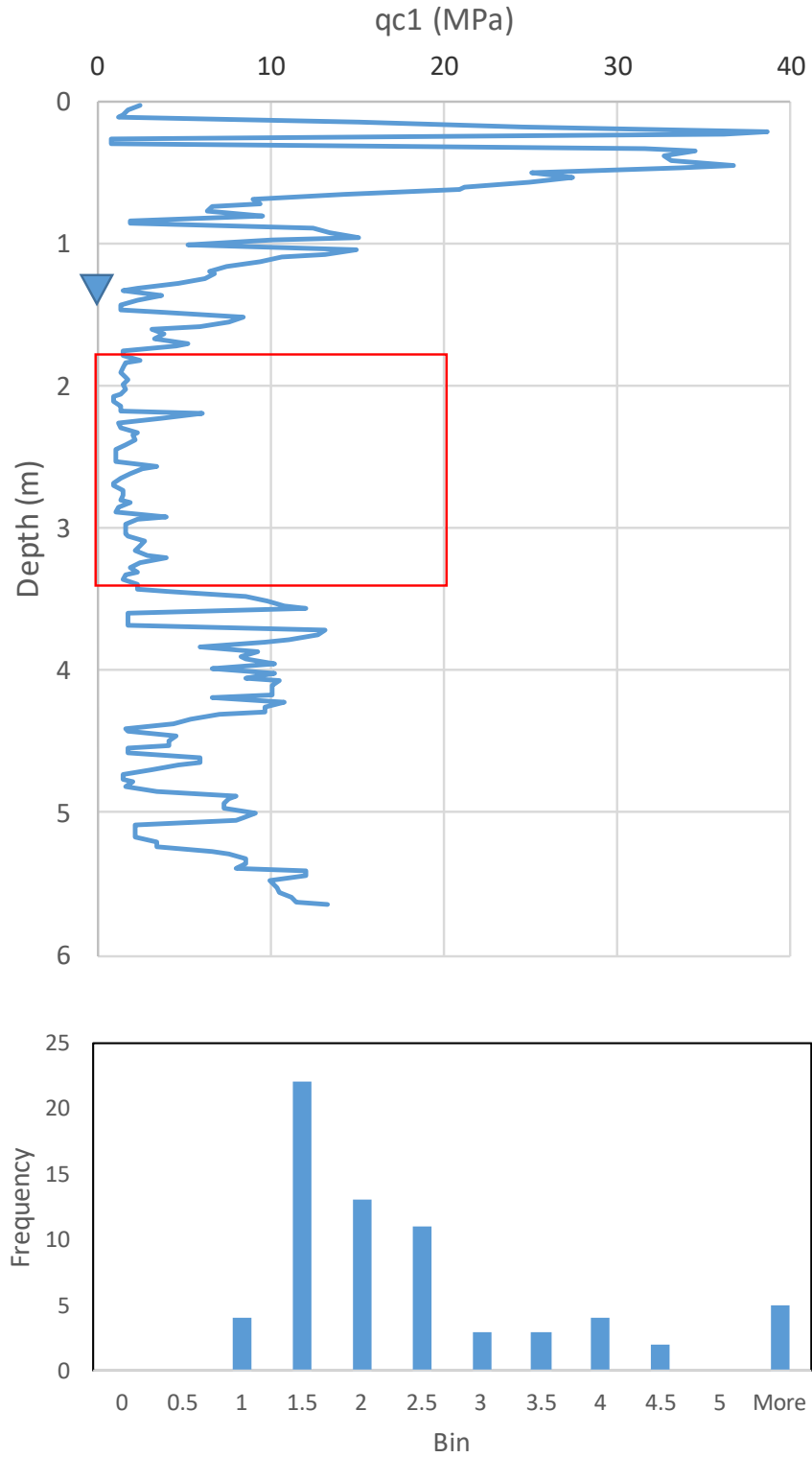


Figure 7.2 CPT1 overburden corrected tip resistance with histogram of boxed region thought to best represent the tailings material susceptible to liquefaction and flow failure. The mean and median are approximately 1.83 MPa with a CoV of 0.40.

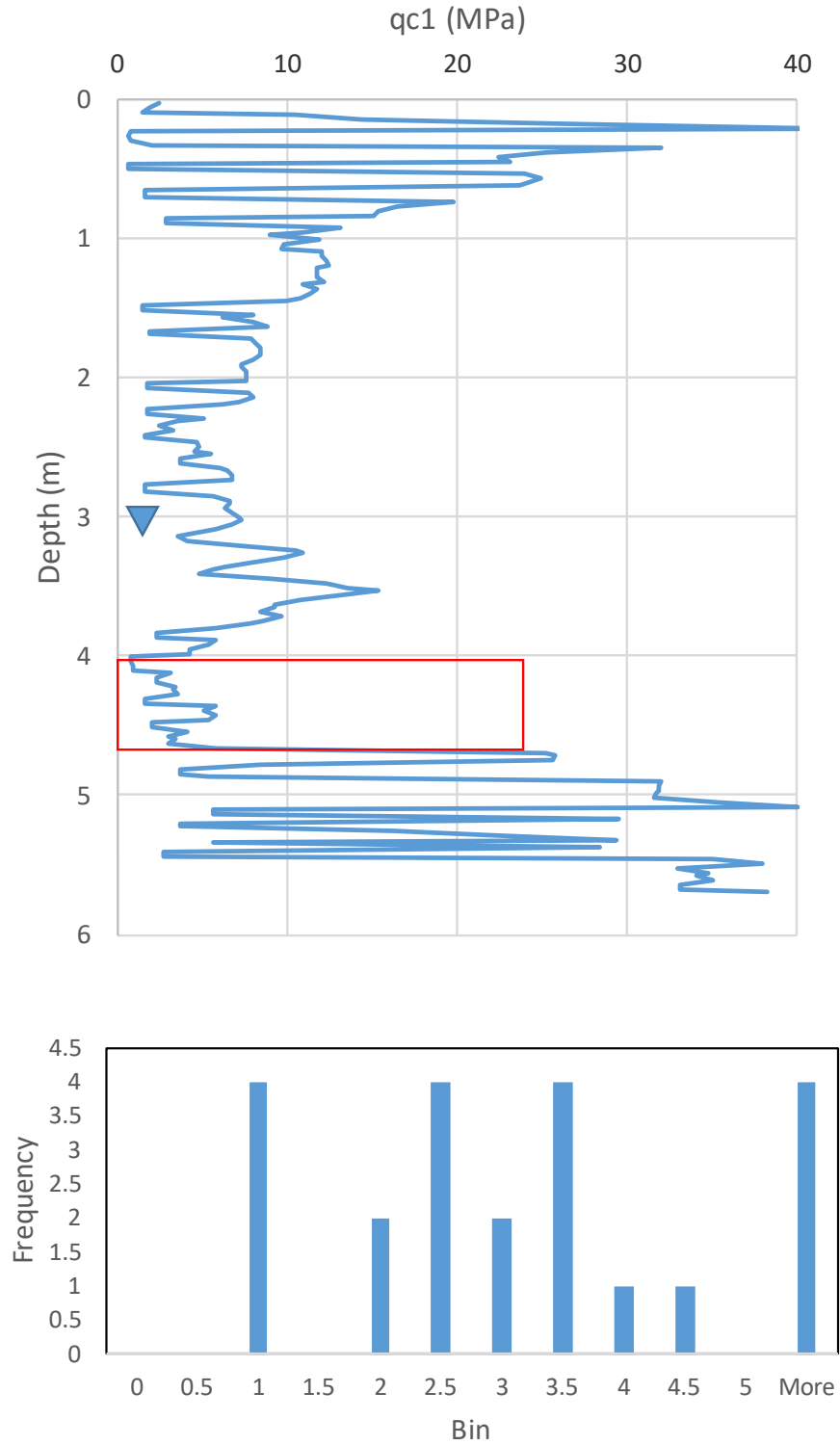


Figure 7.3 CPT2 overburden corrected tip resistance. This sounding is thought to represent material not highly susceptible to liquefaction because of wall material and interlayering. The boxed region mean is 2.94 MPa, median 1.86 MPa, with a CoV of 0.52.

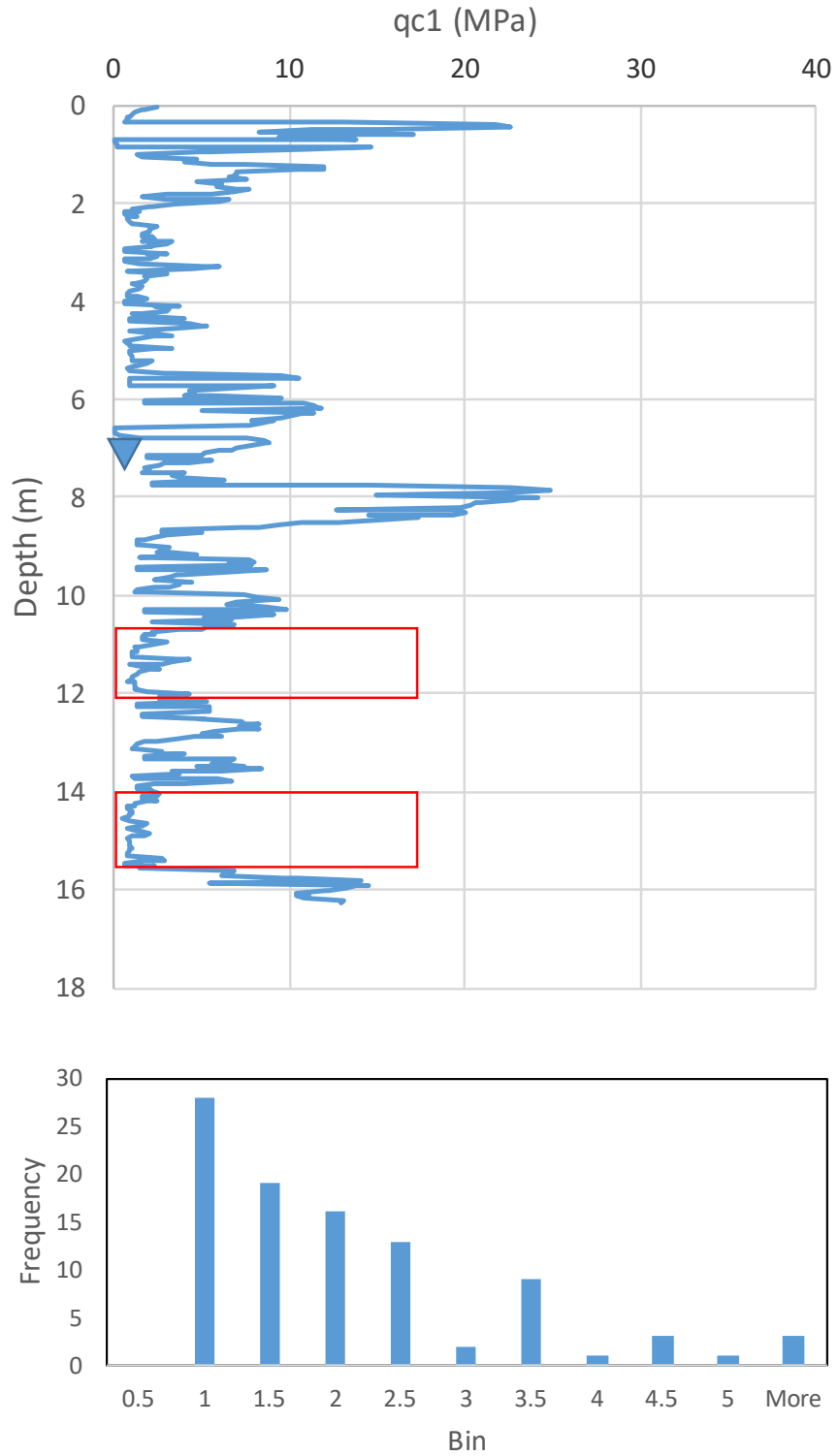


Figure 7.4 CPT3 overburden corrected tip resistance. This sounding is in the center of a region that experienced liquefaction but did not exhibit failure in a flow failure. The boxed regions have a mean of 1.3 MPa, median 1.4 MPa, with a CoV of 0.06.

7.2 RESIDUAL STRENGTH

A post-liquefaction residual strength ≈ 7.8 kPa (163 psf) and ≈ 8.7 kPa (181 psf) represent bounds for a layered failure analysis, and a residual strength ≈ 8.4 kPa (175 psf) represents a complete flow-failure analysis. The average of these three residual strengths ≈ 8.3 kPa (173 psf), which represents the estimated mobilized post-liquefaction residual strength for this case study, with a nominal coefficient of variation of 5.5% estimated from the sensitivity analysis.

To provide confidence in this value, a sensitivity analysis was conducted; the results shown in Figure 7.5. The sensitivity analysis included alternate failure modes, differing ground water conditions, and variable unit weight of the uncompacted tailings embankment and ponded material.

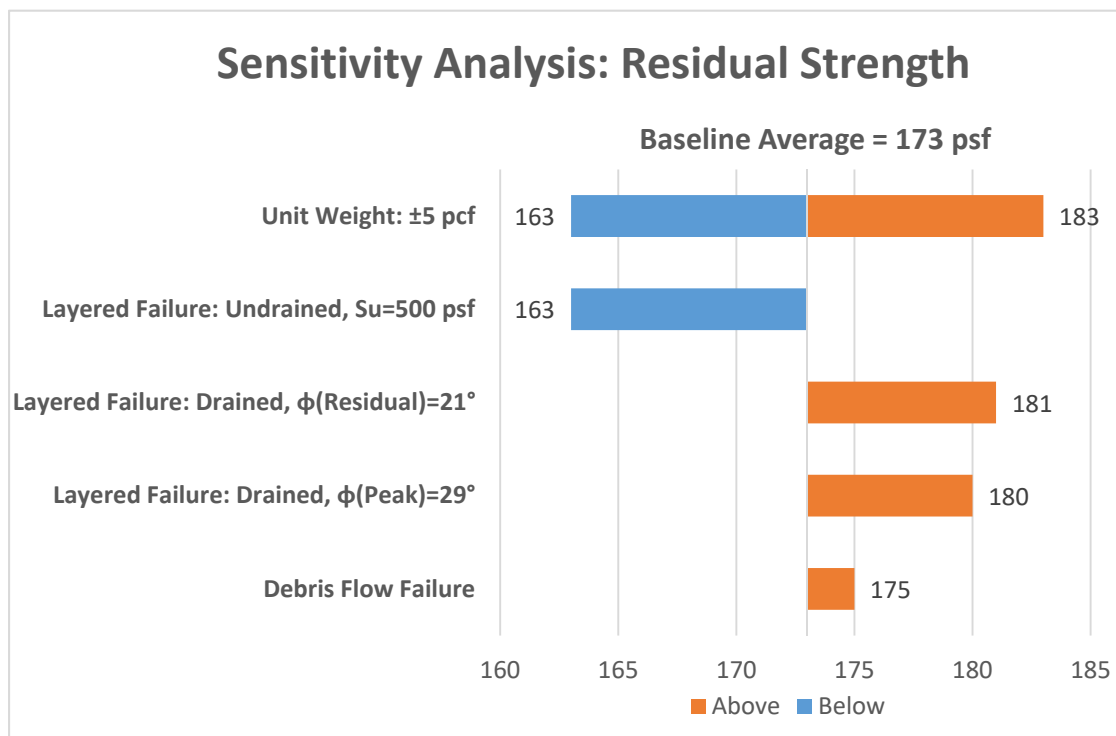


Figure 7.5 Tornado plot sensitivity analysis of post-liquefaction residual strength (from Gebhart [2016]).

7.3 EFFECTIVE STRESS

For this study, the location selected to represent initial vertical effective stress (or soil overburden) was the assumed failure interface between tailings and underlying competent native material. Values and geometry used for calculation are per Figure 7.6. An initial vertical effective stress of approximately 2.0 atmospheres (202.5 kPa or 4,300 psf) was the best estimate for this case history, with an estimated coefficient of variation of 5% [Kulhawy and Mayne 1990].

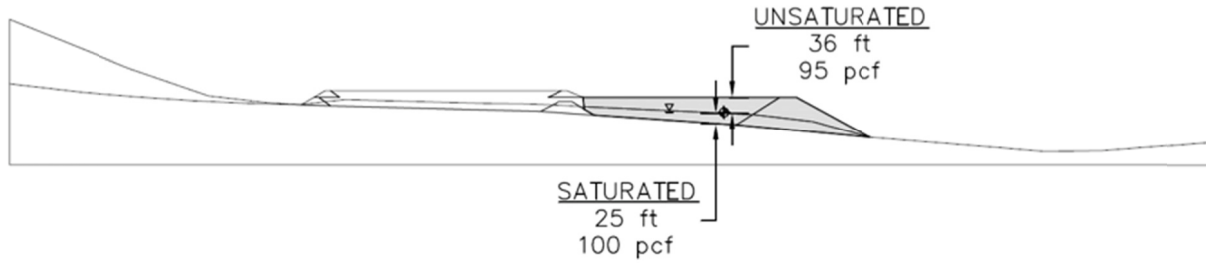


Figure 7.6 Geometry used to estimate the effective stress on the failure plane at the time of failure (from Gebhart [2016]).

7.4 COMPARISON WITH EXISTING DATABASE

The results are plotted against prior case histories in the format of residual strength predictive plots: Seed and Harder [1990] (Figure 7.7); Olson and Stark [2002] (Figures 7.8 and 7.9); Kramer and Wang [2015] (Figure 7.10); and Weber et al. [2015] (Figure 7.11). The data from this case history is shown as an ellipse capturing the quantified uncertainty in penetration resistance and residual strength.

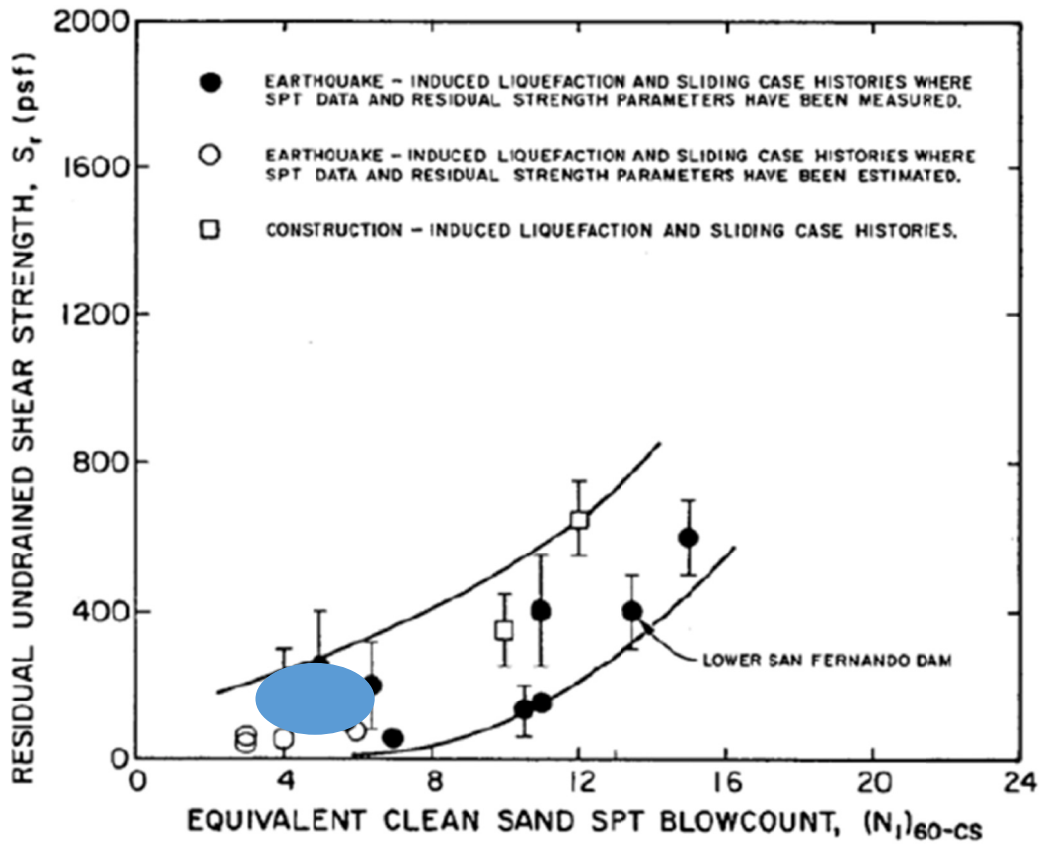


Figure 7.7 Las Palmas data ellipse with respect to Seed and Harder [1990].

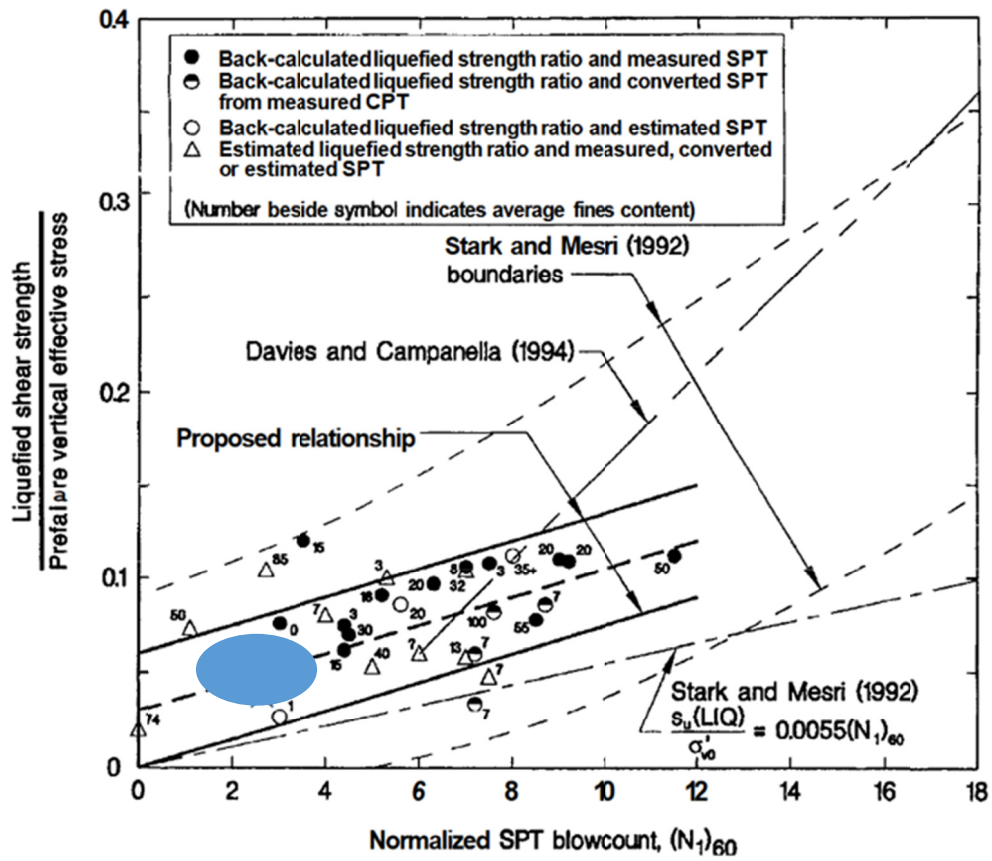


Figure 7.8 Las Palmas data point (SPT) with respect to Olson and Stark [2002].

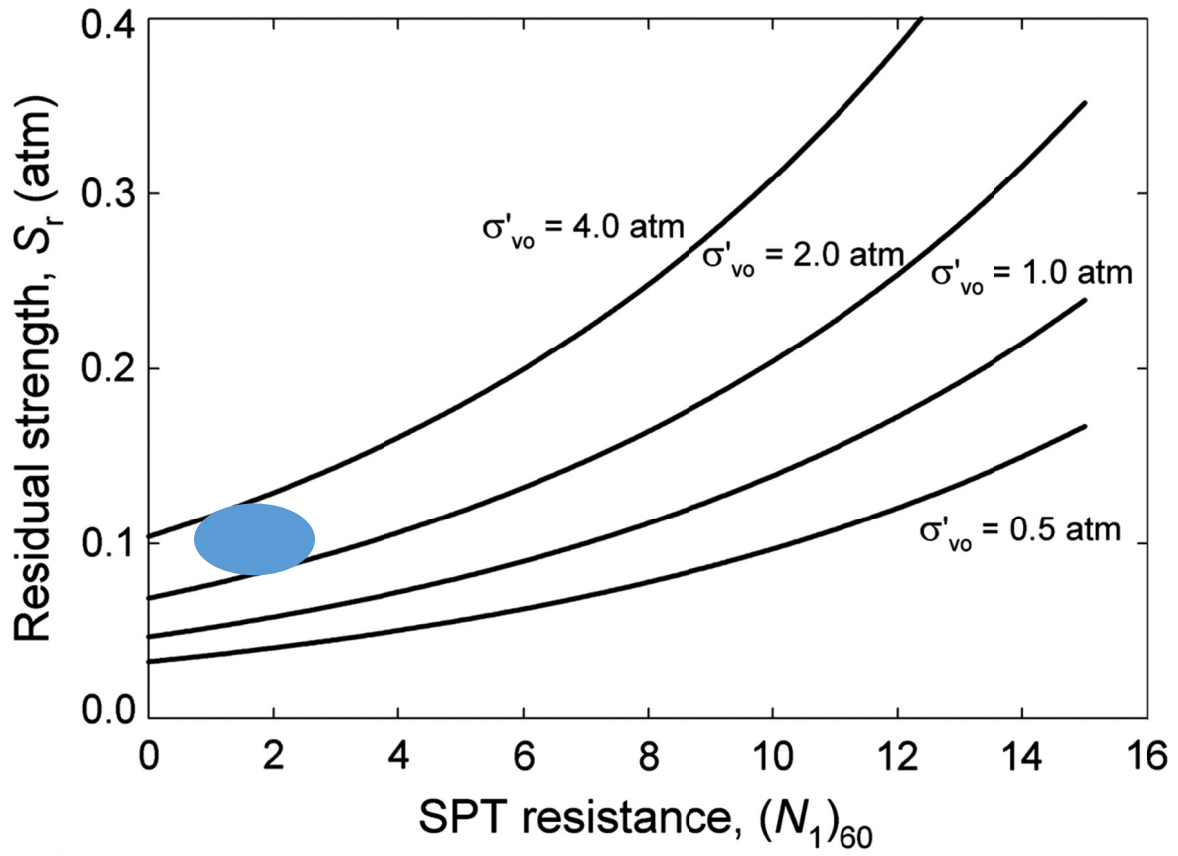


Figure 7.10 Las Palmas data point with respect to Kramer and Wang [2015].

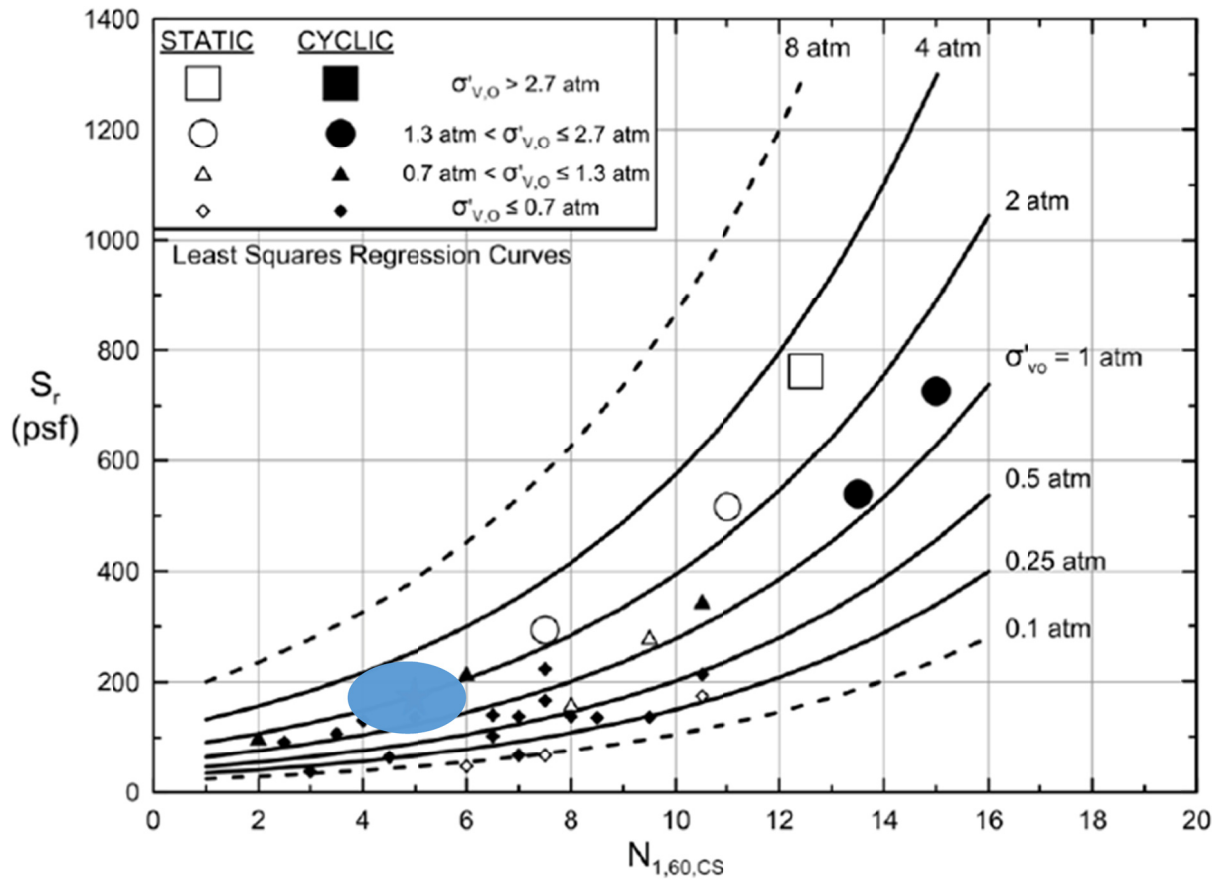


Figure 7.11 Las Palmas data point with respect to Weber et al. [2015].

8 Summary and Conclusions

The goal of this study was to provide a well-documented case history of a liquefaction flow failure. The 2010 Maule, Chile, event triggered the flow failure in the Las Palmas tailings dam, resulting in a run out of upwards of 350 m. The documentation herein includes; reconnaissance information by GEER [2010], drilling and standard penetration measurements (SPT) by DICTUC [2012], and back analysis of the residual strength by Gebhart [2016], as well as the results of cone penetration tests (CPT) and shear-wave velocity (VS) measurements presented here for the first time.

Based on the information evaluated, analyzed, and measured, the Las Palmas flow failure can be summarized with the following mean values and estimated coefficients of variation.

Table 8.1 Summary mean and coefficient of variation.

Resistance	SPT	$N_{1,60} \approx 2.5$ and $N_{1,60,CS} \approx 5$	COV~25%
	CPT	$q_{c1} \approx 1.3$ MPa and $Q_{tn} \approx 11.7$	10%
	VS	$VS_1 \approx 172$ m/sec	10%
Residual strength	Sur ≈ 8.3 kPa (173 psf)		5.5%
Effective stress	$\sigma'_v \approx 2.0$ atmospheres (202.5 kPa, 4300 psf)		5.0%

REFERENCES

- Aki K. (1957). Space and time spectra of stationary stochastic waves, with special reference to microtremors, *Bull. Earthq. Res. Inst.*, 25: 415-457.
- Andrus R.D., Stokoe II K.H. (2000). Liquefaction resistance of soils from shear-wave velocity, ASCE, *J. Geotech Geoenviron. Eng.*, 126(11): 1015-1025.
- Boroschek R.L., Contreras V., Kwak D.Y., Stewart J.P. (2012). Strong ground motion attributes of the 2010 Mw 8.8 Maule, Chile, earthquake, *Earthq. Spectra*, 28(S1): S19-S38.
- DICTUC (2012). Estudio del colapso del tranque de relaves de la mina Las Palmas,” Dirección de Investigaciones Científicas y Tecnológicas de la Pontificia Universidad Católica de Chile (in Spanish).
- Gebhart T. (2016), *Post-Liquefaction Residual Strength Assessment of the Las Palmas, Chile Tailing Failure*, Thesis in partial fulfillment for Master’s Degree, California Polytechnic State University, September.
- GEER (2010). Geo-Engineering Reconnaissance of the Feb 27, 2010 Maule, Chile, Earthquake. (http://www.geerassociation.org/administrator/components/com_geer_reports/geerfiles/Ver2_Cover_Chile_2010.html) Accessed Sept 15, 2017
- Geogiga (2017). (<http://www.geogiga.com/en/surfaceplus.php>). Accessed September 15, 2017.
- Hayes G. (2010) https://earthquake.usgs.gov/earthquakes/eventpage/official20100227063411530_30#finite-fault. Accessed September 23, 2018.
- Kramer S.L., Wang C. (2015). Empirical model for estimation of the residual strength of liquefied soil, ASCE, *J. Geotech Geoenviron. Eng.*, 141(9), DOI: 10.1061/(ASCE)GT.1943-5606.0001317.
- Kulhawy F.H., Mayne P.W. (1990). Manual on estimating soil properties for foundation design (No. EPRI-EL-6800). Electric Power Research Inst., Palo Alto, CA.
- Moss R.E.S. (2008). Quantifying measurement uncertainty of thirty-meter shear-wave velocity, *Bull. Seismol. Soc. Am.*, 98(3): 1399-1411.
- Moss R.E.S., Seed R.B., Kayen R.E., Stewart J.P., Der Kiureghian A., Cetin, K.O. (2006). CPT-based probabilistic and deterministic assessment of in situ seismic soil liquefaction potential, ASCE. *J. Geotech Geoenviron. Eng.*, 132(8): 1032-1051.
- Olson S.M., Stark T.D. (2002). Liquefied strength ratio from liquefaction flow failure case histories, *Canadian Geotech. J.*, 39: 629-647.
- Robertson P.K., Cabal K.L. (2015). *Guide to Cone Penetration Testing*, 6th Ed., <http://www.cpt-robertson.com/doc/view?docid=xnhqTpmrnRdPTvYHHRsr6hcNdKJLWy>). Accessed September 15 2017.
- Seed R.B., Harder L.F., Jr. (1990). SPT-based analysis of cyclic pore pressure generation and undrained residual strength, *Proceedings, H. Bolton Seed Memorial Symposium*, Bi- Tech Publishing Ltd., 2: 351-376.
- USGS (2010). https://earthquake.usgs.gov/earthquakes/eventpage/official20100227063411530_30#executive, U.S. Geological Survey. Accessed September 15, 2017.
- Weber J.P., Seed R.B., Pestana J.M., Moss R.E.S., Nweke C., Deger T.T., Chowdhury, K. (2015). *Engineering Evaluation of Post-Liquefaction Strength*, prepared for the U.S. Nuclear Regulatory Commission.

Appendix Geophysical Data Processing

This appendix shows the passive surface wave geophysical data analysis used to arrive at the shear-wave velocity profiles. The data processing was carried out using the Surface Plus module in the Geogiga software suite. Measured and estimated dispersion curves are shown. All data was recorded using;

- circular arrays
- 12 geophones (4.5Hz)
- 2 m/sec sampling rate
- 32 sec recording length x 10 recordings all concatenated

CPT1 (G1) s35.184242 w71.759540 (coincident with SPT4)
1000-1009 is a 10-m array
1100-1109 is a 20-m array

CPT2 (G2) s35184297 w71.760284
2000-2009 is a 20-m array
2100-2109 is a 10-m array

CPT3 (G3) s35.184350 w71.761196 (coincident with SPT2)
3000-3009 is a 20-m array
3100-3109 is a 10-m array

G5 (debris flow material) s35.185729 w71.758658
5000-5009 is a 10-m array
5100-5109 is a 20-m array
5200-5209 is a 5-m array

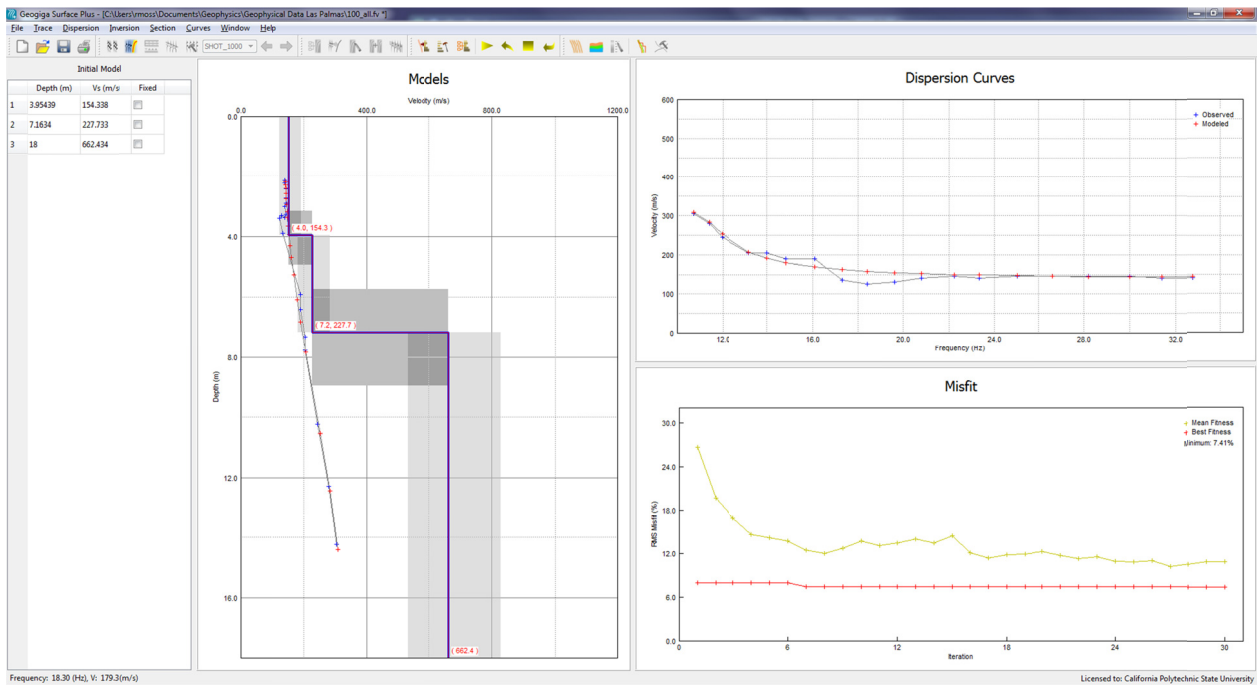
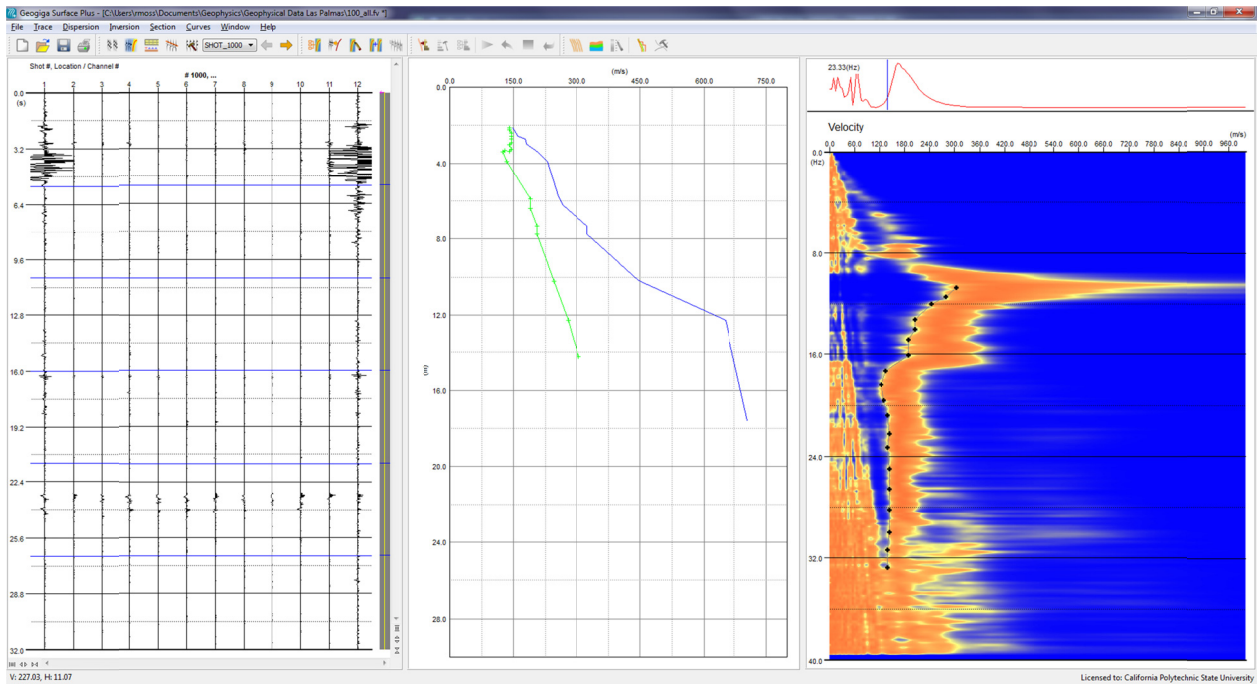
G6 (translated mass) s35.186669 w71.758161
6000-6009 is a 10-m array
6100-6104 is a 20-m array
6200-6209 is a 5-m array

CPT1 (G1) s35.184242 w71.759540 (coincident with SPT4)

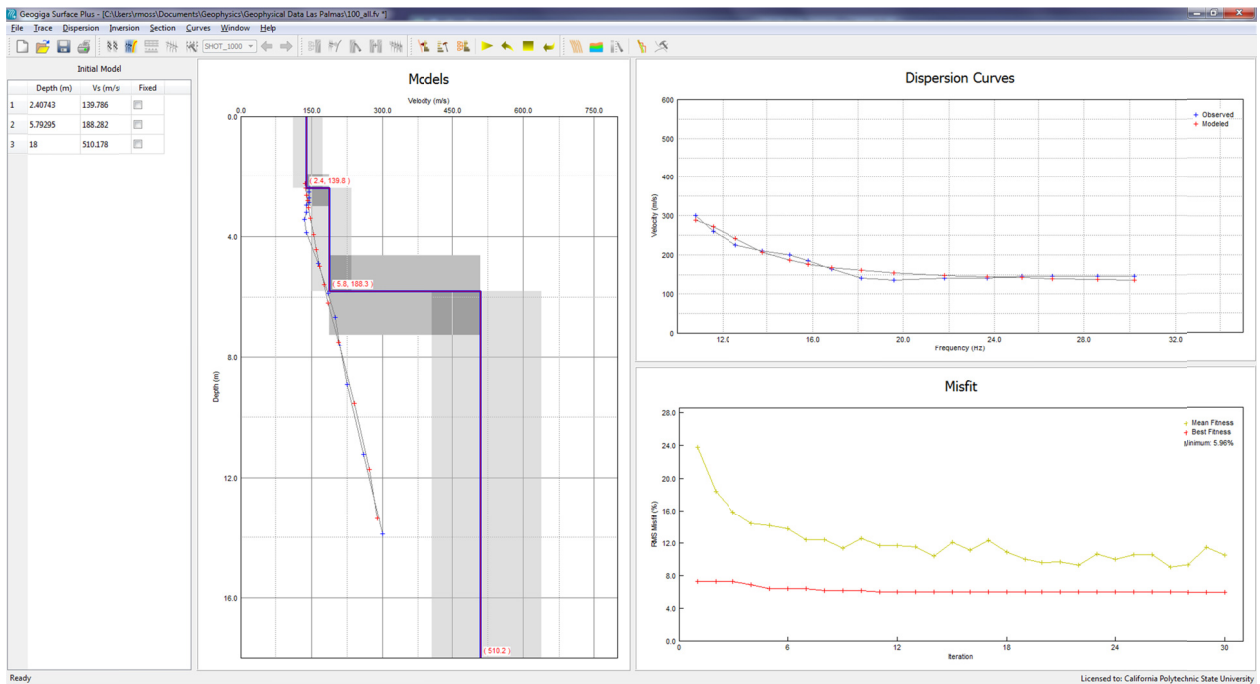
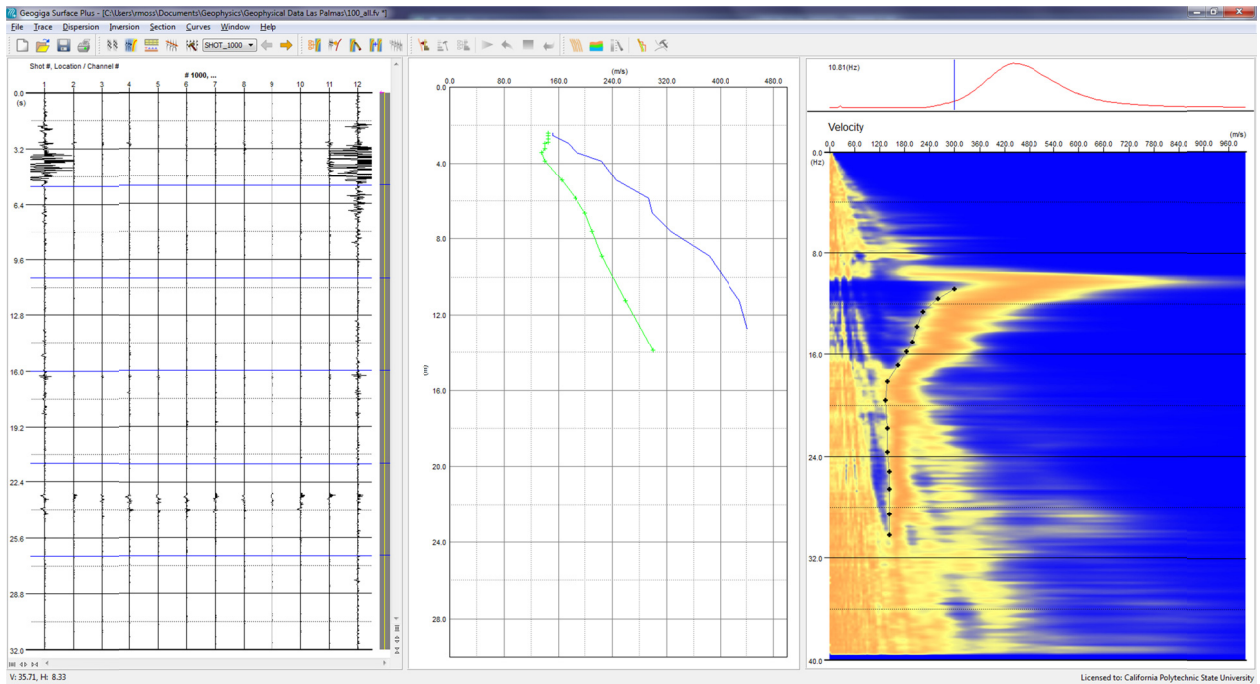
PROJECT INFORMATION						DRILLING INFORMATION						
PROJECT: Las Palmas Tailings Dam						DRILL RIG:						
DRILLING LOCATION: Tailings						HOLE DIAMETER:						
DATE DRILLED:						SAMPLING METHOD:						
LOGGED BY:						HOLE ELEVATION:						
▼ Depth of Groundwater: 17 Feet						Boring Terminated At: 28 Feet						
DEPTH	SOIL DESCRIPTION	USCS	LITHOLOGY	SAMPLE	BLOWS/ 12 IN (N ₁) ₆₀	FRICITION ANGLE, (degrees)	COHESION, C (psf)	WATER CONTENT (%)	MAXIMUM DRY DENSITY (pcf)	EXPANSION INDEX (EI)	FINES CONTENT (%)	PLASTICITY INDEX (PI)

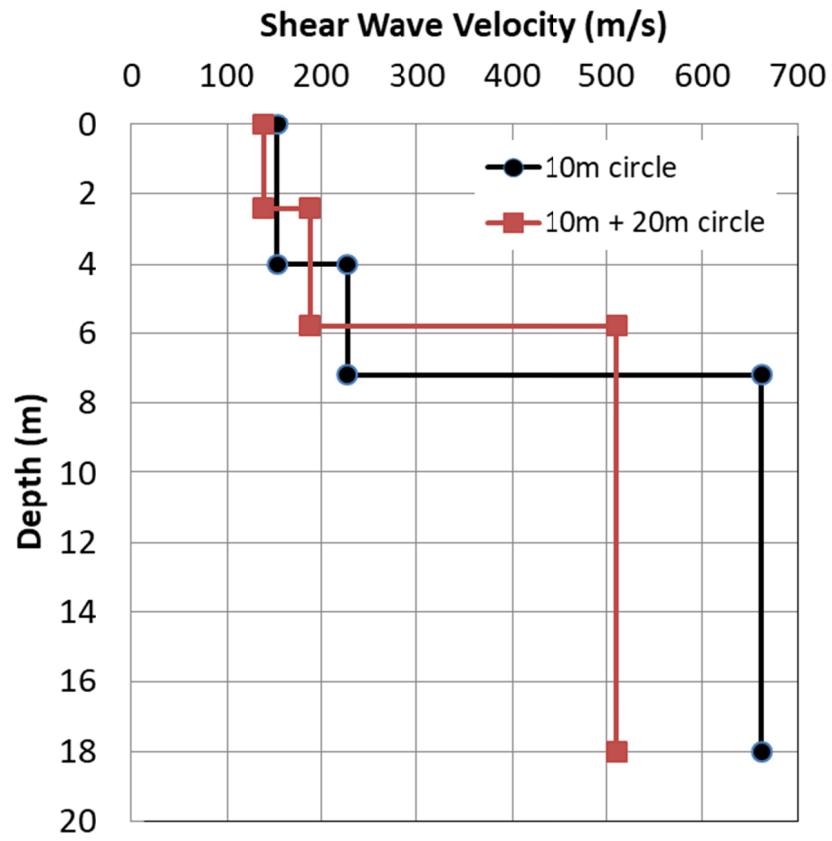
0	SANDY SILT	ML						3-19%				N/A
-1					6	9					88	
-2												
-3												
-4												
-5					4	6					87	
-6												
-7												
-8												
-9					3	4					97	
-10												
-11	SILTY SAND	SM						8%				N/A
-12					12	12					32	
-13												
-14												
-15	SANDY SILT	ML						18%				N/A
-16					7	7					59	
-17												
-18	BEDROCK											
-19												
-20												
-21												
-22												
-23												
-24												
-25												
-26												
-27												
-28												
-29												
-30												

10-m circle only

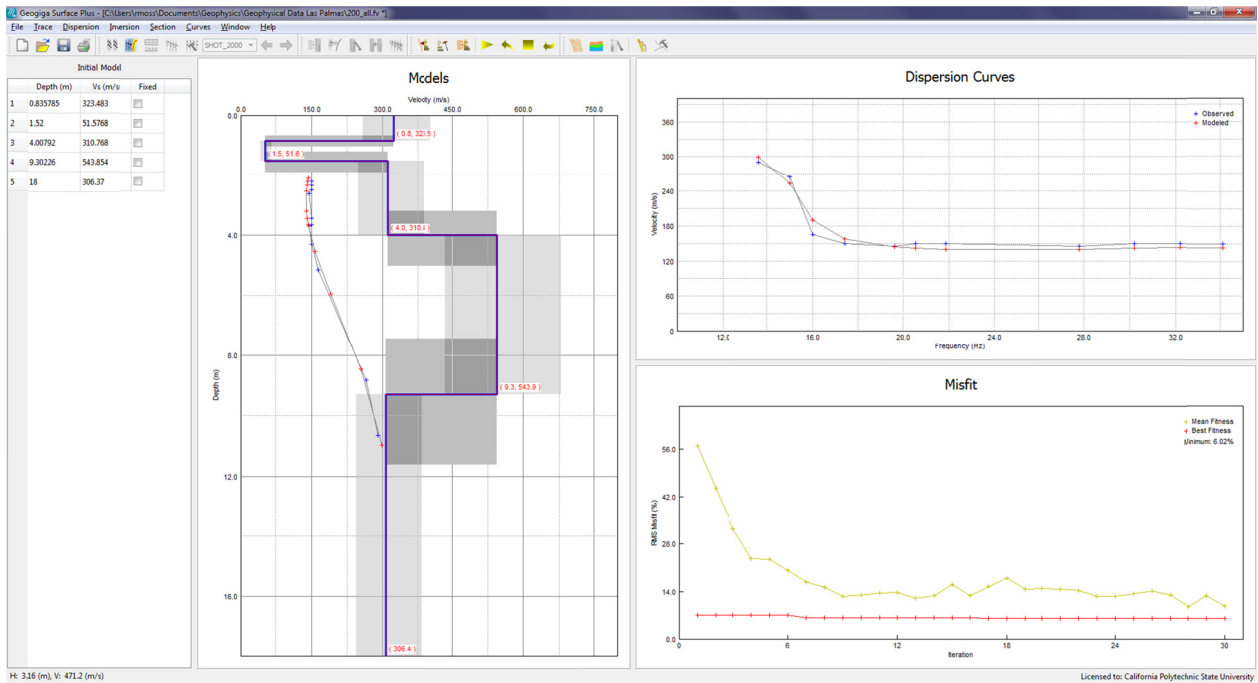
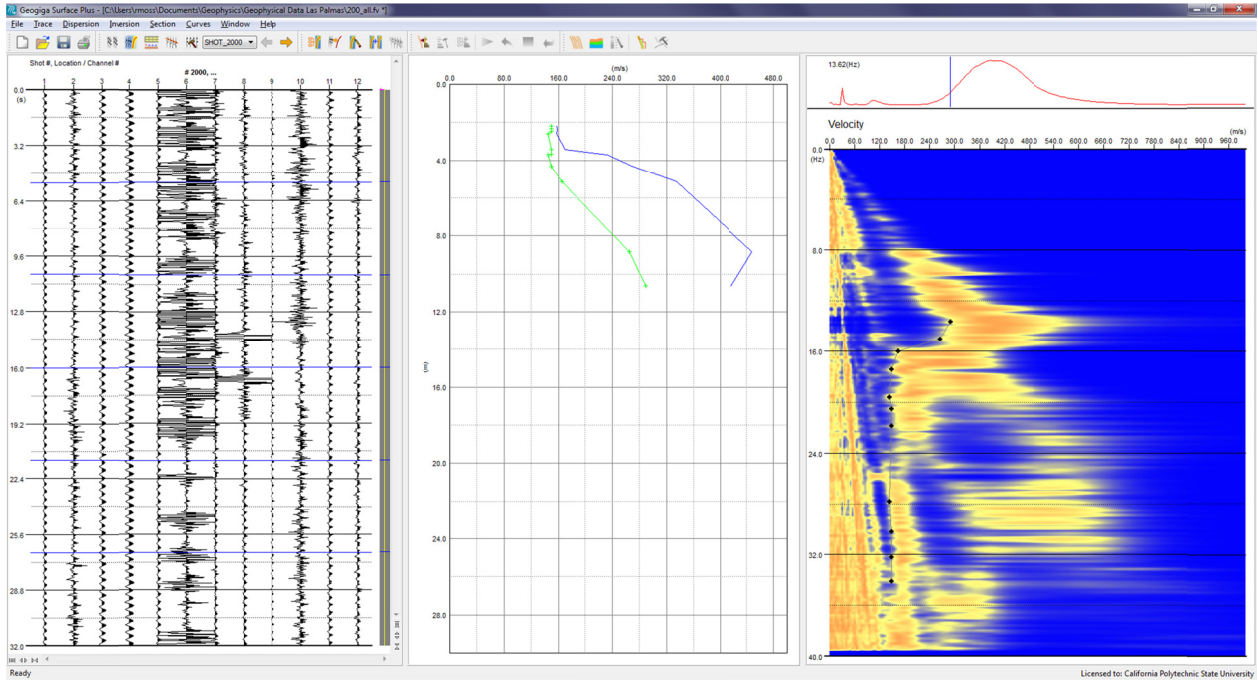


10-m + 20-m circle combined

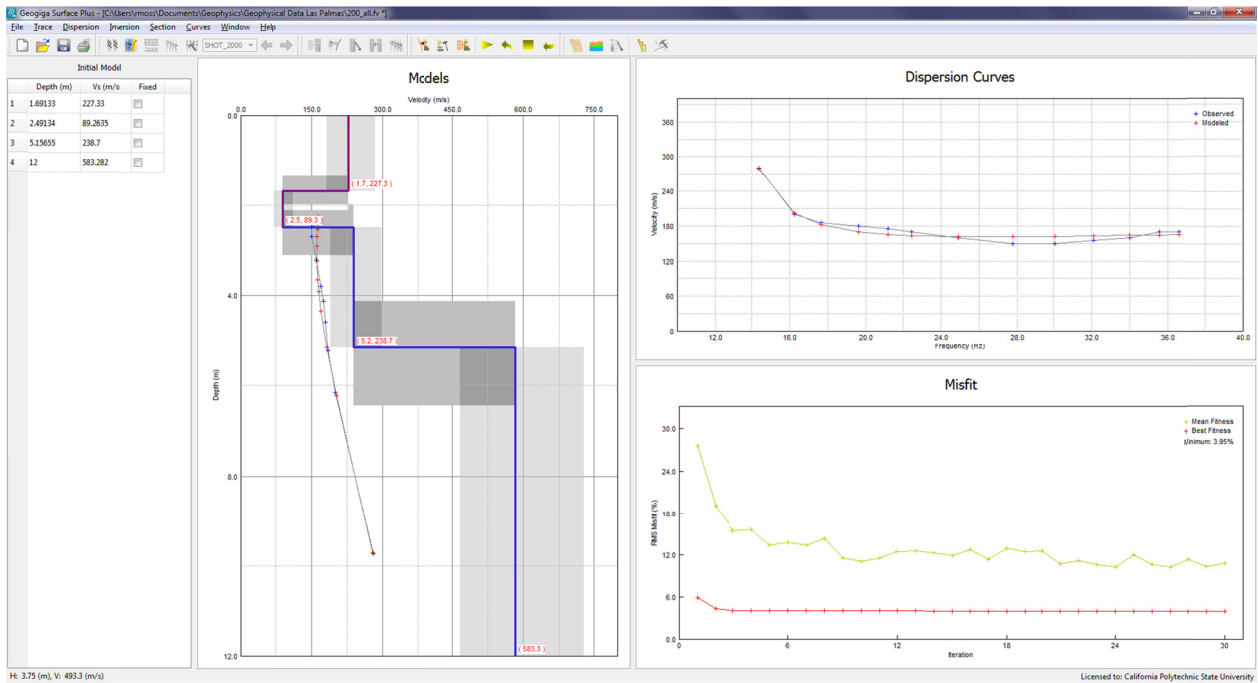
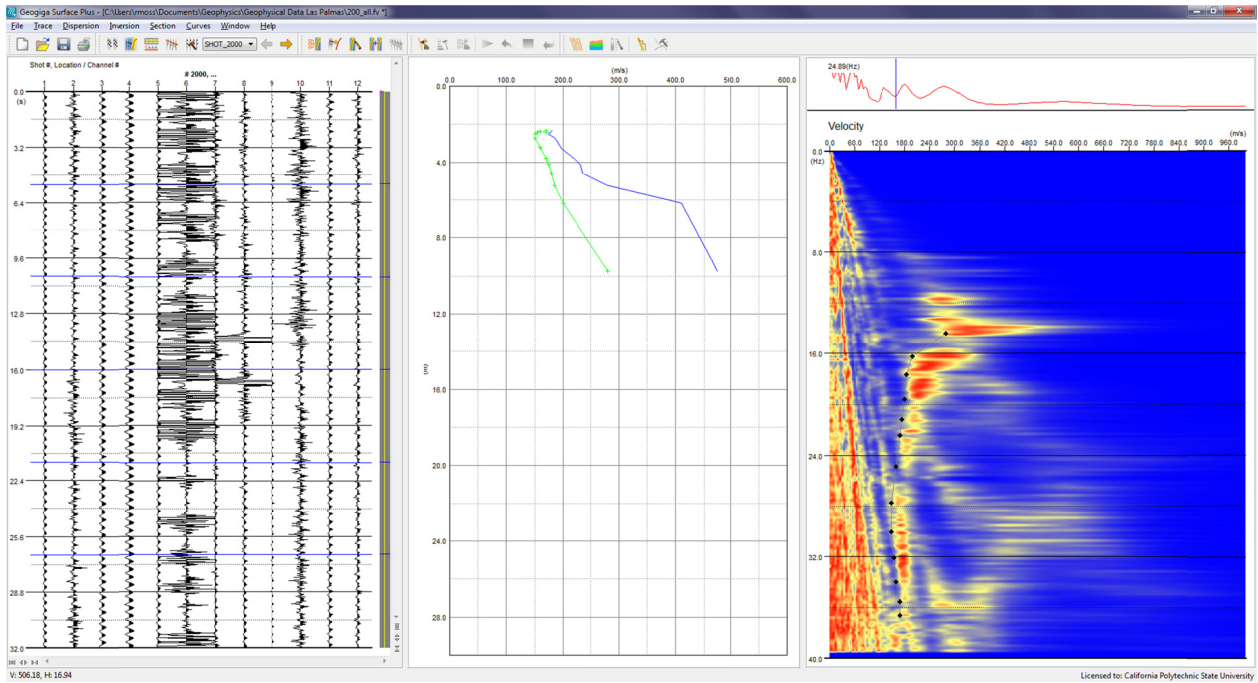


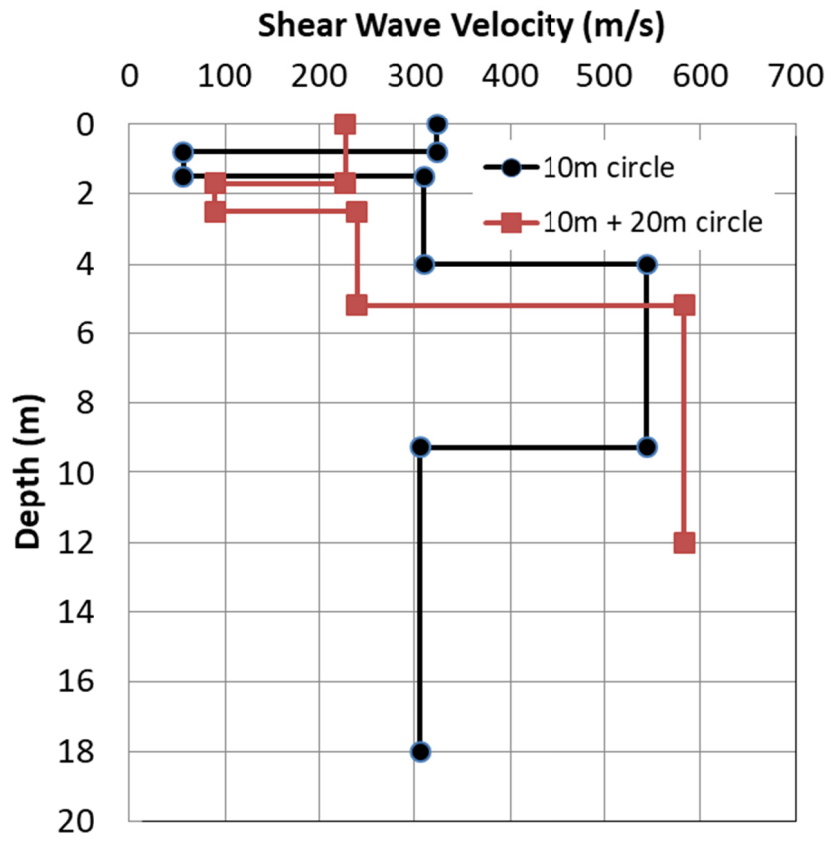


CPT2 (G2) s35184297 w71.760284
10-m circle



10-m + 20-m circle



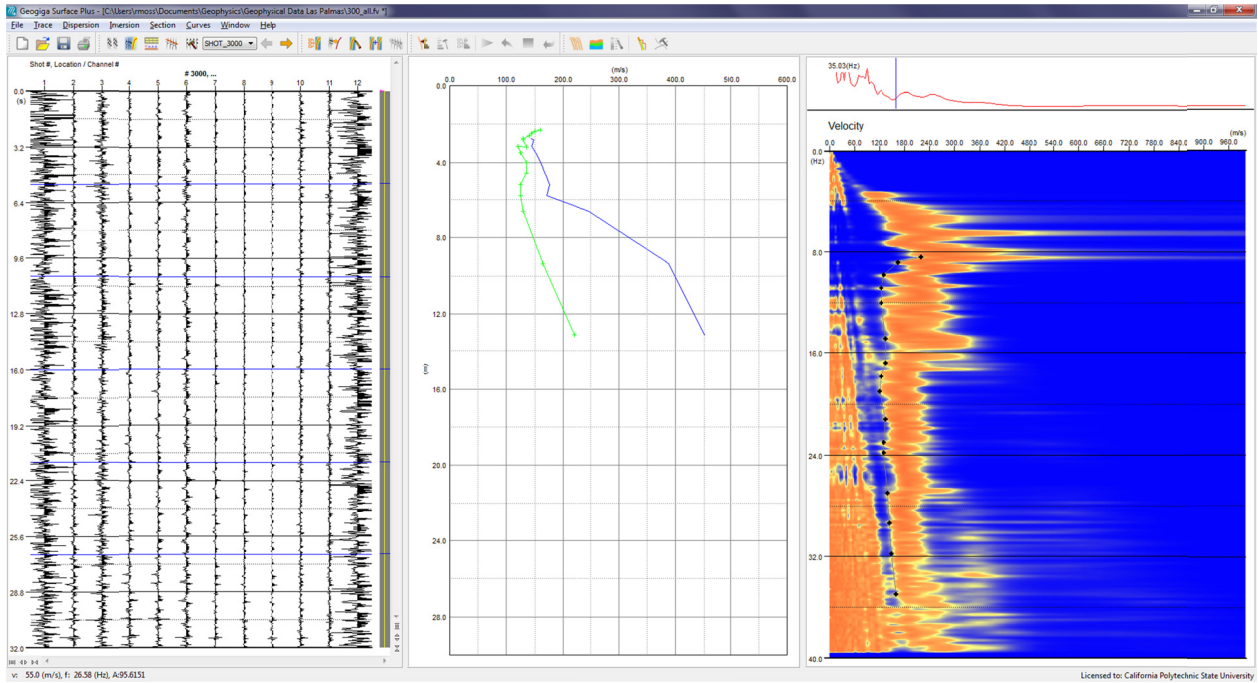


CPT3 (G3) s35.184350 w71.761196 (coincident with SPT2)

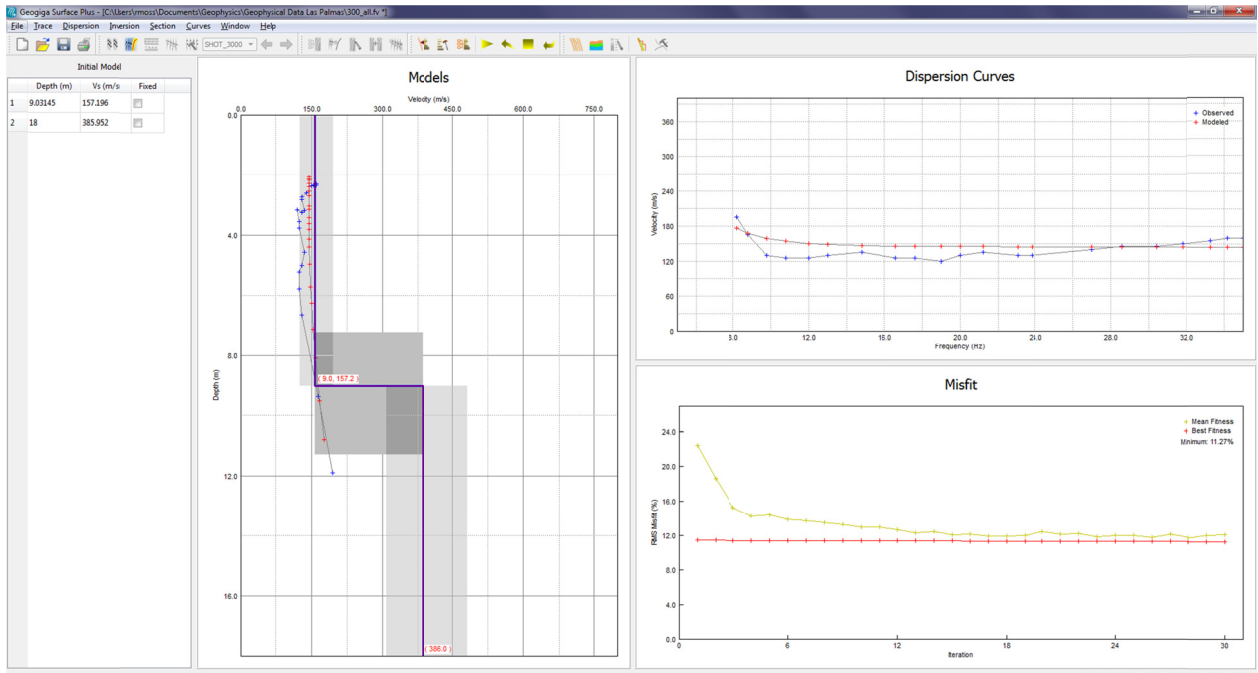
PROJECT INFORMATION					DRILLING INFORMATION								
PROJECT: Las Palmas Tailings Dam					DRILL RIG:								
DRILLING LOCATION: Tailings					HOLE DIAMETER:								
DATE DRILLED:					SAMPLING METHOD:								
LOGGED BY:					HOLE ELEVATION:								
▼ Depth of Groundwater: 40 Feet					Boring Terminated At: 53 Feet								
DEPTH	SOIL DESCRIPTION	USCS	LITHOLOGY	SAMPLE	BLOWS/12 IN	(N ₁) ₆₀	FRICITION ANGLE, (degrees)	COHESION, C (psf)	WATER CONTENT (%)	MAXIMUM DRY DENSITY (pcf)	EXPANSION INDEX (EI)	FINES CONTENT (%)	PLASTICITY INDEX (PI)

0	SANDY SILT	ML	[Lithology Column]	[Sample Column]	8	12			12-32%			93	NP-4			
-1																
-2																
-3																
-4																
-5									1	2						93
-6									4	5						93
-7																
-8																
-9																
-10									4	4						96
-11																
-12																
-13									5	5						93
-14																
-15																
-16																
-17																
-18					6	5					90					
-19																
-20																
-21					5	5					91					
-22																
-23																
-24					4	3					95					
-25																
-26																
-27																
-28					3	2					92					
-29																
-30																
-31					1	1					99					
-32																
-33																
-34					2	2					94					
-35																
-36																
-37																
-38					4	3					88					
-39																
-40																
-41					3	2					82					
-42																
-43																
-44																
-45					2	1					98					
-46																
-47																
-48					4	3					99					
-49																
-50																
-51																
-52					2	1					99					
-53																
-54																
-55																

20-m circle

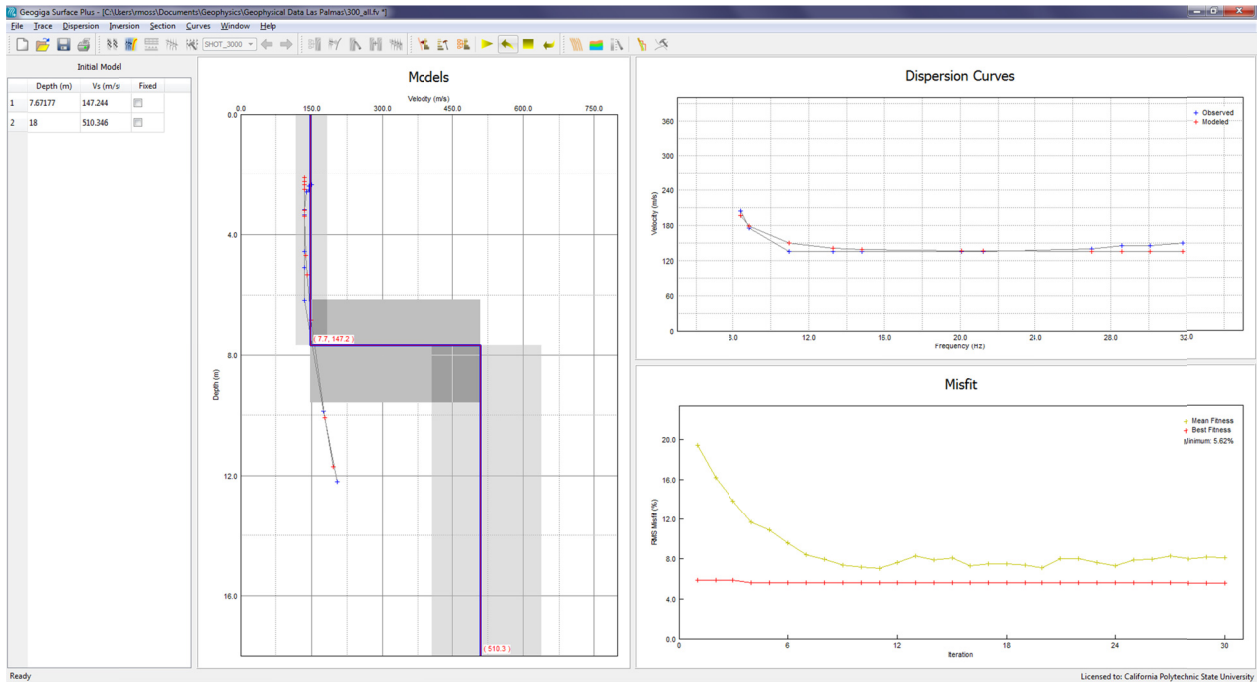
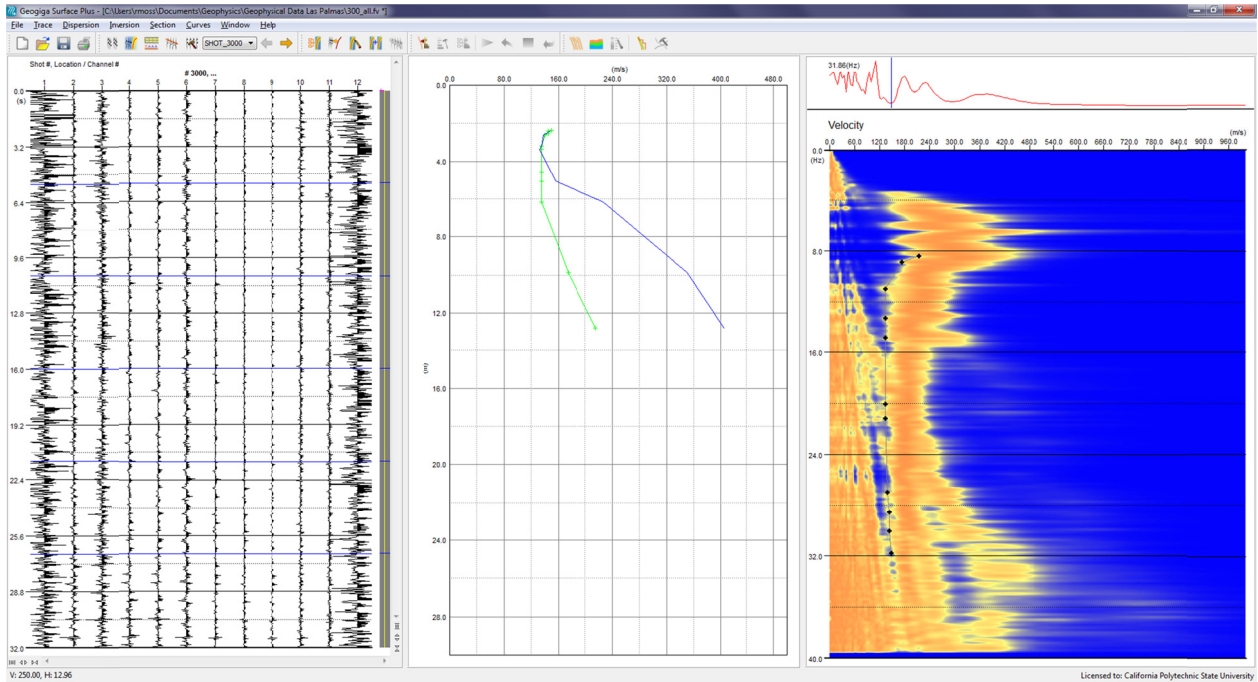


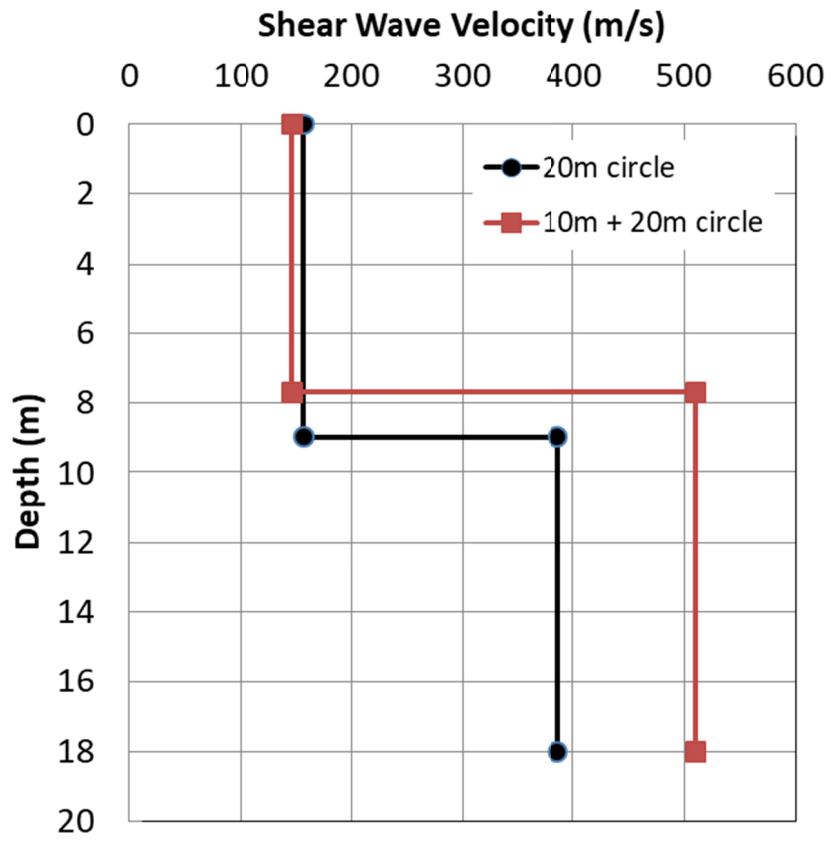
Licensed to: California Polytechnic State University



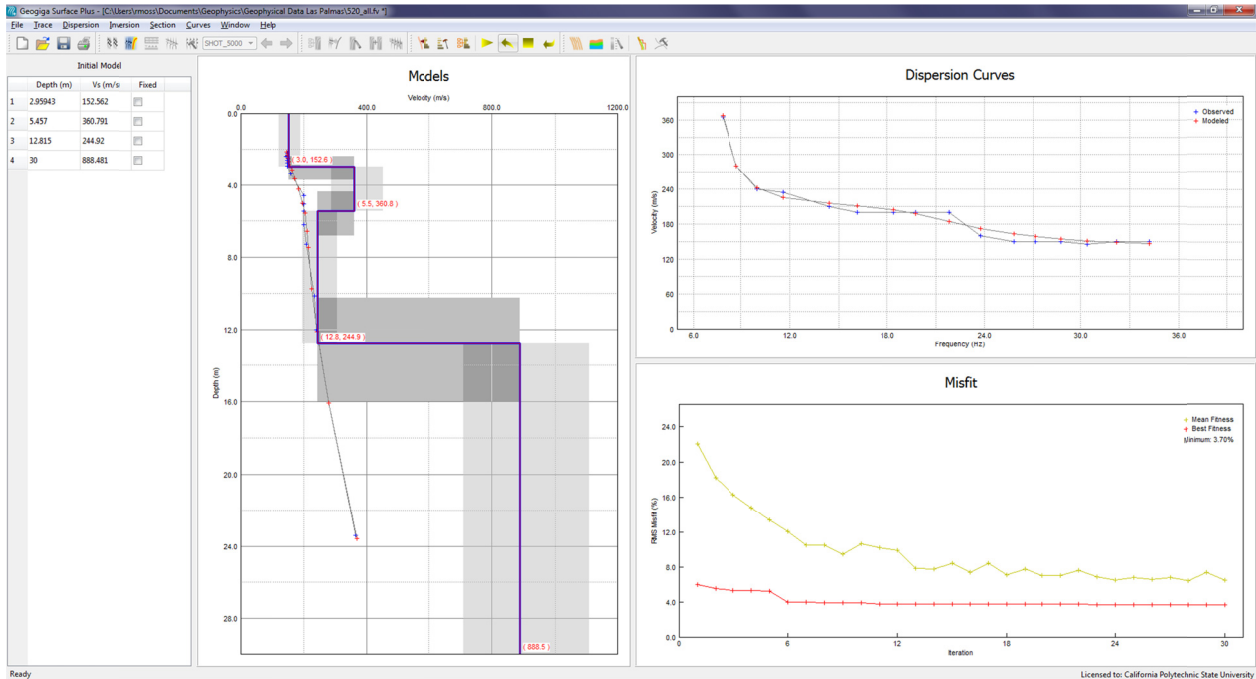
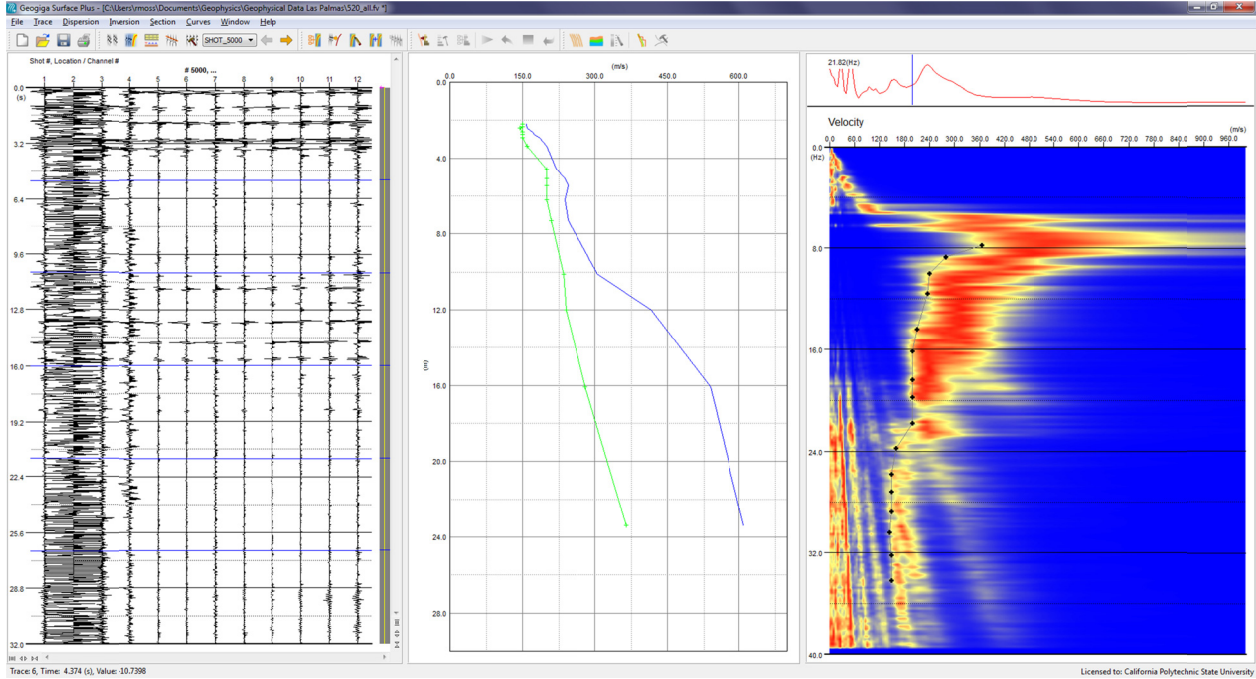
Licensed to: California Polytechnic State University

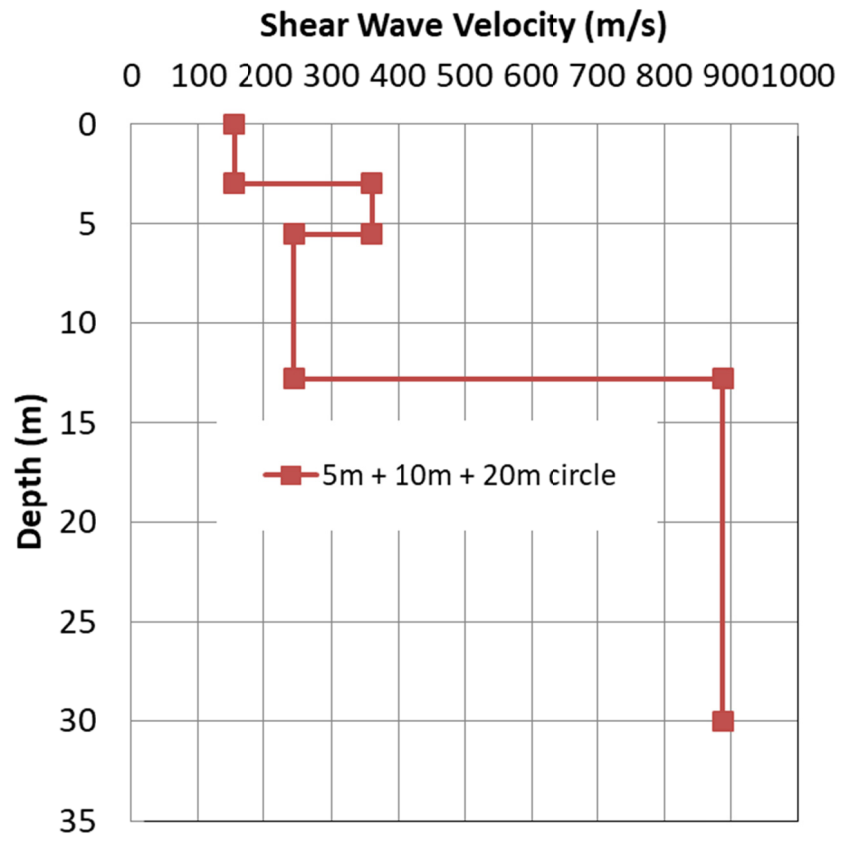
10-m + 20-m circle



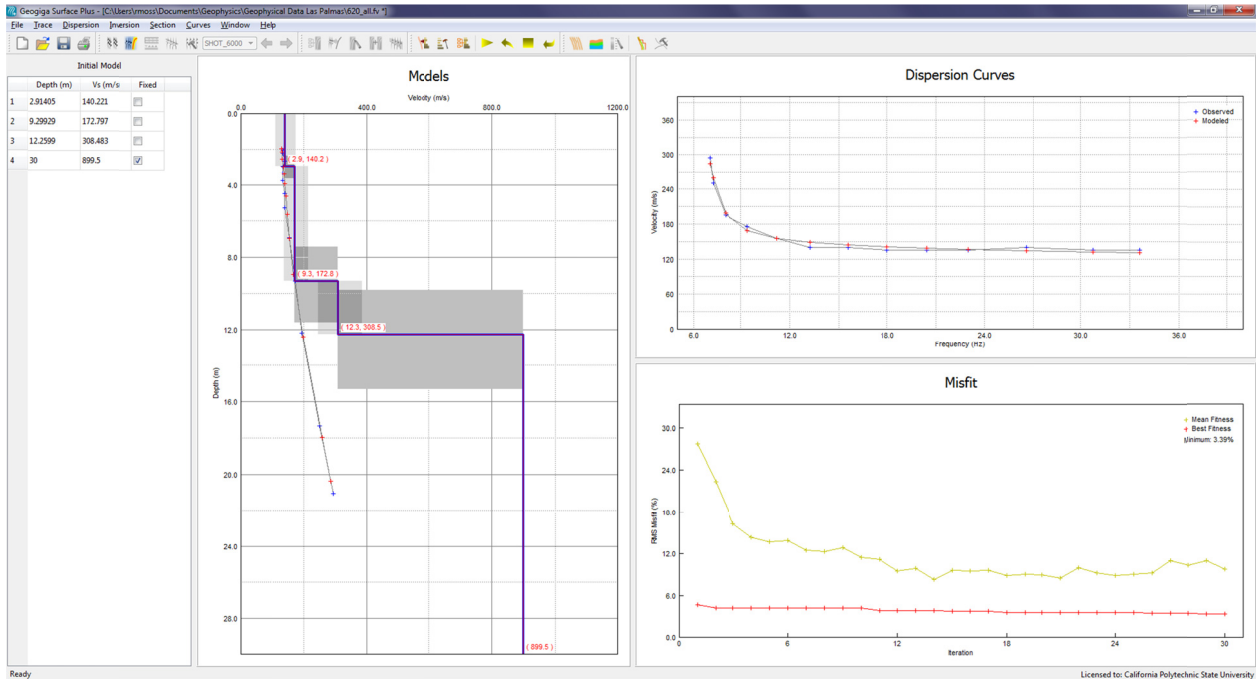
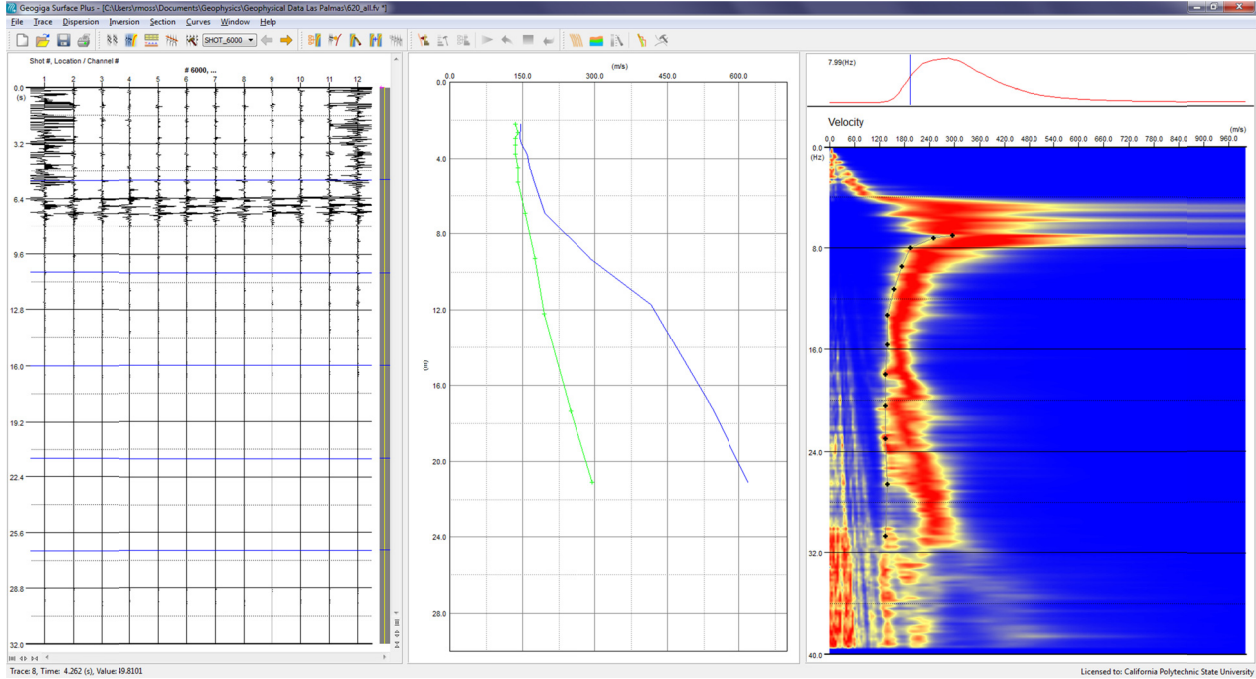


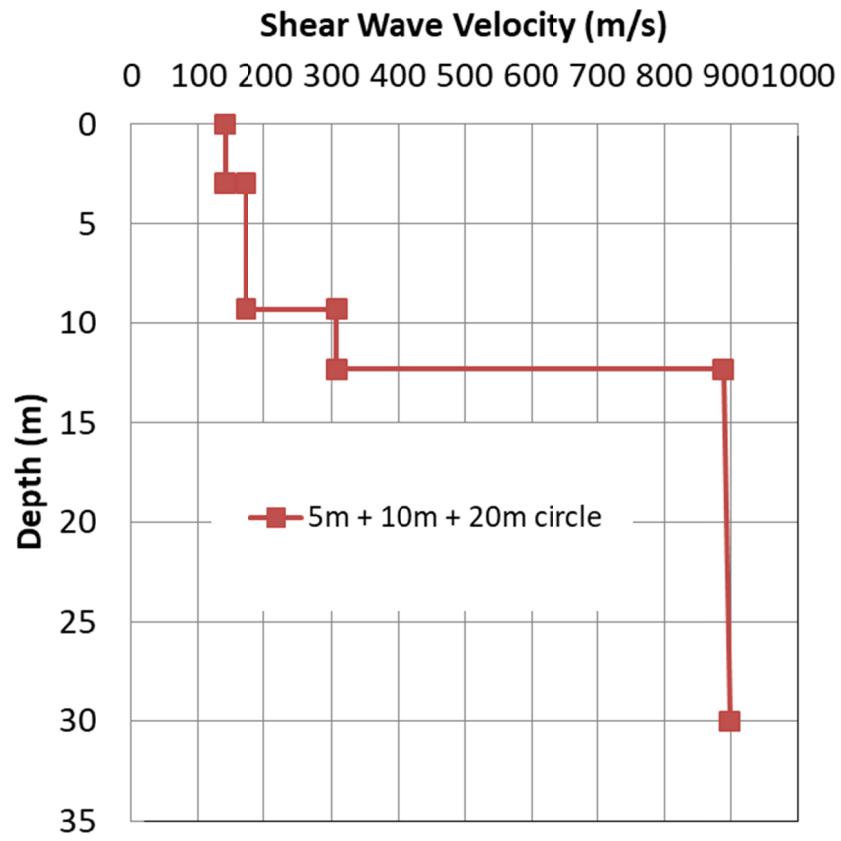
G5 (flow failure material) s35.185729 w71.758658
5000-5009 is a 10-m array
5100-5109 is a 20-m array
5200-5209 is a 5-m array

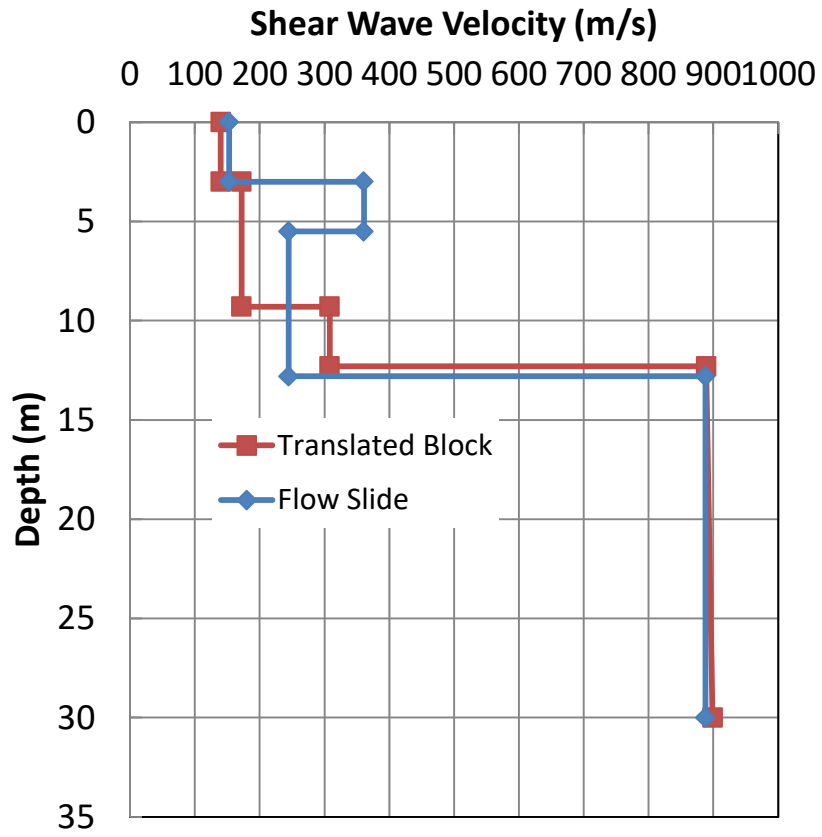




G6 (translated block) s35.186669 w71.758161
 6000-6009 is a 10-m array
 6100-6104 is a 20-m array
 6200-6209 is a 5-m array







PEER REPORTS

PEER reports are available as a free PDF download from <https://peer.berkeley.edu/peer-reports>. In addition, printed hard copies of PEER reports can be ordered directly from our printer by following the instructions at <https://peer.berkeley.edu/peer-reports>. For other related questions about the PEER Report Series, contact the Pacific Earthquake Engineering Research Center, 325 Davis Hall, Mail Code 1792, Berkeley, CA 94720. Tel.: (510) 642-3437; and Email: peer_center@berkeley.edu.

- PEER 2018/08** *Central and Eastern North America Ground-Motion Characterization: NGA-East Final Report.* Christine Goulet, Yousef Bozorgnia, Norman Abrahamson, Nicolas Kuehn, Linda Al Atik, Robert Youngs, Robert Graves, and Gail Atkinson. December 2018.
- PEER 2018/07** *An Empirical Model for Fourier Amplitude Spectra using the NGA-West2 Database.* Jeff Bayless, and Norman A. Abrahamson. December 2018.
- PEER 2018/06** *Estimation of Shear Demands on Rock-Socketed Drilled Shafts subjected to Lateral Loading.* Pedro Arduino, Long Chen, and Christopher R. McGann. December 2018.
- PEER 2018/05** *Selection of Random Vibration Procedures for the NGA-East Project.* Albert Kottke, Norman A. Abrahamson, David M. Boore, Yousef Bozorgnia, Christine Goulet, Justin Hollenback, Tadahiro Kishida, Armen Der Kiureghian, Olga-Joan Ktenidou, Nicolas Kuehn, Ellen M. Rathje, Walter J. Silva, Eric Thompson, and Xiaoyue Wang. December 2018.
- PEER 2018/04** *Capturing Directivity Effects in the Mean and Aleatory Variability of the NGA-West 2 Ground Motion Prediction Equations.* Jennie A. Watson-Lamprey. November 2018.
- PEER 2018/03** *Probabilistic Seismic Hazard Analysis Code Verification.* Christie Hale, Norman Abrahamson, and Yousef Bozorgnia. July 2018.
- PEER 2018/02** *Update of the BChydro Subduction Ground-Motion Model using the NGA-Subduction Dataset.* Norman Abrahamson, Nicolas Kuehn, Zeynep Gulerce, Nicholas Gregor, Yousef Bozorgnia, Grace Parker, Jonathan Stewart, Brian Chiou, I. M. Idriss, Kenneth Campbell, and Robert Youngs. June 2018.
- PEER 2018/01** *PEER Annual Report 2017–2018.* Khalid Mosalam, Amarnath Kasalanati, and Selim Günay. June 2018.
- PEER 2017/12** *Experimental Investigation of the Behavior of Vintage and Retrofit Concentrically Braced Steel Frames under Cyclic Loading.* Barbara G. Simpson, Stephen A. Mahin, and Jiun-Wei Lai, December 2017.
- PEER 2017/11** *Preliminary Studies on the Dynamic Response of a Seismically Isolated Prototype Gen-IV Sodium-Cooled Fast Reactor (PGSFR).* Benschun Shao, Andreas H. Schellenberg, Matthew J. Schoettler, and Stephen A. Mahin. December 2017.
- PEER 2017/10** *Development of Time Histories for IEEE693 Testing and Analysis (including Seismically Isolated Equipment).* Shakhzod M. Takhirov, Eric Fujisaki, Leon Kempner, Michael Riley, and Brian Low. December 2017.
- PEER 2017/09** *“R” Package for Computation of Earthquake Ground-Motion Response Spectra.* Pengfei Wang, Jonathan P. Stewart, Yousef Bozorgnia, David M. Boore, and Tadahiro Kishida. December 2017.
- PEER 2017/08** *Influence of Kinematic SSI on Foundation Input Motions for Bridges on Deep Foundations.* Benjamin J. Turner, Scott J. Brandenburg, and Jonathan P. Stewart. November 2017.
- PEER 2017/07** *A Nonlinear Kinetic Model for Multi-Stage Friction Pendulum Systems.* Paul L. Drazin and Sanjay Govindjee. September 2017.
- PEER 2017/06** *Guidelines for Performance-Based Seismic Design of Tall Buildings, Version 2.02.* TBI Working Group led by co-chairs Ron Hamburger and Jack Moehle: Jack Baker, Jonathan Bray, C.B. Crouse, Greg Deierlein, John Hooper, Marshall Lew, Joe Maffei, Stephen Mahin, James Malley, Farzad Naeim, Jonathan Stewart, and John Wallace. May 2017.
- PEER 2017/05** *Recommendations for Ergodic Nonlinear Site Amplification in Central and Eastern North America.* Youssef M.A. Hashash, Joseph A. Harmon, Okan Ilhan, Grace A. Parker, and Jonathan P. Stewart. March 2017.
- PEER 2017/04** *Expert Panel Recommendations for Ergodic Site Amplification in Central and Eastern North America.* Jonathan P. Stewart, Grace A. Parker, Joseph P. Harmon, Gail M. Atkinson, David M. Boore, Robert B. Darragh, Walter J. Silva, and Youssef M.A. Hashash. March 2017.
- PEER 2017/03** *NGA-East Ground-Motion Models for the U.S. Geological Survey National Seismic Hazard Maps.* Christine A. Goulet, Yousef Bozorgnia, Nicolas Kuehn, Linda Al Atik, Robert R. Youngs, Robert W. Graves, and Gail M. Atkinson. March 2017.

- PEER 2017/02** *U.S.–New Zealand–Japan Workshop: Liquefaction-Induced Ground Movements Effects, University of California, Berkeley, California, 2–4 November 2016.* Jonathan D. Bray, Ross W. Boulanger, Misko Cubrinovski, Kohji Tokimatsu, Steven L. Kramer, Thomas O'Rourke, Ellen Rathje, Russell A. Green, Peter K. Robinson, and Christine Z. Beyzaei. March 2017.
- PEER 2017/01** *2016 PEER Annual Report.* Khalid M. Mosalam, Amarnath Kasalanati, and Grace Kang. March 2017.
- PEER 2016/10** *Performance-Based Robust Nonlinear Seismic Analysis with Application to Reinforced Concrete Bridge Systems.* Xiao Ling and Khalid M. Mosalam. December 2016.
- PEER 2017/09** *Segmental Displacement Control Design for Seismically Isolated Bridges,* Kenneth A. Ogorzalek and Stephen A. Mahin. December 2016.
- PEER 2016/08** *Resilience of Critical Structures, Infrastructure, and Communities.* Gian Paolo Cimellaro, Ali Zamani-Noori, Omar Kamouh, Vesna Terzic, and Stephen A. Mahin. December 2016.
- PEER 2016/07** *Hybrid Simulation Theory for a Classical Nonlinear Dynamical System.* Paul L. Drazin and Sanjay Govindjee. September 2016.
- PEER 2016/06** *California Earthquake Early Warning System Benefit Study.* Laurie A. Johnson, Sharyl Rabinovici, Grace S. Kang, and Stephen A. Mahin. July 2006.
- PEER 2016/05** *Ground-Motion Prediction Equations for Arias Intensity Consistent with the NGA-West2 Ground-Motion Models.* Charlotte Abrahamson, Hao-Jun Michael Shi, and Brian Yang. July 2016.
- PEER 2016/04** *The M_w 6.0 South Napa Earthquake of August 24, 2014: A Wake-Up Call for Renewed Investment in Seismic Resilience Across California.* Prepared for the California Seismic Safety Commission, Laurie A. Johnson and Stephen A. Mahin. May 2016.
- PEER 2016/03** *Simulation Confidence in Tsunami-Driven Overland Flow.* Patrick Lynett. May 2016.
- PEER 2016/02** *Semi-Automated Procedure for Windowing time Series and Computing Fourier Amplitude Spectra for the NGA-West2 Database.* Tadahiro Kishida, Olga-Joan Ktenidou, Robert B. Darragh, and Walter J. Silva. May 2016.
- PEER 2016/01** *A Methodology for the Estimation of Kappa (κ) from Large Datasets: Example Application to Rock Sites in the NGA-East Database and Implications on Design Motions.* Olga-Joan Ktenidou, Norman A. Abrahamson, Robert B. Darragh, and Walter J. Silva. April 2016.
- PEER 2015/13** *Self-Centering Precast Concrete Dual-Steel-Shell Columns for Accelerated Bridge Construction: Seismic Performance, Analysis, and Design.* Gabriele Guerrini, José I. Restrepo, Athanassios Vervelidis, and Milena Massari. December 2015.
- PEER 2015/12** *Shear-Flexure Interaction Modeling for Reinforced Concrete Structural Walls and Columns under Reversed Cyclic Loading.* Kristijan Kolozvari, Kutay Orakcal, and John Wallace. December 2015.
- PEER 2015/11** *Selection and Scaling of Ground Motions for Nonlinear Response History Analysis of Buildings in Performance-Based Earthquake Engineering.* N. Simon Kwong and Anil K. Chopra. December 2015.
- PEER 2015/10** *Structural Behavior of Column-Bent Cap Beam-Box Girder Systems in Reinforced Concrete Bridges Subjected to Gravity and Seismic Loads. Part II: Hybrid Simulation and Post-Test Analysis.* Mohamed A. Moustafa and Khalid M. Mosalam. November 2015.
- PEER 2015/09** *Structural Behavior of Column-Bent Cap Beam-Box Girder Systems in Reinforced Concrete Bridges Subjected to Gravity and Seismic Loads. Part I: Pre-Test Analysis and Quasi-Static Experiments.* Mohamed A. Moustafa and Khalid M. Mosalam. September 2015.
- PEER 2015/08** *NGA-East: Adjustments to Median Ground-Motion Models for Center and Eastern North America.* August 2015.
- PEER 2015/07** *NGA-East: Ground-Motion Standard-Deviation Models for Central and Eastern North America.* Linda Al Atik. June 2015.
- PEER 2015/06** *Adjusting Ground-Motion Intensity Measures to a Reference Site for which $V_{S30} = 3000$ m/sec.* David M. Boore. May 2015.
- PEER 2015/05** *Hybrid Simulation of Seismic Isolation Systems Applied to an APR-1400 Nuclear Power Plant.* Andreas H. Schellenberg, Alireza Sarebanha, Matthew J. Schoettler, Gilberto Mosqueda, Gianmario Benzoni, and Stephen A. Mahin. April 2015.
- PEER 2015/04** *NGA-East: Median Ground-Motion Models for the Central and Eastern North America Region.* April 2015.
- PEER 2015/03** *Single Series Solution for the Rectangular Fiber-Reinforced Elastomeric Isolator Compression Modulus.* James M. Kelly and Niel C. Van Engelen. March 2015.

- PEER 2015/02** *A Full-Scale, Single-Column Bridge Bent Tested by Shake-Table Excitation.* Matthew J. Schoettler, José I. Restrepo, Gabriele Guerrini, David E. Duck, and Francesco Carrea. March 2015.
- PEER 2015/01** *Concrete Column Blind Prediction Contest 2010: Outcomes and Observations.* Vesna Terzic, Matthew J. Schoettler, José I. Restrepo, and Stephen A Mahin. March 2015.
- PEER 2014/20** *Stochastic Modeling and Simulation of Near-Fault Ground Motions for Performance-Based Earthquake Engineering.* Mayssa Dabaghi and Armen Der Kiureghian. December 2014.
- PEER 2014/19** *Seismic Response of a Hybrid Fiber-Reinforced Concrete Bridge Column Detailed for Accelerated Bridge Construction.* Wilson Nguyen, William Trono, Marios Panagiotou, and Claudia P. Ostertag. December 2014.
- PEER 2014/18** *Three-Dimensional Beam-Truss Model for Reinforced Concrete Walls and Slabs Subjected to Cyclic Static or Dynamic Loading.* Yuan Lu, Marios Panagiotou, and Ioannis Koutromanos. December 2014.
- PEER 2014/17** *PEER NGA-East Database.* Christine A. Goulet, Tadahiro Kishida, Timothy D. Ancheta, Chris H. Cramer, Robert B. Darragh, Walter J. Silva, Youssef M.A. Hashash, Joseph Harmon, Jonathan P. Stewart, Katie E. Wooddell, and Robert R. Youngs. October 2014.
- PEER 2014/16** *Guidelines for Performing Hazard-Consistent One-Dimensional Ground Response Analysis for Ground Motion Prediction.* Jonathan P. Stewart, Kioumars Afshari, and Youssef M.A. Hashash. October 2014.
- PEER 2014/15** *NGA-East Regionalization Report: Comparison of Four Crustal Regions within Central and Eastern North America using Waveform Modeling and 5%-Damped Pseudo-Spectral Acceleration Response.* Jennifer Dreiling, Marius P. Isken, Walter D. Mooney, Martin C. Chapman, and Richard W. Godbee. October 2014.
- PEER 2014/14** *Scaling Relations between Seismic Moment and Rupture Area of Earthquakes in Stable Continental Regions.* Paul Somerville. August 2014.
- PEER 2014/13** *PEER Preliminary Notes and Observations on the August 24, 2014, South Napa Earthquake.* Grace S. Kang and Stephen A. Mahin, Editors. September 2014.
- PEER 2014/12** *Reference-Rock Site Conditions for Central and Eastern North America: Part II – Attenuation (Kappa) Definition.* Kenneth W. Campbell, Youssef M.A. Hashash, Byungmin Kim, Albert R. Kottke, Ellen M. Rathje, Walter J. Silva, and Jonathan P. Stewart. August 2014.
- PEER 2014/11** *Reference-Rock Site Conditions for Central and Eastern North America: Part I - Velocity Definition.* Youssef M.A. Hashash, Albert R. Kottke, Jonathan P. Stewart, Kenneth W. Campbell, Byungmin Kim, Ellen M. Rathje, Walter J. Silva, Sissy Nikolaou, and Cheryl Moss. August 2014.
- PEER 2014/10** *Evaluation of Collapse and Non-Collapse of Parallel Bridges Affected by Liquefaction and Lateral Spreading.* Benjamin Turner, Scott J. Brandenberg, and Jonathan P. Stewart. August 2014.
- PEER 2014/09** *PEER Arizona Strong-Motion Database and GMPEs Evaluation.* Tadahiro Kishida, Robert E. Kayen, Olga-Joan Ktenidou, Walter J. Silva, Robert B. Darragh, and Jennie Watson-Lamprey. June 2014.
- PEER 2014/08** *Unbonded Pretensioned Bridge Columns with Rocking Detail.* Jeffrey A. Schaefer, Bryan Kennedy, Marc O. Eberhard, and John F. Stanton. June 2014.
- PEER 2014/07** *Northridge 20 Symposium Summary Report: Impacts, Outcomes, and Next Steps.* May 2014.
- PEER 2014/06** *Report of the Tenth Planning Meeting of NEES/E-Defense Collaborative Research on Earthquake Engineering.* December 2013.
- PEER 2014/05** *Seismic Velocity Site Characterization of Thirty-One Chilean Seismometer Stations by Spectral Analysis of Surface Wave Dispersion.* Robert Kayen, Brad D. Carkin, Skye Corbet, Camilo Pinilla, Allan Ng, Edward Gorbis, and Christine Truong. April 2014.
- PEER 2014/04** *Effect of Vertical Acceleration on Shear Strength of Reinforced Concrete Columns.* Hyerin Lee and Khalid M. Mosalam. April 2014.
- PEER 2014/03** *Retest of Thirty-Year-Old Neoprene Isolation Bearings.* James M. Kelly and Niel C. Van Engelen. March 2014.
- PEER 2014/02** *Theoretical Development of Hybrid Simulation Applied to Plate Structures.* Ahmed A. Bakhty, Khalid M. Mosalam, and Sanjay Govindjee. January 2014.
- PEER 2014/01** *Performance-Based Seismic Assessment of Skewed Bridges.* Peyman Kaviani, Farzin Zareian, and Ertugrul Taciroglu. January 2014.
- PEER 2013/26** *Urban Earthquake Engineering.* Proceedings of the U.S.-Iran Seismic Workshop. December 2013.
- PEER 2013/25** *Earthquake Engineering for Resilient Communities: 2013 PEER Internship Program Research Report Collection.* Heidi Tremayne (Editor), Stephen A. Mahin (Editor), Jorge Archbold Monterossa, Matt Brosman, Shelly Dean, Katherine deLaveaga, Curtis Fong, Donovan Holder, Rakeeb Khan, Elizabeth Jachens, David Lam, Daniela

Martinez Lopez, Mara Minner, Geffen Oren, Julia Pavicic, Melissa Quinonez, Lorena Rodriguez, Sean Salazar, Kelli Slaven, Vivian Steyert, Jenny Taing, and Salvador Tena. December 2013.

- PEER 2013/24** *NGA-West2 Ground Motion Prediction Equations for Vertical Ground Motions.* September 2013.
- PEER 2013/23** *Coordinated Planning and Preparedness for Fire Following Major Earthquakes.* Charles Scawthorn. November 2013.
- PEER 2013/22** *GEM-PEER Task 3 Project: Selection of a Global Set of Ground Motion Prediction Equations.* Jonathan P. Stewart, John Douglas, Mohammad B. Javanbarg, Carola Di Alessandro, Yousef Bozorgnia, Norman A. Abrahamson, David M. Boore, Kenneth W. Campbell, Elise Delavaud, Mustafa Erdik, and Peter J. Stafford. December 2013.
- PEER 2013/21** *Seismic Design and Performance of Bridges with Columns on Rocking Foundations.* Grigorios Antonellis and Marios Panagiotou. September 2013.
- PEER 2013/20** *Experimental and Analytical Studies on the Seismic Behavior of Conventional and Hybrid Braced Frames.* Jiun-Wei Lai and Stephen A. Mahin. September 2013.
- PEER 2013/19** *Toward Resilient Communities: A Performance-Based Engineering Framework for Design and Evaluation of the Built Environment.* Michael William Mieler, Bozidar Stojadinovic, Robert J. Budnitz, Stephen A. Mahin, and Mary C. Comerio. September 2013.
- PEER 2013/18** *Identification of Site Parameters that Improve Predictions of Site Amplification.* Ellen M. Rathje and Sara Navidi. July 2013.
- PEER 2013/17** *Response Spectrum Analysis of Concrete Gravity Dams Including Dam-Water-Foundation Interaction.* Arnkjell Løkke and Anil K. Chopra. July 2013.
- PEER 2013/16** *Effect of Hoop Reinforcement Spacing on the Cyclic Response of Large Reinforced Concrete Special Moment Frame Beams.* Marios Panagiotou, Tea Visnjic, Grigorios Antonellis, Panagiotis Galanis, and Jack P. Moehle. June 2013.
- PEER 2013/15** *A Probabilistic Framework to Include the Effects of Near-Fault Directivity in Seismic Hazard Assessment.* Shrey Kumar Shahi, Jack W. Baker. October 2013.
- PEER 2013/14** *Hanging-Wall Scaling using Finite-Fault Simulations.* Jennifer L. Donahue and Norman A. Abrahamson. September 2013.
- PEER 2013/13** *Semi-Empirical Nonlinear Site Amplification and its Application in NEHRP Site Factors.* Jonathan P. Stewart and Emel Seyhan. November 2013.
- PEER 2013/12** *Nonlinear Horizontal Site Response for the NGA-West2 Project.* Ronnie Kamai, Norman A. Abramson, Walter J. Silva. May 2013.
- PEER 2013/11** *Epistemic Uncertainty for NGA-West2 Models.* Linda Al Atik and Robert R. Youngs. May 2013.
- PEER 2013/10** *NGA-West 2 Models for Ground-Motion Directionality.* Shrey K. Shahi and Jack W. Baker. May 2013.
- PEER 2013/09** *Final Report of the NGA-West2 Directivity Working Group.* Paul Spudich, Jeffrey R. Bayless, Jack W. Baker, Brian S.J. Chiou, Badie Rowshandel, Shrey Shahi, and Paul Somerville. May 2013.
- PEER 2013/08** *NGA-West2 Model for Estimating Average Horizontal Values of Pseudo-Absolute Spectral Accelerations Generated by Crustal Earthquakes.* I. M. Idriss. May 2013.
- PEER 2013/07** *Update of the Chiou and Youngs NGA Ground Motion Model for Average Horizontal Component of Peak Ground Motion and Response Spectra.* Brian Chiou and Robert Youngs. May 2013.
- PEER 2013/06** *NGA-West2 Campbell-Bozorgnia Ground Motion Model for the Horizontal Components of PGA, PGV, and 5%-Damped Elastic Pseudo-Acceleration Response Spectra for Periods Ranging from 0.01 to 10 sec.* Kenneth W. Campbell and Yousef Bozorgnia. May 2013.
- PEER 2013/05** *NGA-West 2 Equations for Predicting Response Spectral Accelerations for Shallow Crustal Earthquakes.* David M. Boore, Jonathan P. Stewart, Emel Seyhan, and Gail M. Atkinson. May 2013.
- PEER 2013/04** *Update of the AS08 Ground-Motion Prediction Equations Based on the NGA-West2 Data Set.* Norman Abrahamson, Walter Silva, and Ronnie Kamai. May 2013.
- PEER 2013/03** *PEER NGA-West2 Database.* Timothy D. Ancheta, Robert B. Darragh, Jonathan P. Stewart, Emel Seyhan, Walter J. Silva, Brian S.J. Chiou, Katie E. Wooddell, Robert W. Graves, Albert R. Kottke, David M. Boore, Tadahihiro Kishida, and Jennifer L. Donahue. May 2013.
- PEER 2013/02** *Hybrid Simulation of the Seismic Response of Squat Reinforced Concrete Shear Walls.* Catherine A. Whyte and Bozidar Stojadinovic. May 2013.

- PEER 2013/01** *Housing Recovery in Chile: A Qualitative Mid-program Review.* Mary C. Comerio. February 2013.
- PEER 2012/08** *Guidelines for Estimation of Shear Wave Velocity.* Bernard R. Wair, Jason T. DeJong, and Thomas Shantz. December 2012.
- PEER 2012/07** *Earthquake Engineering for Resilient Communities: 2012 PEER Internship Program Research Report Collection.* Heidi Tremayne (Editor), Stephen A. Mahin (Editor), Collin Anderson, Dustin Cook, Michael Erceg, Carlos Esparza, Jose Jimenez, Dorian Krausz, Andrew Lo, Stephanie Lopez, Nicole McCurdy, Paul Shipman, Alexander Strum, Eduardo Vega. December 2012.
- PEER 2012/06** *Fragilities for Precarious Rocks at Yucca Mountain.* Matthew D. Purvance, Rasool Anooshehpour, and James N. Brune. December 2012.
- PEER 2012/05** *Development of Simplified Analysis Procedure for Piles in Laterally Spreading Layered Soils.* Christopher R. McGann, Pedro Arduino, and Peter Mackenzie-Helwein. December 2012.
- PEER 2012/04** *Unbonded Pre-Tensioned Columns for Bridges in Seismic Regions.* Phillip M. Davis, Todd M. Janes, Marc O. Eberhard, and John F. Stanton. December 2012.
- PEER 2012/03** *Experimental and Analytical Studies on Reinforced Concrete Buildings with Seismically Vulnerable Beam-Column Joints.* Sangjoon Park and Khalid M. Mosalam. October 2012.
- PEER 2012/02** *Seismic Performance of Reinforced Concrete Bridges Allowed to Uplift during Multi-Directional Excitation.* Andres Oscar Espinoza and Stephen A. Mahin. July 2012.
- PEER 2012/01** *Spectral Damping Scaling Factors for Shallow Crustal Earthquakes in Active Tectonic Regions.* Sanaz Rezaeian, Yousef Bozorgnia, I. M. Idriss, Kenneth Campbell, Norman Abrahamson, and Walter Silva. July 2012.
- PEER 2011/10** *Earthquake Engineering for Resilient Communities: 2011 PEER Internship Program Research Report Collection.* Heidi Faison and Stephen A. Mahin, Editors. December 2011.
- PEER 2011/09** *Calibration of Semi-Stochastic Procedure for Simulating High-Frequency Ground Motions.* Jonathan P. Stewart, Emel Seyhan, and Robert W. Graves. December 2011.
- PEER 2011/08** *Water Supply in regard to Fire Following Earthquake.* Charles Scawthorn. November 2011.
- PEER 2011/07** *Seismic Risk Management in Urban Areas.* Proceedings of a U.S.-Iran-Turkey Seismic Workshop. September 2011.
- PEER 2011/06** *The Use of Base Isolation Systems to Achieve Complex Seismic Performance Objectives.* Troy A. Morgan and Stephen A. Mahin. July 2011.
- PEER 2011/05** *Case Studies of the Seismic Performance of Tall Buildings Designed by Alternative Means.* Task 12 Report for the Tall Buildings Initiative. Jack Moehle, Yousef Bozorgnia, Nirmal Jayaram, Pierson Jones, Mohsen Rahnama, Nilesh Shome, Zeynep Tuna, John Wallace, Tony Yang, and Farzin Zareian. July 2011.
- PEER 2011/04** *Recommended Design Practice for Pile Foundations in Laterally Spreading Ground.* Scott A. Ashford, Ross W. Boulanger, and Scott J. Brandenburg. June 2011.
- PEER 2011/03** *New Ground Motion Selection Procedures and Selected Motions for the PEER Transportation Research Program.* Jack W. Baker, Ting Lin, Shrey K. Shahi, and Nirmal Jayaram. March 2011.
- PEER 2011/02** *A Bayesian Network Methodology for Infrastructure Seismic Risk Assessment and Decision Support.* Michelle T. Bensi, Armen Der Kiureghian, and Daniel Straub. March 2011.
- PEER 2011/01** *Demand Fragility Surfaces for Bridges in Liquefied and Laterally Spreading Ground.* Scott J. Brandenburg, Jian Zhang, Pirooz Kashighandi, Yili Huo, and Minxing Zhao. March 2011.
- PEER 2010/05** *Guidelines for Performance-Based Seismic Design of Tall Buildings.* Developed by the Tall Buildings Initiative. November 2010.
- PEER 2010/04** *Application Guide for the Design of Flexible and Rigid Bus Connections between Substation Equipment Subjected to Earthquakes.* Jean-Bernard Dastous and Armen Der Kiureghian. September 2010.
- PEER 2010/03** *Shear Wave Velocity as a Statistical Function of Standard Penetration Test Resistance and Vertical Effective Stress at Caltrans Bridge Sites.* Scott J. Brandenburg, Naresh Bellana, and Thomas Shantz. June 2010.
- PEER 2010/02** *Stochastic Modeling and Simulation of Ground Motions for Performance-Based Earthquake Engineering.* Sanaz Rezaeian and Armen Der Kiureghian. June 2010.
- PEER 2010/01** *Structural Response and Cost Characterization of Bridge Construction Using Seismic Performance Enhancement Strategies.* Ady Aviram, Božidar Stojadinović, Gustavo J. Parra-Montesinos, and Kevin R. Mackie. March 2010.

- PEER 2009/03** *The Integration of Experimental and Simulation Data in the Study of Reinforced Concrete Bridge Systems Including Soil-Foundation-Structure Interaction.* Matthew Dryden and Gregory L. Fenves. November 2009.
- PEER 2009/02** *Improving Earthquake Mitigation through Innovations and Applications in Seismic Science, Engineering, Communication, and Response.* Proceedings of a U.S.-Iran Seismic Workshop. October 2009.
- PEER 2009/01** *Evaluation of Ground Motion Selection and Modification Methods: Predicting Median Interstory Drift Response of Buildings.* Curt B. Haselton, Editor. June 2009.
- PEER 2008/10** *Technical Manual for Strata.* Albert R. Kottke and Ellen M. Rathje. February 2009.
- PEER 2008/09** *NGA Model for Average Horizontal Component of Peak Ground Motion and Response Spectra.* Brian S.-J. Chiou and Robert R. Youngs. November 2008.
- PEER 2008/08** *Toward Earthquake-Resistant Design of Concentrically Braced Steel Structures.* Patxi Uriz and Stephen A. Mahin. November 2008.
- PEER 2008/07** *Using OpenSees for Performance-Based Evaluation of Bridges on Liquefiable Soils.* Stephen L. Kramer, Pedro Arduino, and HyungSuk Shin. November 2008.
- PEER 2008/06** *Shaking Table Tests and Numerical Investigation of Self-Centering Reinforced Concrete Bridge Columns.* Hyung IL Jeong, Junichi Sakai, and Stephen A. Mahin. September 2008.
- PEER 2008/05** *Performance-Based Earthquake Engineering Design Evaluation Procedure for Bridge Foundations Undergoing Liquefaction-Induced Lateral Ground Displacement.* Christian A. Ledezma and Jonathan D. Bray. August 2008.
- PEER 2008/04** *Benchmarking of Nonlinear Geotechnical Ground Response Analysis Procedures.* Jonathan P. Stewart, Annie On-Lei Kwok, Youssef M. A. Hashash, Neven Matasovic, Robert Pyke, Zhiliang Wang, and Zhaohui Yang. August 2008.
- PEER 2008/03** *Guidelines for Nonlinear Analysis of Bridge Structures in California.* Ady Aviram, Kevin R. Mackie, and Božidar Stojadinović. August 2008.
- PEER 2008/02** *Treatment of Uncertainties in Seismic-Risk Analysis of Transportation Systems.* Evangelos Stergiou and Anne S. Kiremidjian. July 2008.
- PEER 2008/01** *Seismic Performance Objectives for Tall Buildings.* William T. Holmes, Charles Kircher, William Petak, and Nabih Youssef. August 2008.
- PEER 2007/12** *An Assessment to Benchmark the Seismic Performance of a Code-Conforming Reinforced Concrete Moment-Frame Building.* Curt Haselton, Christine A. Goulet, Judith Mitrani-Reiser, James L. Beck, Gregory G. Deierlein, Keith A. Porter, Jonathan P. Stewart, and Ertugrul Taciroglu. August 2008.
- PEER 2007/11** *Bar Buckling in Reinforced Concrete Bridge Columns.* Wayne A. Brown, Dawn E. Lehman, and John F. Stanton. February 2008.
- PEER 2007/10** *Computational Modeling of Progressive Collapse in Reinforced Concrete Frame Structures.* Mohamed M. Talaat and Khalid M. Mosalam. May 2008.
- PEER 2007/09** *Integrated Probabilistic Performance-Based Evaluation of Benchmark Reinforced Concrete Bridges.* Kevin R. Mackie, John-Michael Wong, and Božidar Stojadinović. January 2008.
- PEER 2007/08** *Assessing Seismic Collapse Safety of Modern Reinforced Concrete Moment-Frame Buildings.* Curt B. Haselton and Gregory G. Deierlein. February 2008.
- PEER 2007/07** *Performance Modeling Strategies for Modern Reinforced Concrete Bridge Columns.* Michael P. Berry and Marc O. Eberhard. April 2008.
- PEER 2007/06** *Development of Improved Procedures for Seismic Design of Buried and Partially Buried Structures.* Linda Al Atik and Nicholas Sitar. June 2007.
- PEER 2007/05** *Uncertainty and Correlation in Seismic Risk Assessment of Transportation Systems.* Renee G. Lee and Anne S. Kiremidjian. July 2007.
- PEER 2007/04** *Numerical Models for Analysis and Performance-Based Design of Shallow Foundations Subjected to Seismic Loading.* Sivapalan Gajan, Tara C. Hutchinson, Bruce L. Kutter, Prishati Raychowdhury, José A. Ugalde, and Jonathan P. Stewart. May 2008.
- PEER 2007/03** *Beam-Column Element Model Calibrated for Predicting Flexural Response Leading to Global Collapse of RC Frame Buildings.* Curt B. Haselton, Abbie B. Liel, Sarah Taylor Lange, and Gregory G. Deierlein. May 2008.
- PEER 2007/02** *Campbell-Bozorgnia NGA Ground Motion Relations for the Geometric Mean Horizontal Component of Peak and Spectral Ground Motion Parameters.* Kenneth W. Campbell and Yousef Bozorgnia. May 2007.

- PEER 2007/01** *Boore-Atkinson NGA Ground Motion Relations for the Geometric Mean Horizontal Component of Peak and Spectral Ground Motion Parameters.* David M. Boore and Gail M. Atkinson. May 2007.
- PEER 2006/12** *Societal Implications of Performance-Based Earthquake Engineering.* Peter J. May. May 2007.
- PEER 2006/11** *Probabilistic Seismic Demand Analysis Using Advanced Ground Motion Intensity Measures, Attenuation Relationships, and Near-Fault Effects.* Polsak Tothong and C. Allin Cornell. March 2007.
- PEER 2006/10** *Application of the PEER PBEE Methodology to the I-880 Viaduct.* Sashi Kunnath. February 2007.
- PEER 2006/09** *Quantifying Economic Losses from Travel Forgone Following a Large Metropolitan Earthquake.* James Moore, Sungbin Cho, Yue Yue Fan, and Stuart Werner. November 2006.
- PEER 2006/08** *Vector-Valued Ground Motion Intensity Measures for Probabilistic Seismic Demand Analysis.* Jack W. Baker and C. Allin Cornell. October 2006.
- PEER 2006/07** *Analytical Modeling of Reinforced Concrete Walls for Predicting Flexural and Coupled-Shear-Flexural Responses.* Kutay Orakcal, Leonardo M. Massone, and John W. Wallace. October 2006.
- PEER 2006/06** *Nonlinear Analysis of a Soil-Drilled Pier System under Static and Dynamic Axial Loading.* Gang Wang and Nicholas Sitar. November 2006.
- PEER 2006/05** *Advanced Seismic Assessment Guidelines.* Paolo Bazzurro, C. Allin Cornell, Charles Menun, Maziar Motahari, and Nicolas Luco. September 2006.
- PEER 2006/04** *Probabilistic Seismic Evaluation of Reinforced Concrete Structural Components and Systems.* Tae Hyung Lee and Khalid M. Mosalam. August 2006.
- PEER 2006/03** *Performance of Lifelines Subjected to Lateral Spreading.* Scott A. Ashford and Teerawut Juinarongrit. July 2006.
- PEER 2006/02** *Pacific Earthquake Engineering Research Center Highway Demonstration Project.* Anne Kiremidjian, James Moore, Yue Yue Fan, Nesrin Basoz, Ozgur Yazali, and Meredith Williams. April 2006.
- PEER 2006/01** *Bracing Berkeley. A Guide to Seismic Safety on the UC Berkeley Campus.* Mary C. Comerio, Stephen Tobriner, and Ariane Fehrenkamp. January 2006.
- PEER 2005/17** *Earthquake Simulation Tests on Reducing Residual Displacements of Reinforced Concrete Bridges.* Junichi Sakai, Stephen A Mahin, and Andres Espinoza. December 2005.
- PEER 2005/16** *Seismic Response and Reliability of Electrical Substation Equipment and Systems.* Junho Song, Armen Der Kiureghian, and Jerome L. Sackman. April 2006.
- PEER 2005/15** *CPT-Based Probabilistic Assessment of Seismic Soil Liquefaction Initiation.* R. E. S. Moss, R. B. Seed, R. E. Kayen, J. P. Stewart, and A. Der Kiureghian. April 2006.
- PEER 2005/14** *Workshop on Modeling of Nonlinear Cyclic Load-Deformation Behavior of Shallow Foundations.* Bruce L. Kutter, Geoffrey Martin, Tara Hutchinson, Chad Harden, Sivapalan Gajan, and Justin Phalen. March 2006.
- PEER 2005/13** *Stochastic Characterization and Decision Bases under Time-Dependent Aftershock Risk in Performance-Based Earthquake Engineering.* Gee Liek Yeo and C. Allin Cornell. July 2005.
- PEER 2005/12** *PEER Testbed Study on a Laboratory Building: Exercising Seismic Performance Assessment.* Mary C. Comerio, Editor. November 2005.
- PEER 2005/11** *Van Nuys Hotel Building Testbed Report: Exercising Seismic Performance Assessment.* Helmut Krawinkler, Editor. October 2005.
- PEER 2005/10** *First NEES/E-Defense Workshop on Collapse Simulation of Reinforced Concrete Building Structures.* September 2005.
- PEER 2005/09** *Test Applications of Advanced Seismic Assessment Guidelines.* Joe Maffei, Karl Telleen, Danya Mohr, William Holmes, and Yuki Nakayama. August 2006.
- PEER 2005/08** *Damage Accumulation in Lightly Confined Reinforced Concrete Bridge Columns.* R. Tyler Ranf, Jared M. Nelson, Zach Price, Marc O. Eberhard, and John F. Stanton. April 2006.
- PEER 2005/07** *Experimental and Analytical Studies on the Seismic Response of Freestanding and Anchored Laboratory Equipment.* Dimitrios Konstantinidis and Nicos Makris. January 2005.
- PEER 2005/06** *Global Collapse of Frame Structures under Seismic Excitations.* Luis F. Ibarra and Helmut Krawinkler. September 2005.
- PEER 2005/05** *Performance Characterization of Bench- and Shelf-Mounted Equipment.* Samit Ray Chaudhuri and Tara C. Hutchinson. May 2006.

- PEER 2005/04** *Numerical Modeling of the Nonlinear Cyclic Response of Shallow Foundations.* Chad Harden, Tara Hutchinson, Geoffrey R. Martin, and Bruce L. Kutter. August 2005.
- PEER 2005/03** *A Taxonomy of Building Components for Performance-Based Earthquake Engineering.* Keith A. Porter. September 2005.
- PEER 2005/02** *Fragility Basis for California Highway Overpass Bridge Seismic Decision Making.* Kevin R. Mackie and Božidar Stojadinović. June 2005.
- PEER 2005/01** *Empirical Characterization of Site Conditions on Strong Ground Motion.* Jonathan P. Stewart, Yoojoong Choi, and Robert W. Graves. June 2005.
- PEER 2004/09** *Electrical Substation Equipment Interaction: Experimental Rigid Conductor Studies.* Christopher Stearns and André Filiatrault. February 2005.
- PEER 2004/08** *Seismic Qualification and Fragility Testing of Line Break 550-kV Disconnect Switches.* Shakhzod M. Takhirov, Gregory L. Fenves, and Eric Fujisaki. January 2005.
- PEER 2004/07** *Ground Motions for Earthquake Simulator Qualification of Electrical Substation Equipment.* Shakhzod M. Takhirov, Gregory L. Fenves, Eric Fujisaki, and Don Clyde. January 2005.
- PEER 2004/06** *Performance-Based Regulation and Regulatory Regimes.* Peter J. May and Chris Koski. September 2004.
- PEER 2004/05** *Performance-Based Seismic Design Concepts and Implementation: Proceedings of an International Workshop.* Peter Fajfar and Helmut Krawinkler, Editors. September 2004.
- PEER 2004/04** *Seismic Performance of an Instrumented Tilt-up Wall Building.* James C. Anderson and Vitelmo V. Bertero. July 2004.
- PEER 2004/03** *Evaluation and Application of Concrete Tilt-up Assessment Methodologies.* Timothy Graf and James O. Malley. October 2004.
- PEER 2004/02** *Analytical Investigations of New Methods for Reducing Residual Displacements of Reinforced Concrete Bridge Columns.* Junichi Sakai and Stephen A. Mahin. August 2004.
- PEER 2004/01** *Seismic Performance of Masonry Buildings and Design Implications.* Kerri Anne Taeko Tokoro, James C. Anderson, and Vitelmo V. Bertero. February 2004.
- PEER 2003/18** *Performance Models for Flexural Damage in Reinforced Concrete Columns.* Michael Berry and Marc Eberhard. August 2003.
- PEER 2003/17** *Predicting Earthquake Damage in Older Reinforced Concrete Beam-Column Joints.* Catherine Pagni and Laura Lowes. October 2004.
- PEER 2003/16** *Seismic Demands for Performance-Based Design of Bridges.* Kevin Mackie and Božidar Stojadinović. August 2003.
- PEER 2003/15** *Seismic Demands for Nondeteriorating Frame Structures and Their Dependence on Ground Motions.* Ricardo Antonio Medina and Helmut Krawinkler. May 2004.
- PEER 2003/14** *Finite Element Reliability and Sensitivity Methods for Performance-Based Earthquake Engineering.* Terje Haukaas and Armen Der Kiureghian. April 2004.
- PEER 2003/13** *Effects of Connection Hysteretic Degradation on the Seismic Behavior of Steel Moment-Resisting Frames.* Janise E. Rodgers and Stephen A. Mahin. March 2004.
- PEER 2003/12** *Implementation Manual for the Seismic Protection of Laboratory Contents: Format and Case Studies.* William T. Holmes and Mary C. Comerio. October 2003.
- PEER 2003/11** *Fifth U.S.-Japan Workshop on Performance-Based Earthquake Engineering Methodology for Reinforced Concrete Building Structures.* February 2004.
- PEER 2003/10** *A Beam-Column Joint Model for Simulating the Earthquake Response of Reinforced Concrete Frames.* Laura N. Lowes, Nilanjan Mitra, and Arash Altoontash. February 2004.
- PEER 2003/09** *Sequencing Repairs after an Earthquake: An Economic Approach.* Marco Casari and Simon J. Wilkie. April 2004.
- PEER 2003/08** *A Technical Framework for Probability-Based Demand and Capacity Factor Design (DCFD) Seismic Formats.* Fatemeh Jalayer and C. Allin Cornell. November 2003.
- PEER 2003/07** *Uncertainty Specification and Propagation for Loss Estimation Using FOSM Methods.* Jack W. Baker and C. Allin Cornell. September 2003.

- PEER 2003/06** *Performance of Circular Reinforced Concrete Bridge Columns under Bidirectional Earthquake Loading.* Mahmoud M. Hachem, Stephen A. Mahin, and Jack P. Moehle. February 2003.
- PEER 2003/05** *Response Assessment for Building-Specific Loss Estimation.* Eduardo Miranda and Shahram Taghavi. September 2003.
- PEER 2003/04** *Experimental Assessment of Columns with Short Lap Splices Subjected to Cyclic Loads.* Murat Melek, John W. Wallace, and Joel Conte. April 2003.
- PEER 2003/03** *Probabilistic Response Assessment for Building-Specific Loss Estimation.* Eduardo Miranda and Hesameddin Aslani. September 2003.
- PEER 2003/02** *Software Framework for Collaborative Development of Nonlinear Dynamic Analysis Program.* Jun Peng and Kincho H. Law. September 2003.
- PEER 2003/01** *Shake Table Tests and Analytical Studies on the Gravity Load Collapse of Reinforced Concrete Frames.* Kenneth John Elwood and Jack P. Moehle. November 2003.
- PEER 2002/24** *Performance of Beam to Column Bridge Joints Subjected to a Large Velocity Pulse.* Natalie Gibson, André Filiatrault, and Scott A. Ashford. April 2002.
- PEER 2002/23** *Effects of Large Velocity Pulses on Reinforced Concrete Bridge Columns.* Greg L. Orozco and Scott A. Ashford. April 2002.
- PEER 2002/22** *Characterization of Large Velocity Pulses for Laboratory Testing.* Kenneth E. Cox and Scott A. Ashford. April 2002.
- PEER 2002/21** *Fourth U.S.-Japan Workshop on Performance-Based Earthquake Engineering Methodology for Reinforced Concrete Building Structures.* December 2002.
- PEER 2002/20** *Barriers to Adoption and Implementation of PBEE Innovations.* Peter J. May. August 2002.
- PEER 2002/19** *Economic-Engineered Integrated Models for Earthquakes: Socioeconomic Impacts.* Peter Gordon, James E. Moore II, and Harry W. Richardson. July 2002.
- PEER 2002/18** *Assessment of Reinforced Concrete Building Exterior Joints with Substandard Details.* Chris P. Pantelides, Jon Hansen, Justin Nadauld, and Lawrence D. Reaveley. May 2002.
- PEER 2002/17** *Structural Characterization and Seismic Response Analysis of a Highway Overcrossing Equipped with Elastomeric Bearings and Fluid Dampers: A Case Study.* Nicos Makris and Jian Zhang. November 2002.
- PEER 2002/16** *Estimation of Uncertainty in Geotechnical Properties for Performance-Based Earthquake Engineering.* Allen L. Jones, Steven L. Kramer, and Pedro Arduino. December 2002.
- PEER 2002/15** *Seismic Behavior of Bridge Columns Subjected to Various Loading Patterns.* Asadollah Esmaeily-Gh. and Yan Xiao. December 2002.
- PEER 2002/14** *Inelastic Seismic Response of Extended Pile Shaft Supported Bridge Structures.* T.C. Hutchinson, R.W. Boulanger, Y.H. Chai, and I.M. Idriss. December 2002.
- PEER 2002/13** *Probabilistic Models and Fragility Estimates for Bridge Components and Systems.* Paolo Gardoni, Armen Der Kiureghian, and Khalid M. Mosalam. June 2002.
- PEER 2002/12** *Effects of Fault Dip and Slip Rake on Near-Source Ground Motions: Why Chi-Chi Was a Relatively Mild M7.6 Earthquake.* Brad T. Aagaard, John F. Hall, and Thomas H. Heaton. December 2002.
- PEER 2002/11** *Analytical and Experimental Study of Fiber-Reinforced Strip Isolators.* James M. Kelly and Shakhzod M. Takhirov. September 2002.
- PEER 2002/10** *Centrifuge Modeling of Settlement and Lateral Spreading with Comparisons to Numerical Analyses.* Sivapalan Gajan and Bruce L. Kutter. January 2003.
- PEER 2002/09** *Documentation and Analysis of Field Case Histories of Seismic Compression during the 1994 Northridge, California, Earthquake.* Jonathan P. Stewart, Patrick M. Smith, Daniel H. Whang, and Jonathan D. Bray. October 2002.
- PEER 2002/08** *Component Testing, Stability Analysis and Characterization of Buckling-Restrained Unbonded Braces™.* Cameron Black, Nicos Makris, and Ian Aiken. September 2002.
- PEER 2002/07** *Seismic Performance of Pile-Wharf Connections.* Charles W. Roeder, Robert Graff, Jennifer Soderstrom, and Jun Han Yoo. December 2001.
- PEER 2002/06** *The Use of Benefit-Cost Analysis for Evaluation of Performance-Based Earthquake Engineering Decisions.* Richard O. Zerbe and Anthony Falit-Baiamonte. September 2001.

- PEER 2002/05** *Guidelines, Specifications, and Seismic Performance Characterization of Nonstructural Building Components and Equipment.* André Filiatrault, Constantin Christopoulos, and Christopher Stearns. September 2001.
- PEER 2002/04** *Consortium of Organizations for Strong-Motion Observation Systems and the Pacific Earthquake Engineering Research Center Lifelines Program: Invited Workshop on Archiving and Web Dissemination of Geotechnical Data, 4–5 October 2001.* September 2002.
- PEER 2002/03** *Investigation of Sensitivity of Building Loss Estimates to Major Uncertain Variables for the Van Nuys Testbed.* Keith A. Porter, James L. Beck, and Rustem V. Shaikhutdinov. August 2002.
- PEER 2002/02** *The Third U.S.-Japan Workshop on Performance-Based Earthquake Engineering Methodology for Reinforced Concrete Building Structures.* July 2002.
- PEER 2002/01** *Nonstructural Loss Estimation: The UC Berkeley Case Study.* Mary C. Comerio and John C. Stallmeyer. December 2001.
- PEER 2001/16** *Statistics of SDF-System Estimate of Roof Displacement for Pushover Analysis of Buildings.* Anil K. Chopra, Rakesh K. Goel, and Chatpan Chintanapakdee. December 2001.
- PEER 2001/15** *Damage to Bridges during the 2001 Nisqually Earthquake.* R. Tyler Ranf, Marc O. Eberhard, and Michael P. Berry. November 2001.
- PEER 2001/14** *Rocking Response of Equipment Anchored to a Base Foundation.* Nicos Makris and Cameron J. Black. September 2001.
- PEER 2001/13** *Modeling Soil Liquefaction Hazards for Performance-Based Earthquake Engineering.* Steven L. Kramer and Ahmed-W. Elgamal. February 2001.
- PEER 2001/12** *Development of Geotechnical Capabilities in OpenSees.* Boris Jeremić. September 2001.
- PEER 2001/11** *Analytical and Experimental Study of Fiber-Reinforced Elastomeric Isolators.* James M. Kelly and Shakhzod M. Takhirov. September 2001.
- PEER 2001/10** *Amplification Factors for Spectral Acceleration in Active Regions.* Jonathan P. Stewart, Andrew H. Liu, Yoojoong Choi, and Mehmet B. Baturay. December 2001.
- PEER 2001/09** *Ground Motion Evaluation Procedures for Performance-Based Design.* Jonathan P. Stewart, Shyh-Jeng Chiou, Jonathan D. Bray, Robert W. Graves, Paul G. Somerville, and Norman A. Abrahamson. September 2001.
- PEER 2001/08** *Experimental and Computational Evaluation of Reinforced Concrete Bridge Beam-Column Connections for Seismic Performance.* Clay J. Naito, Jack P. Moehle, and Khalid M. Mosalam. November 2001.
- PEER 2001/07** *The Rocking Spectrum and the Shortcomings of Design Guidelines.* Nicos Makris and Dimitrios Konstantinidis. August 2001.
- PEER 2001/06** *Development of an Electrical Substation Equipment Performance Database for Evaluation of Equipment Fragilities.* Thalia Agninos. April 1999.
- PEER 2001/05** *Stiffness Analysis of Fiber-Reinforced Elastomeric Isolators.* Hsiang-Chuan Tsai and James M. Kelly. May 2001.
- PEER 2001/04** *Organizational and Societal Considerations for Performance-Based Earthquake Engineering.* Peter J. May. April 2001.
- PEER 2001/03** *A Modal Pushover Analysis Procedure to Estimate Seismic Demands for Buildings: Theory and Preliminary Evaluation.* Anil K. Chopra and Rakesh K. Goel. January 2001.
- PEER 2001/02** *Seismic Response Analysis of Highway Overcrossings Including Soil-Structure Interaction.* Jian Zhang and Nicos Makris. March 2001.
- PEER 2001/01** *Experimental Study of Large Seismic Steel Beam-to-Column Connections.* Egor P. Popov and Shakhzod M. Takhirov. November 2000.
- PEER 2000/10** *The Second U.S.-Japan Workshop on Performance-Based Earthquake Engineering Methodology for Reinforced Concrete Building Structures.* March 2000.
- PEER 2000/09** *Structural Engineering Reconnaissance of the August 17, 1999 Earthquake: Kocaeli (Izmit), Turkey.* Halil Sezen, Kenneth J. Elwood, Andrew S. Whittaker, Khalid Mosalam, John J. Wallace, and John F. Stanton. December 2000.
- PEER 2000/08** *Behavior of Reinforced Concrete Bridge Columns Having Varying Aspect Ratios and Varying Lengths of Confinement.* Anthony J. Calderone, Dawn E. Lehman, and Jack P. Moehle. January 2001.
- PEER 2000/07** *Cover-Plate and Flange-Plate Reinforced Steel Moment-Resisting Connections.* Taejin Kim, Andrew S. Whittaker, Amir S. Gilani, Vitelmo V. Bertero, and Shakhzod M. Takhirov. September 2000.

- PEER 2000/06** *Seismic Evaluation and Analysis of 230-kV Disconnect Switches.* Amir S. J. Gilani, Andrew S. Whittaker, Gregory L. Fenves, Chun-Hao Chen, Henry Ho, and Eric Fujisaki. July 2000.
- PEER 2000/05** *Performance-Based Evaluation of Exterior Reinforced Concrete Building Joints for Seismic Excitation.* Chandra Clyde, Chris P. Pantelides, and Lawrence D. Reaveley. July 2000.
- PEER 2000/04** *An Evaluation of Seismic Energy Demand: An Attenuation Approach.* Chung-Che Chou and Chia-Ming Uang. July 1999.
- PEER 2000/03** *Framing Earthquake Retrofitting Decisions: The Case of Hillside Homes in Los Angeles.* Detlof von Winterfeldt, Nels Roselund, and Alicia Kitsuse. March 2000.
- PEER 2000/02** *U.S.-Japan Workshop on the Effects of Near-Field Earthquake Shaking.* Andrew Whittaker, Editor. July 2000.
- PEER 2000/01** *Further Studies on Seismic Interaction in Interconnected Electrical Substation Equipment.* Armen Der Kiureghian, Kee-Jeung Hong, and Jerome L. Sackman. November 1999.
- PEER 1999/14** *Seismic Evaluation and Retrofit of 230-kV Porcelain Transformer Bushings.* Amir S. Gilani, Andrew S. Whittaker, Gregory L. Fenves, and Eric Fujisaki. December 1999.
- PEER 1999/13** *Building Vulnerability Studies: Modeling and Evaluation of Tilt-up and Steel Reinforced Concrete Buildings.* John W. Wallace, Jonathan P. Stewart, and Andrew S. Whittaker, Editors. December 1999.
- PEER 1999/12** *Rehabilitation of Nonductile RC Frame Building Using Encasement Plates and Energy-Dissipating Devices.* Mehrdad Sasani, Vitelmo V. Bertero, James C. Anderson. December 1999.
- PEER 1999/11** *Performance Evaluation Database for Concrete Bridge Components and Systems under Simulated Seismic Loads.* Yael D. Hose and Frieder Seible. November 1999.
- PEER 1999/10** *U.S.-Japan Workshop on Performance-Based Earthquake Engineering Methodology for Reinforced Concrete Building Structures.* December 1999.
- PEER 1999/09** *Performance Improvement of Long Period Building Structures Subjected to Severe Pulse-Type Ground Motions.* James C. Anderson, Vitelmo V. Bertero, and Raul Bertero. October 1999.
- PEER 1999/08** *Envelopes for Seismic Response Vectors.* Charles Menun and Armen Der Kiureghian. July 1999.
- PEER 1999/07** *Documentation of Strengths and Weaknesses of Current Computer Analysis Methods for Seismic Performance of Reinforced Concrete Members.* William F. Cofer. November 1999.
- PEER 1999/06** *Rocking Response and Overturning of Anchored Equipment under Seismic Excitations.* Nicos Makris and Jian Zhang. November 1999.
- PEER 1999/05** *Seismic Evaluation of 550 kV Porcelain Transformer Bushings.* Amir S. Gilani, Andrew S. Whittaker, Gregory L. Fenves, and Eric Fujisaki. October 1999.
- PEER 1999/04** *Adoption and Enforcement of Earthquake Risk-Reduction Measures.* Peter J. May, Raymond J. Burby, T. Jens Feeley, and Robert Wood. August 1999.
- PEER 1999/03** *Task 3 Characterization of Site Response General Site Categories.* Adrian Rodriguez-Marek, Jonathan D. Bray and Norman Abrahamson. February 1999.
- PEER 1999/02** *Capacity-Demand-Diagram Methods for Estimating Seismic Deformation of Inelastic Structures: SDF Systems.* Anil K. Chopra and Rakesh Goel. April 1999.
- PEER 1999/01** *Interaction in Interconnected Electrical Substation Equipment Subjected to Earthquake Ground Motions.* Armen Der Kiureghian, Jerome L. Sackman, and Kee-Jeung Hong. February 1999.
- PEER 1998/08** *Behavior and Failure Analysis of a Multiple-Frame Highway Bridge in the 1994 Northridge Earthquake.* Gregory L. Fenves and Michael Ellery. December 1998.
- PEER 1998/07** *Empirical Evaluation of Inertial Soil-Structure Interaction Effects.* Jonathan P. Stewart, Raymond B. Seed, and Gregory L. Fenves. November 1998.
- PEER 1998/06** *Effect of Damping Mechanisms on the Response of Seismic Isolated Structures.* Nicos Makris and Shih-Po Chang. November 1998.
- PEER 1998/05** *Rocking Response and Overturning of Equipment under Horizontal Pulse-Type Motions.* Nicos Makris and Yiannis Roussos. October 1998.
- PEER 1998/04** *Pacific Earthquake Engineering Research Invitational Workshop Proceedings, May 14–15, 1998: Defining the Links between Planning, Policy Analysis, Economics and Earthquake Engineering.* Mary Comerio and Peter Gordon. September 1998.

- PEER 1998/03** *Repair/Upgrade Procedures for Welded Beam to Column Connections.* James C. Anderson and Xiaojing Duan. May 1998.
- PEER 1998/02** *Seismic Evaluation of 196 kV Porcelain Transformer Bushings.* Amir S. Gilani, Juan W. Chavez, Gregory L. Fennes, and Andrew S. Whittaker. May 1998.
- PEER 1998/01** *Seismic Performance of Well-Confined Concrete Bridge Columns.* Dawn E. Lehman and Jack P. Moehle. December 2000.

PEER REPORTS: ONE HUNDRED SERIES

The following PEER reports are available by Internet only at http://peer.berkeley.edu/publications/peer_reports_complete.html.

- PEER 2012/103** *Performance-Based Seismic Demand Assessment of Concentrically Braced Steel Frame Buildings*. Chui-Hsin Chen and Stephen A. Mahin. December 2012.
- PEER 2012/102** *Procedure to Restart an Interrupted Hybrid Simulation: Addendum to PEER Report 2010/103*. Vesna Terzic and Božidar Stojadinovic. October 2012.
- PEER 2012/101** *Mechanics of Fiber Reinforced Bearings*. James M. Kelly and Andrea Calabrese. February 2012.
- PEER 2011/107** *Nonlinear Site Response and Seismic Compression at Vertical Array Strongly Shaken by 2007 Niigata-ken Chuetsu-oki Earthquake*. Eric Yee, Jonathan P. Stewart, and Kohji Tokimatsu. December 2011.
- PEER 2011/106** *Self Compacting Hybrid Fiber Reinforced Concrete Composites for Bridge Columns*. Pardeep Kumar, Gabriel Jen, William Trono, Marios Panagiotou, and Claudia Ostertag. September 2011.
- PEER 2011/105** *Stochastic Dynamic Analysis of Bridges Subjected to Spatially Varying Ground Motions*. Katerina Konakli and Armen Der Kiureghian. August 2011.
- PEER 2011/104** *Design and Instrumentation of the 2010 E-Defense Four-Story Reinforced Concrete and Post-Tensioned Concrete Buildings*. Takuya Nagae, Kenichi Tahara, Taizo Matsumori, Hitoshi Shiohara, Toshimi Kabeyasawa, Susumu Kono, Minehiro Nishiyama (Japanese Research Team) and John Wallace, Wassim Ghannoum, Jack Moehle, Richard Sause, Wesley Keller, Zeynep Tuna (U.S. Research Team). June 2011.
- PEER 2011/103** *In-Situ Monitoring of the Force Output of Fluid Dampers: Experimental Investigation*. Dimitrios Konstantinidis, James M. Kelly, and Nicos Makris. April 2011.
- PEER 2011/102** *Ground-Motion Prediction Equations 1964–2010*. John Douglas. April 2011.
- PEER 2011/101** *Report of the Eighth Planning Meeting of NEES/E-Defense Collaborative Research on Earthquake Engineering*. Convened by the Hyogo Earthquake Engineering Research Center (NIED), NEES Consortium, Inc. February 2011.
- PEER 2010/111** *Modeling and Acceptance Criteria for Seismic Design and Analysis of Tall Buildings*. Task 7 Report for the Tall Buildings Initiative - Published jointly by the Applied Technology Council. October 2010.
- PEER 2010/110** *Seismic Performance Assessment and Probabilistic Repair Cost Analysis of Precast Concrete Cladding Systems for Multistory Buildings*. Jeffrey P. Hunt and Božidar Stojadinovic. November 2010.
- PEER 2010/109** *Report of the Seventh Joint Planning Meeting of NEES/E-Defense Collaboration on Earthquake Engineering. Held at the E-Defense, Miki, and Shin-Kobe, Japan, September 18–19, 2009*. August 2010.
- PEER 2010/108** *Probabilistic Tsunami Hazard in California*. Hong Kie Thio, Paul Somerville, and Jascha Polet, preparers. October 2010.
- PEER 2010/107** *Performance and Reliability of Exposed Column Base Plate Connections for Steel Moment-Resisting Frames*. Ady Aviram, Božidar Stojadinovic, and Armen Der Kiureghian. August 2010.
- PEER 2010/106** *Verification of Probabilistic Seismic Hazard Analysis Computer Programs*. Patricia Thomas, Ivan Wong, and Norman Abrahamson. May 2010.
- PEER 2010/105** *Structural Engineering Reconnaissance of the April 6, 2009, Abruzzo, Italy, Earthquake, and Lessons Learned*. M. Selim Günay and Khalid M. Mosalam. April 2010.
- PEER 2010/104** *Simulating the Inelastic Seismic Behavior of Steel Braced Frames, Including the Effects of Low-Cycle Fatigue*. Yuli Huang and Stephen A. Mahin. April 2010.
- PEER 2010/103** *Post-Earthquake Traffic Capacity of Modern Bridges in California*. Vesna Terzic and Božidar Stojadinović. March 2010.
- PEER 2010/102** *Analysis of Cumulative Absolute Velocity (CAV) and JMA Instrumental Seismic Intensity (I_{JMA}) Using the PEER–NGA Strong Motion Database*. Kenneth W. Campbell and Yousef Bozorgnia. February 2010.
- PEER 2010/101** *Rocking Response of Bridges on Shallow Foundations*. Jose A. Ugalde, Bruce L. Kutter, and Boris Jeremic. April 2010.
- PEER 2009/109** *Simulation and Performance-Based Earthquake Engineering Assessment of Self-Centering Post-Tensioned Concrete Bridge Systems*. Won K. Lee and Sarah L. Billington. December 2009.

- PEER 2009/108** *PEER Lifelines Geotechnical Virtual Data Center.* J. Carl Stepp, Daniel J. Ponti, Loren L. Turner, Jennifer N. Swift, Sean Devlin, Yang Zhu, Jean Benoit, and John Bobbitt. September 2009.
- PEER 2009/107** *Experimental and Computational Evaluation of Current and Innovative In-Span Hinge Details in Reinforced Concrete Box-Girder Bridges: Part 2: Post-Test Analysis and Design Recommendations.* Matias A. Hube and Khalid M. Mosalam. December 2009.
- PEER 2009/106** *Shear Strength Models of Exterior Beam-Column Joints without Transverse Reinforcement.* Sangjoon Park and Khalid M. Mosalam. November 2009.
- PEER 2009/105** *Reduced Uncertainty of Ground Motion Prediction Equations through Bayesian Variance Analysis.* Robb Eric S. Moss. November 2009.
- PEER 2009/104** *Advanced Implementation of Hybrid Simulation.* Andreas H. Schellenberg, Stephen A. Mahin, Gregory L. Fenves. November 2009.
- PEER 2009/103** *Performance Evaluation of Innovative Steel Braced Frames.* T. Y. Yang, Jack P. Moehle, and Božidar Stojadinovic. August 2009.
- PEER 2009/102** *Reinvestigation of Liquefaction and Nonliquefaction Case Histories from the 1976 Tangshan Earthquake.* Robb Eric Moss, Robert E. Kayen, Liyuan Tong, Songyu Liu, Guojun Cai, and Jiaer Wu. August 2009.
- PEER 2009/101** *Report of the First Joint Planning Meeting for the Second Phase of NEES/E-Defense Collaborative Research on Earthquake Engineering.* Stephen A. Mahin et al. July 2009.
- PEER 2008/104** *Experimental and Analytical Study of the Seismic Performance of Retaining Structures.* Linda Al Atik and Nicholas Sitar. January 2009.
- PEER 2008/103** *Experimental and Computational Evaluation of Current and Innovative In-Span Hinge Details in Reinforced Concrete Box-Girder Bridges. Part 1: Experimental Findings and Pre-Test Analysis.* Matias A. Hube and Khalid M. Mosalam. January 2009.
- PEER 2008/102** *Modeling of Unreinforced Masonry Infill Walls Considering In-Plane and Out-of-Plane Interaction.* Stephen Kadysiewski and Khalid M. Mosalam. January 2009.
- PEER 2008/101** *Seismic Performance Objectives for Tall Buildings.* William T. Holmes, Charles Kircher, William Petak, and Nabih Youssef. August 2008.
- PEER 2007/101** *Generalized Hybrid Simulation Framework for Structural Systems Subjected to Seismic Loading.* Tarek Elkhoraibi and Khalid M. Mosalam. July 2007.
- PEER 2007/100** *Seismic Evaluation of Reinforced Concrete Buildings Including Effects of Masonry Infill Walls.* Alidad Hashemi and Khalid M. Mosalam. July 2007.

The Pacific Earthquake Engineering Research Center (PEER) is a multi-institutional research and education center with headquarters at the University of California, Berkeley. Investigators from over 20 universities, several consulting companies, and researchers at various state and federal government agencies contribute to research programs focused on performance-based earthquake engineering.

These research programs aim to identify and reduce the risks from major earthquakes to life safety and to the economy by including research in a wide variety of disciplines including structural and geotechnical engineering, geology/seismology, lifelines, transportation, architecture, economics, risk management, and public policy.

PEER is supported by federal, state, local, and regional agencies, together with industry partners.



PEER Core Institutions

University of California, Berkeley (Lead Institution)
California Institute of Technology
Oregon State University
Stanford University
University of California, Davis
University of California, Irvine
University of California, Los Angeles
University of California, San Diego
University of Nevada, Reno
University of Southern California
University of Washington

PEER reports can be ordered at <https://peer.berkeley.edu/peer-reports> or by contacting

Pacific Earthquake Engineering Research Center
University of California, Berkeley
325 Davis Hall, Mail Code 1792
Berkeley, CA 94720-1792
Tel: 510-642-3437
Email: peer_center@berkeley.edu

ISSN 2770-8314
<https://doi.org/10.55461/GVIF2980>